# Proceedings of the 7th China International Silk Conference


## Inheritance and Innovation — Modern Silk Road

**Chief Editor: Lun Bai**
**Subeditor: Guo-Qiang Chen**

***Sponsored by***
China National Silk Coordinating Office
China National Silk Association
***Jointly Organized by***
Soochow University
Shinshu University Japan

TRANS TECH PUBLICATIONS

# Silk

Inheritance and Innovation -
Modern Silk Road

Edited by
Lun Bai
Guo-Qiang Chen

# Silk

Inheritance and Innovation - Modern Silk Road

Selected, peer reviewed papers from the
7th China International Silk Conference on
Inheritance and Innovation---Modern Silk Road,
Sep. 10-12, 2010,
Suzhou, P. R. China

*Edited by*

**Lun Bai and Guo-Qiang Chen**

**TRANS TECH PUBLICATIONS LTD**
**Switzerland • UK • USA**

Trans Tech Publications Ltd
Laubisrutistr. 24
CH-8712 Stafa-Zurich
Switzerland
http://www.ttp.net

Volumes 175-176 of
*Advanced Materials Research*
*ISSN 1022-6680*

Full text available online at *http://www.scientific.net*

***Distributed** worldwide by*

Trans Tech Publications Ltd
Laubisrutistr. 24
CH-8712 Stafa-Zurich
Switzerland

Fax: +41 (44) 922 10 33
e-mail: sales@ttp.net

*and in the Americas by*

Trans Tech Publications Inc.
PO Box 699, May Street
Enfield, NH 03748
USA

Phone: +1 (603) 632-7377
Fax: +1 (603) 632-5611
e-mail: sales-usa@ttp.net

# Preface

In the past thousands of years, old-line silk culture has produced the far-reaching implication for east and west. The famous Silk Road, a route for cross-culture and technology exchange between east and west, has promoted the economic and trade development in the world. Nowadays, modern science and technology is injecting new vitality into the traditional silk as the same scenario happened in the other areas. Under the circumstance of the global economy crisis, academic communication is becoming vital for the revolutionary innovation and development of the international textile and silk industry.

On the basis of the successful 6 international silk conferences, the 7th International Silk Conference, Silk: "Inheritance and Innovation---Modern Silk Road" was hold on September 10-12 in Soochow University (Suzhou, P. R. China). The conference promoted the academic communication, accelerated the inheritance and development of silk culture, and exploited novel technology about silk and textile.

The proceedings focus on the new technology in mulberry and silkworm, new textile materials, especially silk-based functional materials and biomaterials, and design, processing techniques in the manufacture of silk and other textile products, chemical treatment technology, and clothing science and culture.

*Sponsored by*

**China National Silk Coordinating Office**

**China National Silk Association**

*Jointly Organized by*

**Soochow University**

**Shinshu University Japan**

**Sep. 10-12, 2010, Suzhou, P. R. China**

# Table of Contents

## Textile Processing and Properties

## Chemical Treatment and Technology

## Clothing Science and Technology

# Mulberry and Silkworm

*Advanced Materials Research Vols. 175-176 (2011) pp 3-7*

*doi:10.4028/www.scientific.net/AMR.175-176.3*

# The Fluorescent Pigment of Mulberry Transferred in the Body of Silkworm, *Bombyx mori*

LIU Xiao-hong[1, a],LI Ye-feng[1, b], XU Jian[1, c], ZHOU Jun[, d], LU Xiao-ping[1*, e]

[1] Gold Mantis school of Architecture and Urban Environment, Soochow University，Suzhou 215123, China;

[2] Plant protection and quarantine station, WuJiang, WuJiang 215200, China;

[a]liuxiaohong0117@163.com; [b]liyefeng.1215@yahoo.com.cn; [c]xujian568@yahoo.com.cn; [d]zj8291@yahoo.com.cn; [e]szlxp@yahoo.com.cn

**Key words**: *Bombyx mori*; mulberry; fluorescent pigment; thin layer chromatography (TLC).

**Abstract.** Using silkworm (*Bombyx mori*, Dazao strain) as material, the fluorescent pigment of mulberry, silkworm blood, silk gland, cocoon shell, silkworm excrement, silkworm urine and moth urine were analyzed by using the technology of thin layer chromatography (TLC). The results indicated that there were 7 bands of fluorescent pigment from the extracts of green cocoon shell after TLC analysis. While, 2 bands in silkworm blood and its urine extracts, 4 bands in the silk gland extracts, as well as 5 bands in moth urine extracts were detected, but no band detection in the silkworm excrement extracts. The blue-violet fluorescent pigment which has the same Rf (0.35) was detected from the extracts of green cocoon shell, silk gland, silkworm urine, moth urine and mulberry after TLC analysis, but it cannot be found in silkworm blood and silkworm excrement. It was revealed that the blue-violet fluorescent pigment may be transferred directly from mulberry leaves, and then accumulated in the silk gland. Most of the pigment remained in the cocoon shell. And only a small amount of this kind of pigment was excreted through urine. There was also some yellow-green fluorescent pigment detected in the silkworm blood, silk gland and cocoon shell extracts, but it cannot be detected in both the mulberry and silkworm urine extracts. It was suggested that yellow-green fluorescent pigment synthesis pathway exist in the body of silkworm (*Bombyx mori*, Dazao strain).

## Introduction

In the early 1970s, Chinese scholars began to study the mechanism of Fluorescent Colors in silkworms. It showed that different varieties of silkworm and research methods could result in significant differences on the types of fluorescent pigment and characteristics. It also showed that there were 7 types of pigment in color cocoon “Zhengbai×B8Banyou strain”, while 9 in Dazao strain [1], among which 5 is the kind of flavonoid pigment and the others are flavonoid pigment analogues after paper chromatography (PC) analysis [2]. With the mothods of UV scanning, HPLC and PC, several kinds of fluorescent pigment were found in cocoon and no differences between male and female [3]. Different relative contents result in different fluorochrome. Some studies [2, 4] showed that the UV absorption peak of cocoon extracts is almost the same (λmax=270 mm, λmax=240 mm), which is a kind of flavonoid pigment and flavonoid pigment analogues. It indicated that this kind of fluorescent pigment, which has the similar molecular structures with flavonols, may be the flavonols analogue with the molecular weight of 340 by Mass Spectrometry and. In our study, we analyzed the fluorescent pigment of mulberry, silkworm blood, silk gland, cocoon shell, silkworm excrement, silkworm urine and moth urine by the technology of thin layer chromatography (TLC). We knew about that the pigment of mulberry was transferred in the silkworm. And we speculated the reasons for the formation of green cocoon, which can provide more important theories for the study and breeding of new varieties in the future.

## Materials and Methods

**Materials.** The mulberry leaves are from Dushu Lake Campus, Soochow University and the variety is the triploid mulberry (L3). Silkworm (Dazao strain) is a kind of green cocoon, which is provided by Professor Sima Yang-hu in Medical College of Soochow University.

*TLC.* Expand agent No.1 is $HOCH_2C(CH_3)_2CH_2OH/CH_3COCH_3$(65:35) and expand agent No.2 is $CH_3(CH_2)_3OH/HCOOH/ H_2O$(4:1:2). The silica gel plates for TLC (HSGF254, 200×100 mm) are produced by the Yantai Institue of Chemical Industry.

*Silkworm fluorescence extraction.* 100% $CH_3OH$ was used to wipe out the protein of silkworm blood, and supernatant solution was used as a sample. Put the silk gland into 100% $CH_3OH$ solution, and then concentrate the solution, which is used as fluorescent silk gland extract sample. Taking a certain amount of silkworm excrement immersed in 100% $CH_3OH$ solution to concentrate. Use the concentrated solution to carry out PC analysis in expand agent No.1 with 3MM filter paper in order to wipe out photosynthetic pigment. Cut stain of Rf = 0 into pieces to immerse in 100% $CH_3OH$ solution to concentrate. Reserve the concentrated solution at 4°C. Cut 2g of cocoon shell into pieces to immerse in 100% $CH_3OH$. Extract the cocoon shell for 72 h by Soxhlet exteaction apparatus in the water bath at 70°C. Filter out the supernatant to concentrate. Finally, put the concentrated solution in 4 □ for reserve [5]. Collect the urine of silkworm and moth directly as two of the samples.

*Mulberry fluorescence extraction.* Using 2g mulberry leaf powder immersed in $CH_3OH$ for 24h concentration under a high temperature. The method of getting fluorescence mulberry extract is the same as that of extracting the silkworm excrement fluorescence.

## Results

**TLC of extracts of mulberry fluorescence.** For studying the differences among different ages and polyploidies, grinded mulberry leaves were used as the samples to carry out TLC (Fig.1). We confirm the location of the fluorescent stain which is dry at room temperature. The same clear blue-violet fluorescence was found among all the samples. It was suggested that whatever the leaf species or age is, the fluorescent pigment is the same. It didn't affect the silkworm fluorescent pigment by the pigment of mulberry.

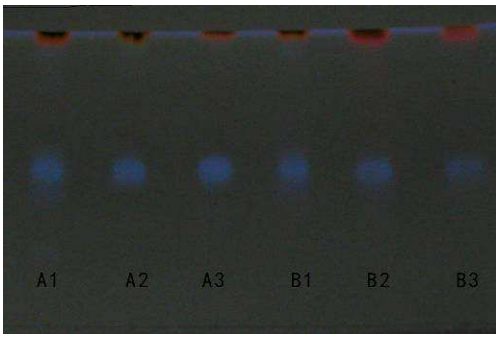


Fig. 1 TLC of extracts of mulberry fluorescence
A1/ B1: the young mulberry; A2/ B2:the middle-aged mulberry; A3/ B3: the elderly mulberry

*TLC of extracts of cocoon shell fluorescence.* In order to investigate the composition of the fluorescent materials and types in cocoon, TLC was used to separate the fluorescent materials of cocoon. Put the spotted silica gel plate into expand agent No.2 to carry out TLC (Fig. 2). When colors were separated, we can clearly see that there were 7 bands under 365 nm UV. We marked the 7 bands as Ⅰ, Ⅱ, Ⅲ, Ⅳ, Ⅴ, Ⅵ and Ⅶ. The Rf of bands are 0, 0.18, 0.35, 0.47, 0.63, 0.79 and 0.97 respectively. Band Ⅰ is the sample point. But it still had a slightly lighte yellow-green fluorescence after TLC. It indicated that certain pigment of the sample could not be carried out in expand agent No.2. Band Ⅱ and Ⅴ are brought in a yellow-green fluorescence, and the colors are similar to that in cocoon. Band Ⅲ and Ⅳ are blue-violet fluorescence. Band Ⅵ is faint

blue-violet fluorescence, while Band Ⅶ is clear blue-violet fluorescence.

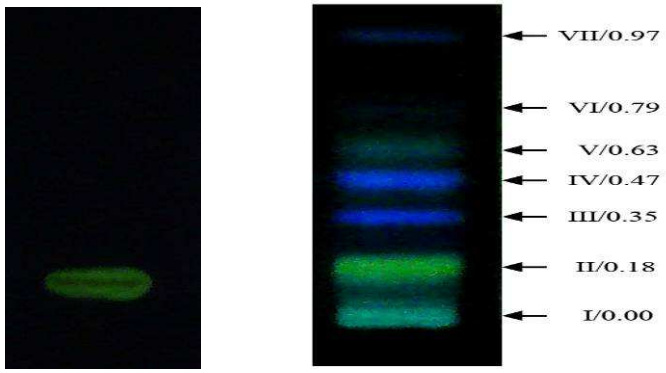


Before TLC After TLC

Fig. 2 TLC results of extracts of the cocoon shell fluorescence

**TLC of extracts of mulberry and silkworm fluorescence.** Put the extracts of mulberry and cocoon shell to carry out TLC(Fig. 3(a)). There is a similar blue-violet fluorescent band which has the Rf of 0.35 after TLC. It indicated that a part of the pigment of mulberry was left in the silkworm after digestion. Then the pigment was transferred to the cocoon. We can obviously find that the extracts of mulberry, silk gland and cocoon shell fluorescence have the same blue-violet fluorescent band after TLC (Fig. 3(b)), but it couldn't be found in silkworm blood. This phenomenon is suggested that the blue-violet fluorescent pigment couldn't stay in the blood, but could massively accumulate in the silk gland. It also can show that the blue-violet fluorescent pigment could not be discharged by silkworm excrement because it could not find the band of blue-violet fluorescent after TLC. Meanwhile, the silk gland and cocoon shell have the same band of yellow-green fluorescent. We can guess that after silkworm ate mulberry, and then a part of pigment was modified into other types of pigment. Fig. 3(c) shows the results of TLC of extracts of silkworm urine and moth urine. There is a band of very weak blue-violet fluorescent which is as same as mulberry's. It is indicated that a very small amount of this pigment was excreted by silkworm urine. Moth urine has a strong blue-violet fluorescent band and a high content. At the same time, we knew that no yellow-green fluorescent band could be found after TLC of silkworm urine and moth urine. As a result, we can speculate that all the yellow-green fluorescent pigment was transferred to the silk. Maybe this yellow-green fluorescent pigment is the reason for the formation of yellow-green cocoon. In a word, the blue-violet fluorescent pigment of mulberry can only accumulate in silk gland, and a part of them were transferred into silk and moth urine. This kind of pigment can not be eliminated by silkworm, but can be expelled from moth urine when it is mature.

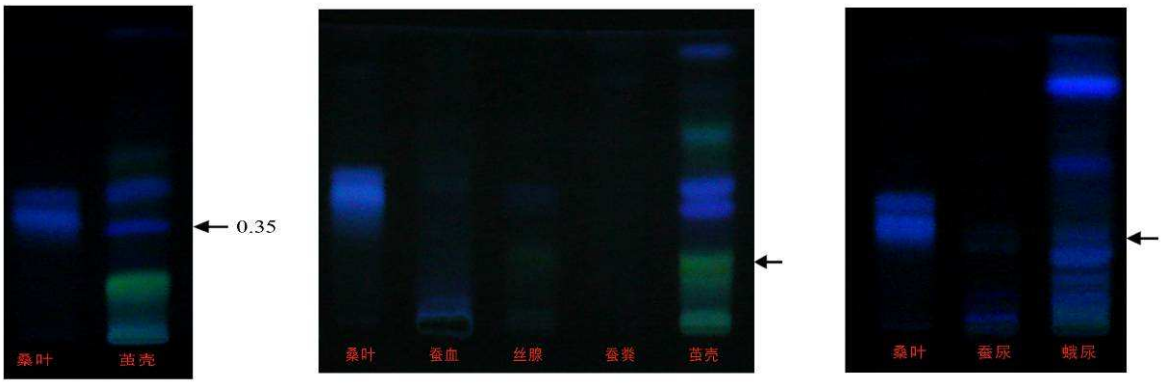


(a) (b) (c)

Fig. 3 TLC results of extracts of mulberry and cocoon shell(a) mulberry and silkworm(b) and mulberry, silkworm urine and moth urine fluorescence(c)

## Discussion

Rich in mulberry in combination of C3 naturally-occurring flavonols, such as rutin quercetin, vision, and glycosidase-catalysed ligands of quercetin[6]. Two major naturally-occurring flavonols are respectively quercetin (3-*O*-β-D-indican quercetin)[7,8] and acacia (3-*O*-β-D-naturally-occurring kaempferol)[9].

Tamera[10] isolated three varieties of 5-indican flavonoids from yellow green cocoon Bi Multi, and using UV Spectra, FT-IR, HPLC, $^{1}H$ and $^{13}C$ NMR and FD-MS analyzed their structure, they are 5,4′-2-O-β-D-pyranoid isothiocyanante quercetin,5,7,4′-3-*O*-β-D-pyranoid isothiocyanante quercetin and 5-*O*-β-D-pyranoid isothiocyanante quercetin. Kurioka[11] got 5-*O*-β-D-indican quercetin, 7-*O*-β-D-indican quercetin, 5-*O*-β-D-indican kaempferol and7-*O*-β-D-indican kaempferol and 4′-*O*-β-D-indican quercetin and their indican, quercetin and kaempferol from cocoon shell ethanol extract of yellow green cocoon(Sasamayu).With UV Spectra, HPLC-ESI-MS methods, they analyzed structures. The cocoon has strong antioxidant capacity mainly because of these flavonoids.Hirayama C[12] got two kinds of flavonoids which contained levoratory proline(6-C-[(2S,5S)-prolin-5-yl], 6-C-[(2S,5R)-ptolin-5-yl]). Using UV Spectrum; ninhydrin reaction; FTICR-MS; HPLC; NMR; DQFCOSY and HSQC,etc, they analyzed structure. This is the first time that it was found flavonoids contained amino group. The flavonoids compounds of combining C5 and glucoside doesn't exist in mulberry, and it can be assumed that it is formed after flavonoids compounds in the mulberry entering the silkworm body. For this conclusion, it was performance in our experiment. Pigment of mulberry that were digested and absorbed were transferred into silkworm, and then most metastasize to the cocoon. Some pigment exist in the cocoon shell but none in mulberry. The pigment may be the pigment of mulberry which was modified by silkworm.

In our study, we got the fluorescent strips after TLC of extracts of fluorescent cocoon shell. There are yellow-green and blue-violet fluorescent bands. But in moth urine there is only blue-violet fluorescent bands. Lots of blue-violet fluorescent pigment was excluded in vitro. They could not be absorbed by silkworm. The yellow-green fluorescent pigment was transferred into silk. From another side, it was revealed that the formation of yellow-green cocoon is mainly because of the yellow-green fluorescent pigment.

The previous studies [13] showed that the yellow-green cocoon is composed of flavonoids pigment. These kinds of pigment mainly existed in the intestines or blood, but in our study, the yellow-green fluorescent pigment was found in silk gland which deviated from the conclusions.

We will continue to study cocoon colors, especially for analysis of fluorescent pigment. We hope our results can provide provide more important theories for the study and breeding of new varieties in the future.

## Acknowledgments

Many thanks to Professor Sima Yang-hu Department of Medicine, Soochow University.

**References**

[1] N. F ujimoto, K. Kawakami. J Seric Sci Jpn. Vol.27 (6) (1958), p. 391

[2] N. Fujimoto, K. Hayashiya and T. Hayashiya. J Seric Sci Jpn. Vol.28 (1) (1959), p. 27

[3] Z.C. Yu , S.Y. Heng. Sericultural science. Vol.28 (2) (2002), p. 151

[4] H. Xu, Y. F. Fen. Silk. Vol. (3) (1990), p.19; (4) (1990), p. 46

[5] Y. Q. Zhang, X. H.Yu and W.D. Shen.Chinese science. Vol.39 (4) (2009), p.372

[6] J. Zhishen, T. Mengcheng and J W. ianming. Food Chem. Vol. (64) (1999), p.555

[7] M. Oku. *Nippon Nogeikagaku Kaishi* . Vol.10(1934), p.1029

[8] C. Hirayama, H. Ono and Y. Tamura. Phytochemistry. Vol. 67 (2006), P.579

[9] K. Naito. *Nippon Nogeikagaku Kaishi* . Vol. 53(1979), p.13

[10] Y. Tamura, K. Nakajima and K. Nagayasu. Phytochemistry . Vol. (59)(2002), p. 275

[11] A. Kurioka, M. Yamazaki. Biosci. Biotechnol. Biochem. Vol. (66) (2002), p. 1396

[12] K. Hayashiya, Y. Hamamera. *Nippon Nogeikagaku Kaishi*. Vol. 30(1956), p. 361

[13] Z. D. Wu, Z. W. Yang, in: Silkworm body anatomy physiology. Edtied by Agriculture publishing, Beijing,(1998), in press

*Advanced Materials Research Vols. 175-176 (2011) pp 8-12*

*doi:10.4028/www.scientific.net/AMR.175-176.8*

# Application of Pebrine Detection by PCR Infected Bombyx mori Eggs

Zhong-Hua Pan[a], Cheng-Liang Gong[b], Xiao-Jian Zheng[c], Rui Guo[d],

Wei-De[e] Shen

Medical College of Soochow University, Suzhou 215123, China

[a]Pzh1971@163.com, [b]chlgong@hotmail.com, [c]zheng_xj6211@yahoo.com.cn, [d]rui_0508@163.com,

[e]shenwd@suda.edu.cn

**Keywords**: Application study; Pebrine infected *Bombyx mori* eggs; PCR detection.

**Abstract.** With the development of the PCR technology, especially the improvement of its reagent and a method of pebrine detection by PCR in infected *Bombyx mori* eggs was established.With the 16sRNA gene of *Nosema bombycis* as target sequence, the results of extraction of genomic DNA from purified microspores showed that $1.3\times10^{-7}$μg DNA can be extracted from each spore. The sensitivity detection showed the detection limit of *Nosema bombycis* DNA was $3.25\times10^{-2}$pg, i.e. 4 spores. (PCR system volume is 25μl). The method of total DNA extraction from pebrine infected silkworm eggs just before hatching was created. The result showed that extracting total DNA from silkworm eggs after the eggs had been treated with 30% KOH met the PCR detection requirements. The result of application study showed the spores in the pebrine infected egg just before hatching can sensitively be found with PCR. The result of a group of eggs just before hatching detection showed that the maximum PCR detection level was of a pebrine infected eggs just before hatching in 300 healthy eggs when the total DNA extraction had been purified with Agarose electrophoresis. The probability of identifying groups of one pebrine spore in infected eggs just before hatching mixed with 100 healthy ones was about 80%.

## Introduction

At present, optical microscope detection is adopted in production to detect the pebrine infection of *Bombyx mori* female moth. Over time, its deficiency has been realized by some professionals, so new detection method needs to be developed.

In 1996, Chen X [1] *et al* first reported the application of PCR in *N. bombycis* detection in China. I primer was designed by using a highly conservative sequence of the DNA of *N. bombycis* and PCR detection was successfully carried out. Cai PZ (1997) [2] *et al* had designed several primers to detect *N. bombycis* with PCR. Qiu BL (2002) [3] *et al* had produced DIG using peculiar DNA sequence of *N. bombycis* to find the spore of *N. bombycis* through dotblot and Southern, the sensitivity reaching 1ng DNA. Hatakeyama (2002) [4] *et al* had reported that multiprimer PCR could be used to detect *N. bombycis* in pebrine infected eggs, but no systematic research had been done. Liu JP (2004)[5] *et al* imitated "pebrine infected eggs"(health eggs added with artificially purified spores) as subject and proved PCR detection limit was 369 spores and some substance in silkworm eggs can cause the inhibition of PCR. The application of PCR in the detection of pebrine is worth studying.

With the development of PCR technology, especially the great improvement of the function of reagent and reaction system, we carried out detailed study on the PCR detection of pebrine infected silkworm eggs based on previous studies. The results showed PCR can be applied in the study on the rate of pebrine infected eggs just before hatching.

## Experimental

**Materials.** *Bombycis mori* (Su5, Su6) (provided by Jiangsu Province *Bombyx mori* Egg management); *N. bombycis* has been preserved and rejuvenated by the Department of Applied Biology of Soochow University.

*Primers.* (Nb5): 5'CACCAGGTTCTGCC'3', (Nb3): 5'TTATGATCCTGCTAATGG'3', Composed by Shang Hai Bo Ya Biological Technical Company Limited.

*Regents.* Pfu-*Tag* DNA, dNTP, λDNA/*Hin*dIII. *Eco*RI et al (provided by Shang Hai Biological Project Company Limited).

**PCR system.** PCR was carried out as follows: after preheating the reaction mixture ultimately containing 10 mmol/L Tris-HCl(pH8.9), 50 mmol/L KCl, 1.5mmol/L $MgCl_2$, 0.2mmol/L dNTP, 0.5μmol/L of the respective primers, and 5 ng of template DNA at 98°C for 5 min and subsequent cooling on ice, 2.5 units of pfu-Taq DNA polymerase were added, followed by 32 cycles of denaturing at 94°C for 30s, annealing at 55°C for 30s, and extension at 72°C for 50s using GeneAmp PCR System 9700. After PCR, a 5μl aliquot of the PCR mixture was mixed with 5 μl TE buffer and 2μl 40% sucrose containing 0.25% BPB and subjected to 2% agarose gel electrophoresis with 200 bp DNA size markers. The gels were stained with ethidium bromide.

**Detecting PCR Sensitivity with Maximum Dilution.** After $10^9$ pure spores, which were initially placed in a 1.5-ml plastic tube, has been soaked in 0.1mol/L $K_2CO_3$+0.1mol/L $KHCO_3$ solution at 27°C for an hour, extract with Phol/chloroform the DNA from spores of *N. bombycis*, and dissolve it with 40μl D.W. Then adjust the total volume to 3ml and measure its ultraviolet absorption ($OD_{260}$). Then dilute to $10^{-1}$, $10^{-2}$, $10^{-3}$, $10^{-4}$, $10^{-5}$, $10^{-6}$, $10^{-7}$, $10^{-8}$, $10^{-9}$ and $10^{-10}$ respectively. Use them as PCR template to detect the sensitivity of the DNA of *N. bombycis*.

**Preparation of "pebrine infected silkworm eggs".** Inoculation of $10^8$ of spores to newly exuviated silkworm larvae at stage 5. That is, an artificial diet soaked in a solution containing spores of *N. bombycis* was ingested by silkworms over 24 h. Thereafter, silkworms were maintained normally to obtain silkworm moths and eggs.

**"Pebrine Infected Eggs" incubation.** Pickling at once, incubating at 25°C about 6 days, until the period of eggs just before hatching, then preserving at -20°C.

**Examining with microscope for "pebrine infected eggs".** Take 100 silkworm eggs randomly, examine with microscope (every egg was ground and examined). Microspores can be found in every silkworm egg, so we can know that other silkworm eggs were all pebrine inspected.

**Extraction of DNA from "pebrine infected eggs".** According to method of Hatakeyama (2002) [5], DNA was extracted from silkworm eggs with the 30% KOH. That is, silkworm eggs were independently placed in an Eppendorf tube, followed by the addition of 500 μl of 30% KOH. The sample solution was allowed to stand for about 20 min until the color of the silkworm eggs turned red. After confirming the color change, KOH was removed, and then the silkworm eggs were washed twice with 500 μl of D.W. and once with 1mol/L HCl in order to return to the neutrality. The silkworm eggs were then washed twice with D.W., and gently swirled after the addition of 500 μl of 2% SDS solution. Subsequently, the same volume of Tris-phenol was added, and the solution was centrifuged after gentle swirling to recover the aqueous phase. Phenol extraction was performed twice, and then ethanol precipitation was performed after washing with chloroform. In addition, the extracted DNA was rinsed twice with 70% ethanol before dissolution in 40 μl of TE solution.

**Purification of total DNA.** Take 10 μl from the above abstracted DNA to carry out electrophoresis. Extract the agarose containing DNA at the same horizontal route as the DNA of *N. bombycis*, and repeatedly freeze and thaw it at ultra-low temperature. Deposit DNA with 75% alcohol, vacuum dry and dissolve it with 5 μl TE.

The healthy silkworm eggs with an amount of 0, 9, 19, 29, 39, 49, 59, 69, 79, 89 and 99 were taken and added one "pebrine infected" egg, respectively, then the total DNA was extracted with 30% KOH method, dissolved with 40μl TE, take 10μl to go through purification with Agarose electrophoresis, then 1μl sample was used as template to carry out PCR.

Study on the possibility of detecting one pebrine infected egg from 100 silkworm eggs with PCR, Take 10 groups (99 grain each group) healthy silkworm eggs, then add one "pebrine infected" egg to each group. After extracting the total DNA from each group with 30% KOH method, dissolve it with TE. Take 10 μl to go through purification with Agarose electrophoresis and then take 1 μl as template to carry out PCR.

**Results**

**The sensitivity of PCR detection to the DNA of *N. bombycis* spore.** After extracting the DNA from $10^9$ spores, the $OD_{260}$ of DNA was 0.8670. Because the DNA of every 1.0 OD /ml was 50 μg, the total DNA was 130.05 μg. We can say that $1.3\times10^{-7}$μg DNA can be extracted from one spore.

Take the diluted samples to carry out PCR. The result shows (Fig. 1) bands can be found in the diluted samples of $10^{-1}$~$10^{-8}$, but not in the samples of $10^{-9}$ and $10^{-10}$. So we could deduce that PCR limit is $3.25\times10^{-2}$ pg (25 μl system volume), i.e. 4 spores.

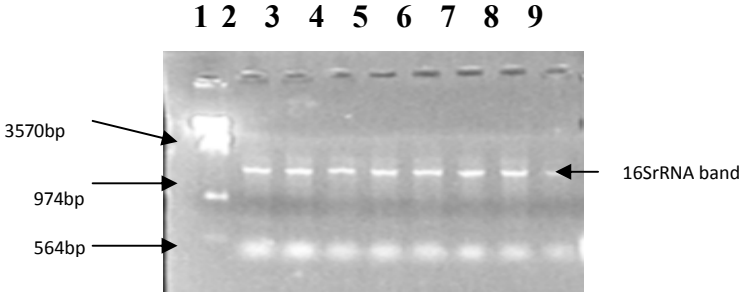


Fig. 1 being found limitation of PCR for *N. bombycis* DNA

1: Marker (λ/*Eco*RI and *Hin*dIII), 2~9: DNA extracted from$10^9$ *N. bombycis* spore which diluted $10^{-1}$~$10^{-8}$, take 1μl as template

**The Purification of total DNA.** Purify the extracted total DNA with Agarose electrophoresis. The result is shown in Fig. 2. It can be observed that lots of irrelevant DNA and RNA were cleared away.

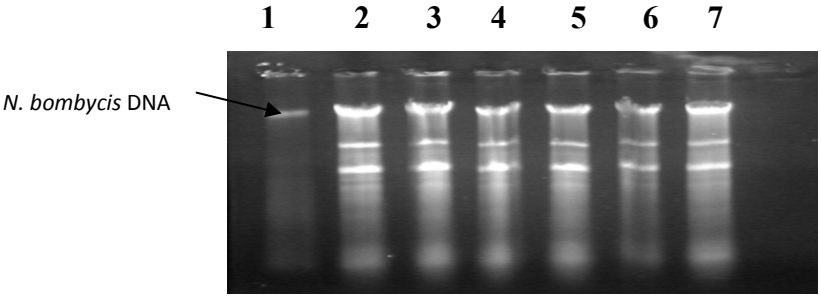


Fig.2 The purification of silkworm eggs total DNA:

1. *N . bombycis* DNA, 2~7: silkworm eggs samples DNA

**The relationship between the rate of being found and different rate of "pebrine infected egg".** PCR was carried out with the above DNA as template. The result showed (Fig. 3) he DNA of *N.bombycis* can be detected sensitively from the 1/10 to 1/100 silkworm egg samples by using the above mentioned method (3.7).

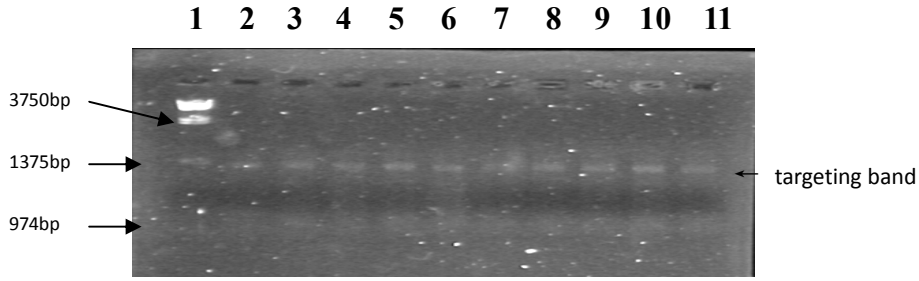


Fig. 3 The relation of different proportion of pebrine silkworm egg and detection efficiency

1. Marker (λ/*Eco*RI and *Hin*dIII); 2~11: respectively point out adding a grain pebrine silkworm egg into every 10, 20, 30, 40, 50, 60, 70, 80, 90 and 100 grain silkworm eggs.

**Study on the possibility of detecting one pebrine infected egg from 100 silkworm eggs with PCR.** Take the DNA of 1/100 as template to carry out PCR, and treat it with No 3.8 method. DNA of *N. bombycid* can be found in 8 of the 10 groups (Fig. 4).

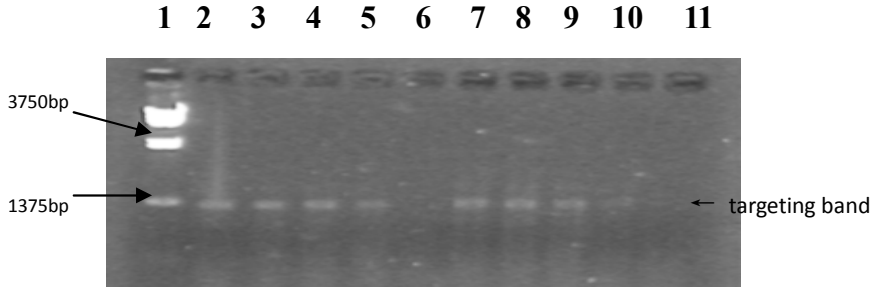


Fig. 4 The successful rate of PCR detection for having a grain pebrine silkworm egg in 100 silkworm eggs

1. Marker (λ/*Eco*RI and *Hin*dIII), 2~11: PCR results (10 times)

## Discussion

Liu R.H (2003) [6] *et al* had showed that spores could only be randomly detected under light microscope if the spore density in solution was lower than $1\times10^4$ grain/ml; if it was lower than $3\times10^3$grain/ml, they can hardly be detected. So we can deduce that the sensitivity of PCR detection was better than that of light microscope. Liu JP (2004) [7] *et al* had extracted the DNA from spores of *N. bombycis* with SDS-Protease and carry out PCR. He thought the detection limit was 1000 grains, but our detection sensitivity had increased by 250 times, which may be relevant to the draw efficiency of DNA, primers, PCR system.

Our study showed after the abstracted total DNA of silkworm was purified with Agarose electrophoresis the detection sensitivity of PCR was improved compared to the previous study of the author (2005)[8]. We can deduce that DNA may disturb the PCR. 1/10~1/100 diseased eggs can be successfully detected by using the systematic approach of this study. Our study verified Hatakeyama's proposition that PCR can be applied to the detection of the *N. bombycis* of silkworm eggs. The study showed that PCR detection probability was about 80% in 1/100 pebrine infected eggs. Due to the small number of test samples, we can not provide accurate mathematical statistics, and further detailed studies need to be carried out. .

This study concentrated on the *Nosema* spores preserved in our laboratory and preliminary conclusions were obtained by using the above method. Due to the complicated situations in production, it needs to be further explored whether this method can be applied to the production. In addition, we used only a pair of primers in this study, so if a few pairs of primers had been used, the experimental results would have been different.

**Acknowledgements:**

Financial support for this work was provided by The National Natural Science Foundation of China (31072085) and The National Basic Research Program of China (973 program, 2005 CB121000)

**References:**

[1] X.Chen, K. W. Huang and Z.Y. Shen: Acta Sericologica Sinica Vol.4 (1996), p. 229

[2] P. Z. Cai, X. Y. Xu and Z. R. Huang: Acta. Sericologica Sinica Vol. 4 (1997), p. 207

[3] B. L. Qiu, X. Y. XU and Z.M. MU: Journal of Shandong Agricultural University Vol.1 (2002), p. 14

[4] J. P. Liu, Y. Cao and J. E. Smith: Acta Sericologica Sinica Vol. 4 (2004), p. 367

[5] Y. Hatakeyama, S. Hayasaka S: JARQ Vol 36 (2)(2002), p. 97

[6] R.H. Liu, Q. B. Liu and Y.J. Wan: Hybrids Bulletin of Sericulture Vol. 40 (3) (2003), p. 86

[7] J.P.Liu, Y. Cao, J.E. Smith: Scientia Agricultura Sinica Vol. 44 (4)(2004), p. 53

[8] Z.H. Pan, X. J. Zheng, and R.Y. Xue: Acta Sericologica Sinica Vol. 48 (2)(2005), p. 90

*Advanced Materials Research Vols. 175-176 (2011) pp 13-18*

*doi:10.4028/www.scientific.net/AMR.175-176.13*

# Cloning and Expression Analysis of Acetylcholinesterase Gene (*Bm-ace*1, *Bm-ace*2) From domesticated silkworm, *Bombyx mori*

Bing Li[1,2,a], Yan-Hong Wang[2,b], Ju-Mei Wang[2,c], Wei-De Shen[1,2,d]

[1]National Engineering Laboratory for Modern Silk, Soochow University, Jiangsu 215123, China.

[2]School of Basic Medicine and Biological Sciences, Soochow University, Jiangsu 215123, China.
[a]email: Lib@suda.edu.cn, [b]email: wangyh2004@163.com, [c]email: 13771764026@139.com,
[d]Corresponding author, shenwd@suda.edu.cn

**Keywords:** *Bombyx mori*; acetylcholinesterase gene; Cloning; Gene expression.

**Abstract.** Acetylcholinesterase (AChE, 2 EC 3.1.1.7), encoded by the *ace* gene, catalyzes the hydrolysis of the neurotransmitter acetylcholine to terminate nerve impulses at the postsynaptic membrane. In this study, AChE genes (*Bm-ace*1*, Bm-ace*2) were cloned from domesticated silkworm *Bombyx mori* (Dazao strain) through RT-PCR. Sequence analysis showed that the ORF of *Bm-ace*1 gene contained 2 025 bp nucleotides, encoding 683 amino acid residues. The predicted protein has a molecular weight (MW) of 76.96 kD and an isoelectric point (pI) of 6.36; The ORF of *Bm-ace*2 gene contained 1 917 bp nucleotides, encoding 638 AA's. The predicted protein has a MW of 71.68 kD and a pI of 5.49. These two acetylcholinesterase genes both contain conserved motifs including a catalytic triad, a choline-binding site and an acyl picket. A clustering analysis showed that *Bm-ace*1 (ABY50088)shared highest similarity with *Bmm-ace*1 (ABM66370) from Chinese wild silkworm (*B. mandarina*), *Bm-ace*2 (ABY50089) shared highest similarity with *Bm-ace*2 (NP_001037366) from *B. mori*. Using semi-quantitative RT-PCR, expression analyses in insect tissues and in development period demonstrated that *Bm-ace*1and *Bm-ace*2 were expressed highly in head and fat bodies; *Bm-ace*1 and *Bm-ace*2 were expressed firstly higher, then lower and higher again from 1$^{st}$ instar to 5$^{th}$ instar stages. *Bm-ace*1 was expressed higher than that of *Bm-ace*2 in all the stages. This result will help understanding of the resistance mechanism of *B. mori* to organophosphosphorous insecticides.

## Introduction

Acetylcholinesterase (AChE, 2 EC 3.1.1.7), encoded by the *ace* gene, catalyzes the hydrolysis of the neurotransmitter acetylcholine to terminate nerve impulses at the postsynaptic membrane[1]. AChE is a target of organophosphate (OP) and carbamate (CB) insecticides[2]. The inhibition of AChE results in acetylcholine accumulation and, ultimately, death[3].

Insect AChE gene was firstly cloned from *Drosophila melanogaster* [4]. Until now, the research progress between gene mutation and AChE function mainly from *Drosophila melanogaster*. Lepidopteran insects were classified as one of the major pests. However, so far there has been no reliable evidence concerning the relationship between mutations in AChE and insecticide resistance in lepidopteran other than the mutation found in the *ace*1 of *Plutella xylostella* [5].

The domesticated silkworm, *Bombyx mori*, a member of the family *Bombycidae*, is a well-studied *Lepidopteran* model insect with rich repertoire of genetic information on mutations affecting morphology, development, and behavious [6]. It was used as a source of silk, and lost some characteristicses because of long-term breeding in artificial conditions. *B. mori* has been tamed for 5

700 years. *B. mori* had a weak resistance to insecticide, and its production was reduced by more than 30% annually because of insecticide poisoning. Organophosphorus insecticide is one of the major pesticides which were used in the farmland, it is important to study the molecular mechanisms of *B. mori* to organophosphorus pesticide.

Recently, the cDNAs of two acetylcholinesterase genes in the hybrid of *B.mori* were cloned and analyzed [7-8]. However, the strain Dazao that was used for genome project, has no information about *ace* genes, even, there are not reports about the expression characteristics of *Bm-ace*1 and *Bm-ace*2 in different tissue, different stages and pesticide poisoning. In this study, the strain Dazao was used to clone the ORF of *Bm-ace*1 and *Bm-ace*2. Furthermore, expression of the genes in different tissues, different stage and pesticide poisoning of *B. mori* was also studied. There were significant to the study of the resistance evolution of *Lepidorptera* as well as the analysis to the mechanism of pesticide resistance of insects.

## Experimental

**Insects.** The larvae of *B. mori*(Dazao strain), maintained in our laboratory, were reared on mulberry leaves under a 12-h light/12-h dark photoperiod.

Twenty grams of fresh mulberry leaves were soaked in the solution containing each working concentration of phoxim for one minute. After dried in the air, the leaves were used to rear the newly molted larvae of *B. mori* in $2^{nd}$ instar. Three independent experimental tests were done, with three repeats in each test. The mortality number of the larvae was counted after 24 hours. The living *B. mori* larvae were selected to analysis gene expression.

**Chemicals.** $T_4$ DNA ligase, plasmid extraction kit and gel Extraction Kit were the products of Shanghai Shenergy Biocolor Bioscience and Technology Company. DNA molecular weight marker, restriction enzymes, reaction buffers and other routine chemical reagents were all purchased from TAKARA Biotechonolgy(Dalian) Co., Ltd. Primers were synthesized by Shanghai Sangon Biological Techonology and Services Co., Ltd. The reagent of phoxim was purchased from Sigma-Aldrich Company.

**Extraction of total RNA and RT-PCR.** The larvae of *B. mori* on the third day of $5^{th}$ instar were dissected, and their respective hemolymph, brain tissue, midgut, fat body and silk gland were selected. In phoxim experiment, the whole bodies of larvae at newly molted and $2^{nd}$ instar phoxim experimental group were selected to test gene expression in the different stage. Total RNAs were extracted from these tissues, respectively, by using TRIzol according to instructions of the manufacturer (TAKARA Biotechonolgy (Dalian) Co., Ltd), and then stored at -70°C for use. RT-PCR was carried out by using M-MLV RTase cDNA Synthesis Kit according to instructions of the manufacturer (TAKARA Biotechonolgy (Dalian) Co., Ltd). Primers, Type P1 (5'-TTG TGG GTG TAG GTG CCA GCG ACG GTA T-3') and Type M1(5'- ACT TAT ATG GTG TAT TTG AAC AGT GCT GTG CCT GTA-3'), were designed according to sequences 26 bp upstream of and 2 029 bp downstream of ATG of *ace*1 of *B. mori* (GenBank Accession No. DQ186605), respectively, and PCR cycling conditions were as follows: 94°C for 3 min; 35 cycles of 98°C for 20 s, 68°C for 3 min 30 s; and a final extension at 72°C for 10 min. Primers, *ace*2 P2 (5'- GAA TCA CAA TGA TCA ACT ACG GCA AGA TT-3' ) and *ace*2 M2 (5'- TAC AAA GCA ATA GTG ATT GCC AAA GTG GTG-3'), were designed according to sequences 8 bp upstream of and 1 869 bp downstream of *ace*2 of *B. mori* (Accession No. DQ115792 ), respectively, and PCR cycling conditions were as follows: 94°C for 3 min; 35 cycles of 94°C for 35 s, 63 °C for 40 s, 72 °C for 150 s; and a final extension at 72°C for 10 min. With the cDNA of brain tissue of *B. mori* as template, RT-PCR was carried out.

**Expression Analysis of the genes.** The following primers for *Actin*-3 were designed: *Actin*-3 P1 (5'- AAC ACC CCG TCC TGC TCA CTG -3') and *Actin*-3 P2 (5'- GGG CGA GAC GTG TGA TTT CCT -3'). The following primers across introns were designed: 814 ace P1 (5'- CCG ACG GAT ATT TGA ACC A -3'), 814 ace P2 (5'- GTG TAG TAA TGA GGC GAA GAC C -3'), 814 ace1P1 (5'- ATG GTC GGA GAC TAT CAT TTC ACT -3') and 814 ace1 P2 (5'- GCG GCT CTG GTT TAT TGG T -3'). The cDNAs of each tissues of *B. mori* were used as templates and normalized by *actin*-3 gene, and then the expression of *ace*1 and *ace*2 was studied in the tissues of *B. mori*. PCR cycling conditions for *actin*-3 were as follows: 94°C for 2 min; 22 cycles of 94 °C for 30 s, 60 °C for 30 s, 72 °C for 30 s; and a final extension at 72 °C for 10 min. PCR cycling conditions for *ace*1 and *ace*2 were as follows: 94 °C for 2 min; 28 cycles of 94 °C for 30 sec, 52.9°C ( for *ace*1) or51.1 °C (or *ace*2) for 30 sec, 72 °C for 30 s; and a final extension at 72 °C for 10 min.

**Sequence analysis.** Sequences were analyzed by using online software (http://www.ncbi.nlm.nih.gov/blast, http://bio-soft.net/sms/ and http://npsa-pbil.ibcp.fr), and phylogenic tree was constructed by using MEGA 4.1. The amino acid sequences were used for alignment available in the GenBank..

## Results

**Cloning of *Bm-ace*1 and *Bm-ace*2 cDNAs.** With the total RNA of brain tissue of *B. mori* as template, two fragments with the length of 2 069 bp and 1 925 bp were amplified by RT-PCR, respectively (Fig. 1). These two PCR fragments were then cloned in to pUCm-T vector to obtain the following two plasmids: pUCm-Bm-ace1, pUCm-Bm-ace2. After restriction mapping with *pst* I and sequencing analysis, the correctness of *ace*1and *ace*2 gene cloning was confirmed. Sequences of the two genes *Bm-ace*1, *Bm-ace*2 have been submitted to GenBank with the following gene accession numbers: ABY50088, ABY50089, respectively.

Sequence analysis showed that *Bm-ace*1 contains a 2 025 bp ORF, which encodes a protein of 683 amino acids with predicted molecular weight of 76.96 kD and pI of 6.36; *Bm-ace*2 contains a 1 917 bp ORF, which encodes a protein of 638 amino acids with predicted molecular weight of 71.68kD and pI of 5.49, respectively. Both ace genes contain the enzymic characteristic domains.

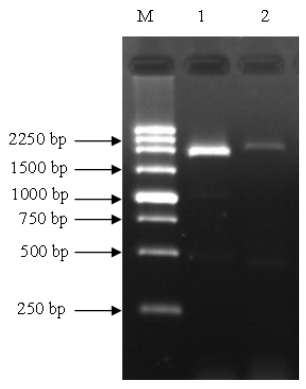


Fig. 1 The results of RT-PCR of *Bm-ace*1 and *Bm-ace*2 genes.
M.DNA molecular weight mark, 1.*Bm-ace*2,

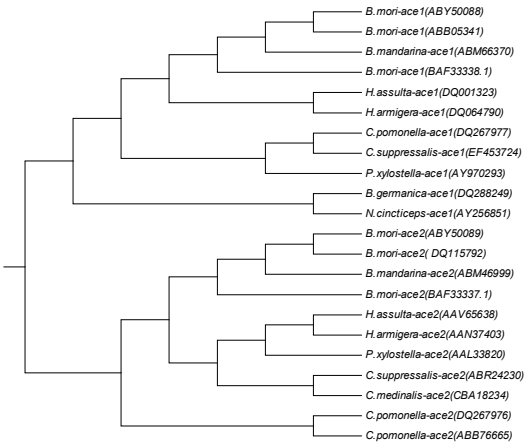


Fig.2 Unrooted phylogenetic tree of the insect *ace* constructed by the neighbor-joining method.

**Phylogenetic analysis.** Phylogenetic analysis showed that *Bmm-ace*1 and *Bmm-ace*2 had the closest genetic relationship with *Bm-ace*1 and *Bm-ace*2, respectively, with amino acid identity of 99.71 % and 99.37 %, respectively (Fig. 2). *Bmm-ace*1 and *Bmm-ace*2 showed only 30.82% identity. Compared with *ace*1, *ace*2 was more evolutionally conserved. These results indicated that *ace*2 might be closely related to insecticide resistance.

**Gene expression analysis.** *Gene expression in tissues.* By RT-PCR assay, the results showed that *Bm-ace*1 was highly expressed both in brain and fat bodies. However, the former was with minor expression while the latter without detectable expression in midgut. *Bm-ace*2 was expressed in the five tissues tested with high expression in brain and fat bodies(Fig. 3).

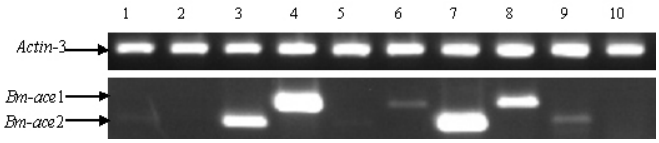


Fig.3 Tissue expression profile of *Bm-ace*1 *and Bm-ace*2 from *B. mori* by semi-quantitative RT-PCR

1,2.hemolymph; 2.brain; 3.midgut; 4.fat body 5.silk gland

*Gene expression in each instar.* The expression patterns of *ace*1 and *ace*2 genes at different development stages in all the five larval instar, were investigated by using semi-quantitative RT-PCR method. The results showed that the expression of *Bm-ace*1 and *Bm-ace*2 decreases first, then increases then from 1st instar to 5th instar stage, with the lowest expression of *Bm-ace*1 at the 3rd instar, and *Bm-ace*2 at 2nd instar (Fig.4).

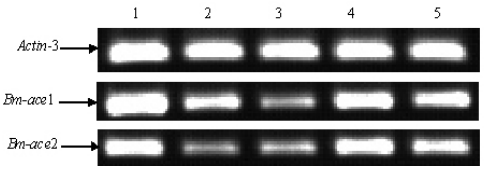


Fig.4 Development expression analysis of ace genes from *B. mo*ri of different instar

1.1st instar; 2.2nd instar; 3.3rd instar; 4.4th instar; 5th instar

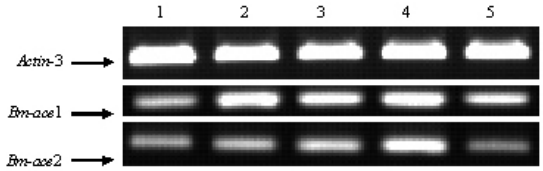


Fig. 5 Expression analysis of *Bm-ace*1and *Bm-ace*2 induced by phoxim of different concentrations

1.CK; 2. 200 ng/mL; 3.238 ng/mL; 4.283 ng/mL;

The expression of the genes after stimulation of the reagent phoxim The results of the inductive expression by phoxim showed that below the value of $I_{50}$, ($LC_{50}$=314 ng/mL) the expression of *aec*1 and *ace*2 genes increased along with the concentrations of phoxim.When phoxim was applied at higher concentrations than $I_{50}$, the expression of *ace*1 and *ace*2 decreased in *B. mori*(Fig. 5).

## Discussion

**Cloning of *Bm-ace1* and *Bm-ace2.*** *B. mori* is rich in variety resources. Their genetic backgrounds are different at certain degree. China and Japan have conducted exploring investigation using their own *B. mori* variety resources [3, 7]. These studies are of importance for further in-depth studies on *Bm-ace*1 and *Bm-ace*2. Since China initiated *B. mori* genome project, its 9x genomic draft map has been completed. In this project, the representative experimental *B. mori* variety Dazao was used. Our group first cloned the ORF of *Bm-ace*1 and *Bm-ace*2 using Dazao as the DNA source. This is

of great significance for directly reference *B. mori* genomic information and in-depth studies on its genetic structure and function.

**Evolutionary analysis and origin of *B. mori.*** The existing study has shown that *ace*2 is relatively conservative among species of *Lepidoptera*. In this study, evolutionary analysis of amino acid sequences encoded by *ace*2 genes of *Saturniidae* published in Genbank indicates that both Chinese and Japanese *B. mori* are originated from Chinese wild silkworm (*B. mandarina*), in consistence with previous report [8]. To our knowledge, this is the first report on the *B. mori* origin based on the evolution of *ace*.

***Bm-ace*1 and *Bm-ace*2 expression in different tissues.** The results showed that *Bm-ace*1 and *Bm-ace*2 are highly expressed in brain and fat bodies. Brain tissue is the central nervous system of *B. mori* and an important composition of nerve transduction. Since AChE is mainly present in the synaptic cleft during synaptic transmission, it is reasonable that *ace* is largely expressed in brain tissue. Fat body is an important organ for detoxification of organic phosphorus pesticide. When *B. mori* is poisoned by organic phosphorus pesticide, some of the pesticides are directly excreted, some are decomposed by fat bodies, and the remaining is mainly stored in the fat bodies. High expression level of *Bm-ace*1 and *Bm-ace*2 in fat bodies may be a physiological defense mechanism of *B. mori*. In addition, the expression of *Bm-ace*1 in brain is higher than that of *Bm-ace*2. By contrast, the expression of *Bm-ace*2 in fat bodies is higher than that of *Bm-ace*1. It needs to be further investigated if *Bm-ace*1 and *Bm-ace*2 have different physiological functions in brain and fat bodies.

**Expression of *Bm-ace*1 and *Bm-ace*2 at developmental stages.** The expressions of both *Bm-ace*1 and *Bm-ace*2 in 1$^{st}$ instar larvae are relatively high, which then gradually decrease in 2$^{nd}$ to 3$^{rd}$ instar larvae and increase again in 4$^{th}$ to 5$^{th}$ instar. The main reason for the higher expression of *ace* in 1$^{st}$ instar larvae is that 1$^{st}$ instar have higher proportion of head and body. Therefore, the higher expression of *Bm-ace*1 and *Bm-ace*2 in brain can result in their higher expression in the whole body sample. Our results are in consistent with the previous report of Shang [3] published in 2007 on AChE activity. As the instar increases, the constantly accumulated fat body in *B. mori* may lead to increase of *Bm-ace*1 and *Bm-ace*2 expression. In addition, the expression of *Bm-ace*1 is higher than that of *Bm-ace*2, which may implicate that *Bm-ace*1 plays a more important role than *Bm-ace*2 in *B. mori*, in agreement with the report of DW Lee published in 2006 [9].

**Phoxim induced expression of *Bm-ace*1 and *Bm-ace*2.** In this study, 2$^{nd}$ instar larvae were fed with pesticide phoxim with different concentrations. 24 h later, the expressions of *Bm-ace*1 and *Bm-ace*2 were examined. The results indicate that at low pesticide concentrations, *B. mori* express more ace mRNA and synthesize more AChE protein to alleviate the damage caused by phoxim-induced inhibition of AChE activity. On the other hand, high concentrations of pesticide can cause disorder of basic physiological function and consequently result in the decline of *Bm-ace*1 and *Bm-ace2* expression. The alteration of *Bm-ace*1 and *Bm-ace*2 expression induced by pesticide poisonousness shows the same pattern, indicating that the basic functions of *Bm-ace*1 and *Bm-ace*2 are same. But the alteration of *Bm-ace*2 expression is more dramatic compared with that of *Bm-ace*1, which suggests that they are regulated by different mechanisms. The interaction of *Bm-ace*1 and *Bm-ace*2 is worth in-depth study.

**Acknowledgments**

This work was supported by Project 31072086 supported by the National Natural Science Foundation of China and the National High Technology Research and Development Program of China (863 Program) (2006AA10A118).

**References:**

[1] D. Fournier, A. Mutero, Comparative Biochemistry and Physiology Part C: Pharmacology, Toxicology and Endocrinology Vol. 108, Issue 1, May (1994), p. 19

[2] F. Matsumura, Toxicology of Insecticides, second. Plenum Press, New York (1985).

[3] J. Y. Shang, Y. M. Shao and G. J. Lang, Insect Science, 14 (6) (2007), p. 443

[4] L. M. Hall, P. Spierer, EMBO J Vol. 5 (1986), p. 2949

[5] J. H. Baek, J. I. Kim and D. W. Lee, Pestic. Biochem. Physiol Vol. 81 (2005), p.164

[6] B. L. Astaurov, M. D. Golysheva and I. S. Rovinskaya, Cytology Vol.1 (1959), p. 327

[7] A. Seino, T. Kazuma and A. J. Tan, Pesticide Biochemistry and Physiology Vol. 88 (2007), p. 92

[8] C. Lu, H. S. Yu and Z. H. Xiang, Science agriculture sinica Vol. 35(1) (2002), p.94

[9] D.W. Lee, S. S. Kim and S. W. Shin, Biochimica et Biolhysica Acta Vol.1760 (2006), p.125

*Advanced Materials Research Vols. 175-176 (2011) pp 19-24*

*doi:10.4028/www.scientific.net/AMR.175-176.19*

# Transcriptional Expression of *Serpin-6* Gene in *Bombyx mori* Larval after Infection of Bacteria at Different Developmental Stages

Hongxian Zha [1,2,a] , Yanfang Yu [1,2,b] , Yanyun Wang [1,2,c], Shanshan Sun[1,2,d], Zhengguo Wei[1,2,e], Bing Li[1,2,f] ,Yuhua Chen[1,2,g], Yaxiang Xu [1,2,h] Weide Shen [1,2,i]

[1]National Engineering Laboratory for Modern Silk, Soochow University, Suzhou 215123, China

[2]School of Basic Medicine and Biological Sciences, Soochow University, Suzhou 215123, China

[a]mtvtlc@163.com, [b]youyouyu325@163.com, [c]yyw1985914@163.com,

[d]ddycysss@yahoo.com.cn, [e]szwei2002@126.com, [f]sdlibing@hotmail.com,
[g]chenyh@suda.edu.com, [h]Corresponding author, szdxxyx@163.com, [i]shenwd@suda.edu.cn

**Key words:** *Bombyx mori*;*Serpin-6*, transcription;Immunostimulatory;Semi-quantitative RT-PCR.

**Abstract.** Serpins can block different steps in the activation cascade of *prophenoloxidase* (proPO) system, and play an important role in immunity of insect. In this paper, Haemolymph was collected from the 4th molting, newly moulted 5th instar and day-3 fifth instar larval challenged by lipopolysaccharide (LPS) or Bacillus thuringiensis, respectively. The results revealed that the transcriptional level of *Bmserpin-6* in different developmental stages showed a trend of rise first, then fall. *Bmserpin-6* of the 4th molting larva expressed highest at 6h post-infection with LPS and 3h post-infection with Bacillus thuringiensis. *Bmserpin-6* of newly moulted 5th instar larva expressed highest at 9h post-infection with LPS and 6h post-infection with Bacillus thuringiensis. *Bmserpin-6* of day-3 fifth instar larva expressed highest at 9h post-infection with Bacillus thuringiensis. *Bmserpin-6* was all highly induced and highly expressed in haemolymph of larval at different developmental stages. But The time to arrive the highest transcriptional level was different. This is inferred that the Serpin gene may play an important role in immunity of *Bombyx mori*.

## Introduction

Serpins are a superfamily of proteins, most of which control protease-mediated processes by inhibiting their cognate enzymes. Serpin-like genes have been identified in animals, poxviruses, plants, bacteria and archaea. Serpins are central factor in controlling many important proteolytic cascades, including the prophenoloxidase (proPO) system activation cascade[1-3]. Serpins have been purified and cloned from insects including *Bombyx mori*[4-5], *Manduca sexta*[6-10], *Drosophila melanogaster*[11], *Anopheles gambiae*[12], *Mythimna unipuncta*[13]and *Aedes aegypti*[14].

Melanization is an important immune response in many invertebrates. Certain microbial products (e.g. peptidoglycans, lipopolysaccharides or b-1,3-glucans) are bound by host recognition proteins. It initiates a serine proteinase cascade that leads to the conversion of zymogenic proPO into catalytically active phenoloxidase and ultimately results in the generation of cytotoxic products and

encapsulation of the pathogen[15-16]. Several controlling mechanisms have already been elucidated. Among them, the function of clip-domain serine protease homologs (SPHs) appears to be most intriguing and somewhat controversial at present [17]. Excessive cytotoxic products may be harmful to the host, and polyphenol oxidase activity was negatively correlated with silkworm cocoon weight, cocoon shell weight and pupal weight[18]. Therefore, to minimize possible cytotoxicity of quinones to host tissues and cells, protease inhibitors, such as serpins, are involved in preventing premature and excessive activation. Serpin and SPHs mediate and regulate the melanization together, not only eliminate the invading pathogens but also protect the host itself.

There were many studies about the relations between serpins and insect immune. *Bombyx mori* is a biochemical and molecular research model of Lepidoptera insects. It is known that there are always five instars for silkworm larval. The larval should grow through molting to be the next instar. It undergoes significant physiological and biochemical changes during the molting. The molting and newly moulted larval are more susceptible to pathogen infection than larval at other developmental stages. There were no studies about transcriptional expression profile of serpin gene in molting or newly molted larva insects post-infection. In this paper, we investigated the transcriptional expression profile of *serpin-6* gene in molting and newly molted silkworm post-infection by semi-quantitative RT-PCR. The result provided the references for studying immune defense of Bombyx mori and other Lepidoptera insects.

## Materials and methods

**Insects and collection of haemolymph.** *B. mori* (Dazao) larvae were reared with mulberry at routine conditions. The 4th molting larve, newly moulted 5 th instar larvae and day-3 fifth instar larvae were injected with LPS (lipopolysaccharide ,10 μL, 1mg/mL,SIGMA,) or Bacillus thuringiensis ($1\times10^5$ cells in 10μL PBS buffer ) respectively. Haemolymph were collected from the injected and control larvae 3,6,9,12 ,24 h post-infection. The larvae injected with Bacillus thuringiensis were all died at 24h after injection.

**RNA extraction and cDNA synthesis.** Total RNAs were extracted from haemolymph of control and induced *B. mori* larvae using RNAiso reagent (TaKaRa) according to the manufacturer's instructions. First-strand cDNA synthesis was performed using M-MLV RTase cDNA Synthesis Kit (TaKaRa) according to the manufacturer's instructions.

**Reverse transcription (RT)-PCR analysis.** *B. mori actin-3* cDNA was used as an internal standard to normalize the templates in a preliminary PCR experiment. After template adjustment, PCRs were performed to detect relative levels of *serpin-6* cDNAs using the primers *serpin6*-F(5'-GTACCCGATGACAACATATTCTT-3) and *serpin6*-R (5'-GAGACACCCAGCTATT GATGTAG-3') as previously described[19] . The thermal cycling conditions for *actin-3* were: 94 °C, 30 s; 60 °C, 30 s; 72 °C, 30 s. The thermal cycling conditions for *serpin-6* were: 94 °C, 30 s; 54 °C, 30 s; 72 °C, 30 s. PCR cycle numbers were empirically chosen to show comparable band intensity and avoid saturation. After separation by 1.2% agarose gel electrophoresis, intensities of the PCR products were quantified and compared using Tanon Gel Analysis Software.

## Results

**Time-course expression of *Bmserpin*-6 in haemocytes of 4th molting larval stimulated by LPS.** *Bmserpin-6* was highly induced in haemolymph of 4th molting larval after injecting with LPS. The transcriptional level of *Bmserpin-6* changed significantly after injection, showed a trend of rise first, then fall. The highest expression was at 6 h after injection(Fig. 1).

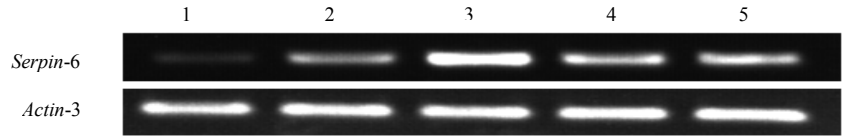


1. CK; 2. 3h post LPS-challenged; 3. 6h post LPS-challenged; 4. 12h post LPS-challenged; 5. 24h post LPS-challenged

Fig. 1 Time-course expression of *Bmserpin*-6 in haemocytes of 4th molting larval stimulated by LPS

**Time-course expression of *Bmserpin*-6 in haemocytes of newly moulted 5th instar larva stimulated by LPS.** The transcriptional level of *Bmserpin-6* changed significantly after injection, showed a trend of rise first, then fall. The highest expression was at 9 h after injection. The transcriptional level at 24h post-infection was slightly higher than control (Fig. 2).

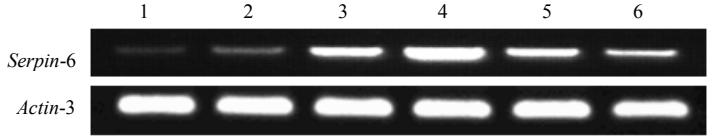


1. CK; 2. 3h post LPS-challenged; 3. 6h post LPS-challenged; 4. 9h post LPS-challenged; 5. 12h post LPS-challenged; 6. 24h post LPS-challenged

Fig. 2 Time-course expression of *Bmserpin*-6 in haemocytes of newly moulted 5th instar larva stimulated by LPS

**Time-course expression of *Bmserpin*-6 in haemocytes of 4th molting larva stimulated by Bt.** The 4th molting larval showed obvious symptoms 12h post-infection of *B. thuringiensis*. All injected larvae died at 24 h post-infection. The transcriptional level of *Bmserpin-6* changed significantly after injection, showed a trend of rise first, then fall. The highest expression was at 3h after injection(Fig. 3).

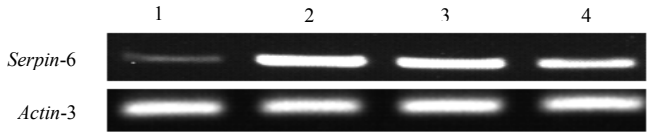


1. CK; 2. 3h post Bt-challenged; 3. 6h post Bt-challenged; 4. 12h post Bt-challenged

Fig. 3 Time-course expression of *Bmserpin*-6 in haemocytes of 4th molting larva stimulated by Bt

**Time-course expression of Bmserpin-6 in haemocytes of newly moulted 5th instar larva stimulated by Bt.** The newly moulted 5th instar larval injected with *B. thuringiensis* showed obvious symptoms at 12h post-infection. All injected larvas died at 24 h of infection. The transcriptional level of *Bmserpin-6* changed significantly after injection, showed a trend of rise first, then fall. The highest expression was at 6h after injection, which decreased dramatically to the control level between 9 to 12 hour post-infection (Fig. 4).

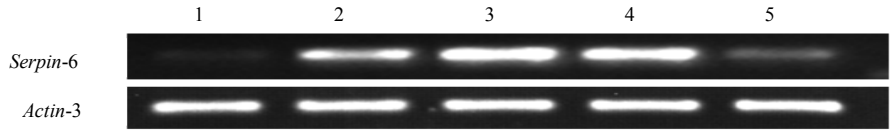


1. CK; 2. 3h post Bt-challenged; 3. 6h post Bt-challenged; 4. 9h post Bt-challenged; 5. 12h post Bt-challenged

Fig. 4 Time-course expression of Bmserpin-6 in haemocytes of newly moulted 5th instar larva stimulated by Bt

**Time-course expression of *Bmserpin*-6 in haemocytes of the third day of 5th instar larva stimulated by Bt.** The third day of 5th instar larval injected with *B. thuringiensis* showed not as obvious symptoms as the molting larval or the newly moulted larval at 12h post-infection. But all the injected larvae died 24 h post-infection. The transcriptional level of *Bmserpin-6* showed a trend of rise first, then fall. The highest expression was at 9h after injection, which decreased slightly later(Fig. 5).

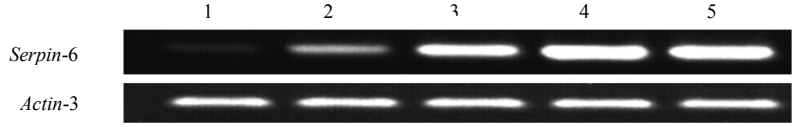


1. CK; 2. 3h post Bt-challenged; 3. 6h post Bt-challenged; 4. 9h post Bt-challenged; 5. 12h post Bt-challenged

Fig. 5 Time-course expression of *Bmserpin*-6 in haemocytes of the third day of 5th instar larva stimulated by Bt

**Discussion**

Serpins regulate the immune defense response by inhibiting serine protease cascade, which is important for normal life activity of insects. Biochemical investigations suggested that most serpins in hemolymph can regulate plasma proteases and its expression level would be higher after stimulation, revealed physiological functions of serpins. For instance, *D .melanogaster serpin-28D* was the strongest induced serpin gene with a peak of about 20-fold induction 1.5 h after injury[20], *M. sexta serpin-2* gene expression increased dramatically after larvae were injected with Micrococcus lysodeikticu[8].*M. sexta serpin-3* is constitutively present in haemolymph at a low concentration of 5-12 mg/ml and increases to 30-75 mg/ml after a microbial challenge[9]. *M. sexta Serpin-4* and *Serpin-5* inhibit PPO cascade activation in the haemolymph, serpin-protease complexes formed after activation of the cascade by exposure of plasma to bacteria or lipopolysaccharide[10]. *M. sexta Serpin-6* is constitutively present in haemolymph of native larvae, and its mRNA and protein levels significantly increase after a bacterial injection[21].For *B.mori*, the mRNA levels of *serpin1, 3, 5, 6, 9, 12, 13, 25, 27, 32* and *34* in fat body and haemocytes increased after larvae were injected with bacteria.

Liu et al. [19] found that *Bmserpin-6* was highly induced and it was highly expressed in the fat body and haemolymph, and the highest expression was at 6 h after injection. Another study revealed that *B.mori* serpin gene showed that *Bmserpin-6* was strongly activated by E. coli and B. subtilis but not by *S. aureus*[22].In this paper, we studied the transcriptional expression profile of *serpin-6* gene of *B.mori* larval after infection at different developmental stages. The result showed that the transcriptional level of *Bmserpin-6* of different stages showed a trend of rise first, then fall. *Bmserpin-6* of the 4th molting larval expressed highest at 6h post-infection with LPS and 3h post-infection with *B.thuringiensis*. *Bmserpin-6* of newly molted 5th instar larval expressed highest at 9h post-infection with LPS and 6h post-infection with *B. thuringiensis*. *Bmserpin-6* of day-3 fifth

instar larval expressed highest at 9h post-infection with *B. thuringiensis*. Overall, *Bmserpin-6* was all highly induced and highly expressed in haemolymph of larvae at different developmental stages and the time to arrive the highest transcriptional level was different. These results were consistent with physiological characteristics of silkworm, as the resistance and susceptibility of larval at different developmental stages are different. The molting and newly molted larval are more susceptible to stimulation. 12 hours after injection with *B. thuringiensis*, all larvae showed obvious infection symptoms, the normal physiological mechanism of the larval may have been seriously damaged, so the transcriptional expression level of *Bmserpin-6* dramatically decreased.

In conclusion, the relationships between *Bmserpin-6* and immune response of *Bombyx mori* were investigated from a new perspective. The results suggest that the serpins play regulatory roles in defense responses. A more in-depth study using the recombinant *serpin-6* is necessary to study its substrate specificity and to see if it is involved in the regulation of the prophenoloxidase cascade.

**Acknowledgments**

This work was supported by The National High Technology Research and Development Program of China (863 Program) (2006AA10A118).

**References**

[1] R. HP. Law, Q. W. Zhang, S. McGowan, A. M. Buckle, G. A. Silverman, W. Wong, C. J. Rosado, C. G. Langendorf, R. N . Pike, P. I. Bird and J. C. Whisstock: Genome Biology. Forum Vol. 7(2006), p. 216

[2] J. A. Irving, R. N. Pike, A. M. Lesk and J. C. Whisstock: Genome Res. Forum Vol. 10(2000), p. 1845

[3] G. A. Silverman, P. I. Bird, R. W. Carrell, F. C. Church, P. B. Coughlin, P. G. W. Gettins, J. A. Irving, D. A. Lomas, C. J. Luke, R. W. Moyer, P. A. Pemberton, E. Remold-O'Donnell, G. S. Salvesen, J. Travis and J. C. Whisstockc: Biological Chmistry. Forum Vol. 36(2001), p. 33293

[4] T. Sasaki, K. Kobayashi: Biochem. Forum Vol. 95(1984), p. 1009

[5] T. Sasaki: Eur. Biochem. Forum Vol. 202(1991), p. 255

[6] M. R. Kanost, S. V. Prasad, M. A. Wells: Biol. Chem. Forum Vol. 264(1989), p. 965

[7] H. B. Jiang, M. R. Kanost: Biol. Chem. Forum Vol. 272(1997), p. 1082

[8] H. Gan, Y. Wang, H. B. Jiang, K. Mita and M. R. Kanost: Insect Biochem. Mol. Biol. Forum Vol. 31(2001), p. 887

[9] Y. Zhu, Y. Wang, M. J. Gorman, H. B. Jiang and M. R. Kanost: Biol. Chem. Forum Vol. 278(2003), p. 46556

[10] Y. Tong, H. B. Jiang and M. R. Kanost: Biol. Chem: Forum Vol. 280(2005), p. 14932

[11] E. De Gregorio, SJ. Han, WJ. Lee, MJ. Baek, T. Osaki, S. I. Kawabata, BL. Lee, S. Iwanaga, B. Lemaitre and P. T. Brey: Developmental Cell. Forum Vol. 3(2002), p. 581

[12] A. Danielli, F. C. Kafatos and T. G. Loukeris: Biol. Chem. Forum Vol. 278(2003), p. 4184

[13] A. Cherqui, N. Cruz and N. Simoes: Insect Biochem. Mol. Biol. Forum Vol. 31(2001), p. 761

[14] K. R. Stark, A. A. James: Biol. Chem. Forum Vol. 273(1998), p. 20802

[15] M. Ashida, P. T. Brey: Proc. Nal. Acad. Sei. USA. Forum Vol. 31(1995), p. 10698

[16] L. Cerenius, B. L. Lee and K. Sderhll: Trends in Immunology. Forum. Vol. 29(2008), p. 264

[17] S. Gupta, Y. Wang and H. B. Jiang: Insect Biochem. Mol. Biol. Forum Vol. 35(2005), p. 241

[18] D. S. Li, E. J. Ling, A. M. Wang: Chinese sericulture. Forum Vol. 24(2003), p. 37

[19] Liu C L, Wang D, Li B, J. M. Guan,Y. F. Yu, H. X. Zha, Y. X. Xu and W. D. Shen: Aeta Entomologica Sinica. Forum Vol. 52(2009), p. 1

[20] C. Scherfer, H. P. Tang, Z. Kambris, N. Lhocine , C. Hashimoto and B. Lemaitre: Developmental Biology. Forum Vol. 323(2008), p. 189

[21] Z. Zou, H. B. Jiang: Biol. Chem. Forum Vol. 280(2005), p. 14341

[22] Z. Zhen, P. Zhao, W. Hua, K. Mita and H. B. Jiang: Genomics. Forum Vol. 93(2009), p. 367

*Advanced Materials Research Vols. 175-176 (2011) pp 25-29*

*doi:10.4028/www.scientific.net/AMR.175-176.25*

# Separation and Identification of Proteins Related to Fruits Ripening in Mulberry (*Morus alba*)

Wenqian Liu[1,a], Lili Zhou[1,b], Mei Su[1,c], Xujuan Chi[1,d], Jianzhong Tan[1,2, e*]

[1]Department of Horticulture, Soochow University, Suzhou Jiangsu, 215123 China

[2]Institute of Sericulture, Soochow University, Suzhou Jiangsu, 215123 China

[a]liu_wq@163.com, [b]wojiayou_2008@126.com, [c]sumei.1212@163.com

[d]lgsg163@163.com, [e]Corresponding author, szutjz@hotmail.com

**Key words:** Mulberry fruits; Ripening stage; Differential proteome; Cell wall invertase.

**Abstract.** To elucidate the physiological mechanism of mulberry fruit ripening in protein level, differential proteome expression of mulberry fruits was analyzed by using 2-DE and mass spectrometry in different ripening stages, green ripe stage(G), half ripe stage(R) and pan ripe stage(P). A mulberry cultivator, "Da10" was used as experimental material. The results showed that separation of proteins with 2-DE were significantly improved by using phenol/SDS buffer for protein extraction. 441, 222, 328 protein spots were detected respectively in ripening stage G, R and P. Among them, differential expression of 31 proteins was more than 2-fold and 6 proteins were stage-specific expression. 8 differential proteins were identified by MALDI-TOF/TOF MS analysis and database search, which were photosynthesis related proteins (ribulose bisphosphate carboxylase/oxygenase activase and ribulose bisphosphate carboxylase small subunit), stress related protein (18kD winter accumulating protein), glucose metabolism related protein (cell wall invertase) and so on, suggesting that these proteins may play the specific physiological role in mulberry fruits ripening.

## Introduction

Changes in morphological characteristics, physiology and biochemistry are significant during fruit ripening, involving gene expression and proteome differential expression. In some fruits, such as tomato, peach, strawberry, banana, grape, and pear, proteome studies have been reported in protein extraction [1-3], 2-DE technology [4,5] and fruit development and ripening related proteins [6,7]. However, so far, there are still no related results shown in mulberry fruit.

Mulberry fruit is nourishing and high economic value, but it softens quickly after ripening, which is difficult in its storage, and transporting. Until now, there are no effective preservation techniques to resolve the problem. The understanding of mulberry fruit ripening and its regulation mechanism in molecular level will be helpful to develop new ways on mulberry ripening regulation and preservation. In this study, protein changes during mulberry fruit ripening were analyzed using differential proteomics technology and meaning results were obtained.

## Materials and methods

**Plant material.** Mulberry fruits of cultivator "Da 10" were picked at the different stages from mulberries in good growth vigor in May 2008, immediately put in low temperature condition, and then stored in -70°C, as experimental material.

**Two dimension electrophoresis of proteins.** Mulberry fruit proteins were extracted by phenol/ SDS buffer referred Wang[1] and dissolved in protein sample buffer (6 $mol \cdot L^{-1}$ urea, 2 $mol \cdot L^{-1}$ thiourea, 2% CHAPS, 0.5% IPG Buffer, 15 $mmol \cdot L^{-1}$ DTT). The total protein concentration was determined according to Bradford method and used for IPG-IEF/SDS-PAGE(2-DE).

Isoelectric focusing (IEF) was performed using IPG strips with nonlinear pH range of 3-10, 17cm. The IPG strips were rehydrated with 350μL of rehydration buffer (6 $mol \cdot L^{-1}$ urea, 2 $mol \cdot L^{-1}$ thiourea, 2% CHAPS, 0.5% IPG Buffer, 15 $mmol \cdot L^{-1}$ DTT, 0.002% bromophenol blue) containing 1mg protein. Isoelectric focusing was conducted in the IEF cell (GE Healthcare) according to the operation instruction. After IEF, strips were equilibrated for 15min in 0.05 $mol \cdot L^{-1}$ Tris-HCl (pH8.8), 6 $mol \cdot L^{-1}$ urea, 30% glycerol, 2% SDS, buffer containing 1% DTT then for 15min in the same buffer containing 1.25% iodoacetamide. Subsequently SDS-PAGE second dimension was performed and the gels were stained with Coomassie Brilliant Blue R-250.

**2-DE image analysis.** Following staining, 2-DE gel patterns were scanned by Image scanner (GE Healthcare) and analyzed using Image Master 2D Platinum 5.0 (GE Healthcare) which allows spot detection, matching and spot 3-D image analysis. The intensity of every spot was expressed as the ratio of the total intensity of the gel image.

**Mass spectrometry identification.** The aim spots were cut from gels and analyzed by MALDI-TOF/TOF MS (4800 Plus MALDI TOF/TOFTM, ABI) after digesting with trypsin for 20 hours, concentrating and desalting using ZipTip. According to MS/MS data analysis, MS/MS Ion Search of NCBInr was searched by Matrix Science software in order to identify protein types of each component in which the error of peptide and MS/MS was 100ppm and 0.8Da and others were analyzed using universal rule and standards.

## Results

**Analysis of differential proteome during mulberry fruits ripening by 2-DE**. The color of mulberry fruits changed greatly during ripening. In appearance the mulberry fruit experiences from green at ripening initiation to red and inherent color of the cultivator, accordingly, it can be divided into three stage - green ripe stage (green mulberry fruit), half ripe stage (red mulberry fruit) and full ripe stage (purple mulberry fruit).

IPG-IEF/SDS-PAGE was conducted with mulberry fruit protein extracted in different ripening stages. Analyzed by 2D image analysis software, 441, 222, 328 protein spots (Fig. 1) were detected respectively from 2-DE maps of green ripe stage, half ripe stage and full ripe stage and 31 protein components were detected to express differentially more than twice in which 15 were up-regulated and 16 were down-regulated. According to the differential analysis of protein expression level in different stages, 6 change types were classified as follow: (Ⅰ) continuous increase (4 spots), (Ⅱ) continuous decrease (9 spots), (Ⅲ) first increase, then decrease, totally increase (6 spots), (Ⅳ) first increase, then decrease, totally decrease (4 spots), (Ⅴ) first decrease, then increase, totally increase (5 spots), (Ⅵ) first decrease, then increase, totally decrease (3 spots). Additionally, 6 spots showed characteristic of stage-specific expression.

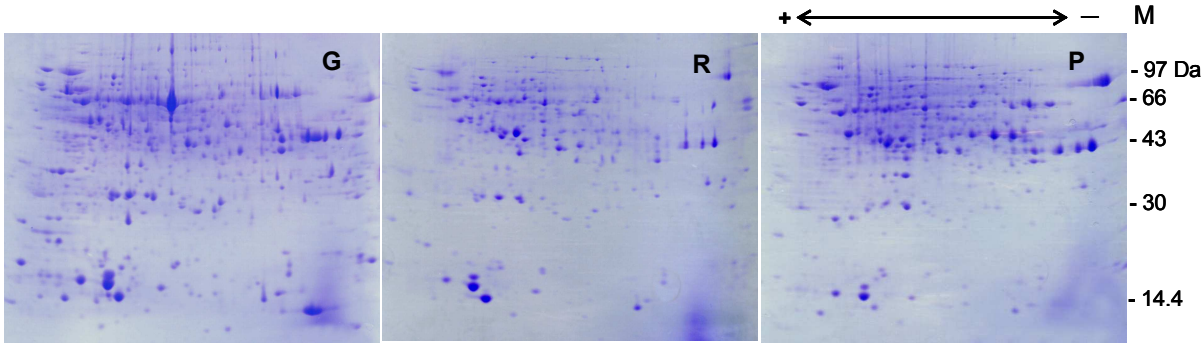


G: Green ripe stage, R: Half ripe stage, P: Full ripe stage; M: protein marker

Fig. 1 The 2-DE separation of mulberry fruit proteins in different ripening stages

**MS identification of differential proteins in mulberry fruit ripening**. 8 of 15 protein spots which were great differential expression and specific expression were identified by MS analysis (Fig. 2, Table 1). They were photosynthesis relative proteins (ribulose bisphosphate carboxylase/oxygenase activase and ribulose bisphosphate carboxylase small subunit), whose expression level reduced in mulberry fruit ripening. 3 isoforms of 18 kD winter accumulating protein were stress relative proteins and their expression level also reduced in mulberry fruit ripening. In contrast the expression level of glucose metabolism-related protein (cell wall invertase, CWI) increased in mulberry fruit ripening. And the function of the soybean protein induced by salicylic acid has not been known clearly so far. The results suggested that these proteins above were considered to be associated with mulberry fruits ripening, though it has still been unknown if they were ripening-inducing factors of mulberry fruit or induced by mulberry fruit ripening.

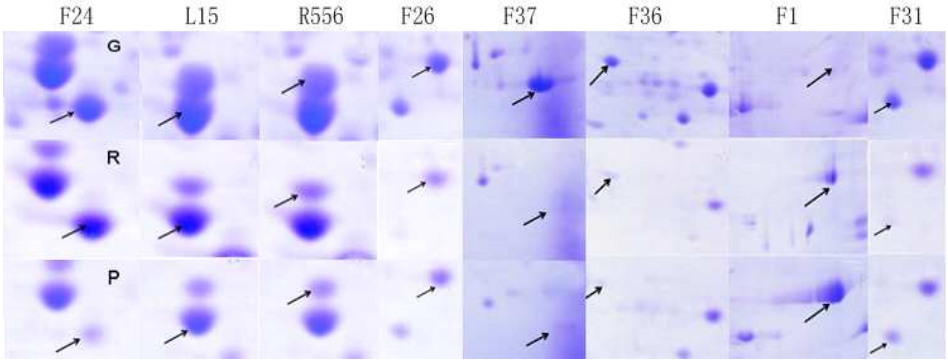


G: Green ripe stag, R: Half ripe stage, P: Full ripe stage

Fig. 2 The differential expressed proteins during mulberry fruits ripening

Table 1 The identification results of differential proteins during mulberry fruit ripening

| Spots | Differential expression | | | Protein naim | Theoretical Mr/pI |
|---|---|---|---|---|---|
| | G | R | P | | |
| F24 | +++ | ++ | + | Ribulose bisphosphate carboxylase/oxygenase activase [*Solanum pennellii*] | 50897/9.12 |
| L15 | ++ | + | + | Ribulose bisphosphate carboxylase small chain [*Musa acuminat*] | 20839.3/9.23 |
| F31 | ++ | — | + | ribulose bisphosphate carboxylase activase [*Nicotiana tabacum*] | 48541/5.48 |
| R556 | +++ | ++ | + | 18 kD winter accumulating protein B[*Morus bombycis*] | 16726.5/5.35 |
| F26 | +++ | + | ++ | 18 kD winter accumulating protein A[*Morus bombycis*] | 16741.5/5.18 |
| F37 | + | — | — | 18 kD winter accumulating protein C[*Morus bombycis*] | 16619/5.36 |
| F1 | — | + | ++ | cell wall invertase precursor[*Fragaria×ananassa*] | 65131.4/9.15 |
| F36 | + | — | — | Gm_ck32857 soybean induced by salicylic acid [*Glycine max*] | 22376/5.32 |

Note: +/- meant the expression level of the identified proteins in ripening G, R and P

## Discussion

Mulberry fruit is classified as special fruit with abundant nutrition and medicinal value, but study on mulberry fruit ripening related genes and proteins has not been reported so far. By using 2-DE and mass spectrometry, differential expressed proteome of mulberry fruit was analyzed in different ripening stages. 31 proteins were detected to express differentially more than 2-fold in green ripe stage, half ripe stage and full ripe stage and 6 proteins were stage-specifically expressed. Among them, 8 proteins were identified which laid a foundation in further study molecular mechanism of mulberry fruit ripening.

It is well known that ribulose bisphosphate carboxylase activase (RAC) is a soluble chloroplast protein encoded by nuclear gene. It is the key enzyme in photosynthetic carbon assimilation of all higher plants and took part in photosynthesis and photorespiration. RCA is only expressed in green tissue such as apple leaves[8], rice leaves and shoots[9], arabidopsis thaliana leaves, shoots, flowers and silique, but it is not expressed in roots and etiolated seedlings[10].

In this study, besides green mulberry fruit, RCA protein components were also detected to exist in red and purple mulberry fruit. Additionally, molecular weight of these components was only half of theoretically predicted value and their expression level decreased with mulberry fruit developing, which inferred these differential protein components might be the peptides from RCA degradation. This phenomenon was also reported in proteome study on rice salt stress and low temperature stress, and the most obvious degradation was directly photosynthesis related proteins which besides RCA, it contained large subunit of rubisco and α-subunit and β-subunit of ATP synthase.

Mulberry fruit ripening is virtually supposed to be a program senescence process whose physiological and biochemical metabolism was similar to adversity-stressed change. In this study, the expression level of small subunit of rubisco precursor was truly reduced with mulberry fruit developing, inferred the degradation of photosynthesis related proteins. Further more, low

temperature stress related proteins were detected, such as spots R556, F26, F37 identified to be isoforms of 18 kD winter accumulating protein [11], whose expression changing trend similar to it of RCA protein and small subunit of rubisco. These changes showed some metabolism characteristic similar to adversity stress.

Previous studies have demonstrated that cell wall invertase (CWI) had multiple physiological functions in plants and may participate fruit ripening. CWI activity rapidly increased near the beginning of ripening and reached a peak at the beginning of ripening in the process of grape developing which benefited to sucrose uploading and leaded to ripening initiation [12]. On the contrary, expression level of CWI in mulberry ripening showed gradually increasing trend and it reached a peak at the full ripe stage. It is likely that CWI plays an important physiological role in the whole process of mulberry fruit ripening, but its regulation mechanism needed further study.

**Acknowledgments**

This work was supported by the National Natural Science Foundation of China (31072087), the foundation of post scientist in National Sericultural System (nycytx-27-gw103), and the program (SNG0719) from the Suzhou Science and Technology Bureau, China.

**References**

[1] W. Wang, M. Scali, R. Vignani, A. Spadafora, E. Sensi, S. Mazzuca and M. Cresti: Electrophoresis, Vol. 24 (2003), p.2369

[2] W. Wang, R. Vignani, M. Scali and M. Cresti: Electrophoresis, Vol.27 (2006), p.2782

[3] R.S. Saravanan and J.K. Rose: Proteomics, Vol.4 (2004), p.2522

[4] Z.Chan, G. Qin, X. Xu, B. Li and S. Tian: J. Proteome Research, Vol.6 (2007), p.1677

[5] J. E. Sarry, N. Sommerer, F. X. Sauvage, A. Bergoin, M. Rossignol, G. Albagnac and C. Romieu: Proteomics, Vol.4 (2004), p.201

[6] M. Faurobert, C. Mihr, N. Bertin, T. Pawlowski, L. Negroni, N. Sommerer and M. Causse: Plant Physiol, Vol.143 (2007), p.1327

[7] M. Rocco, C. D'Ambrosio, S. Arena, M. Faurobert, A. Scaloni and M. Marra: Proteomics, Vol.6 (2006), p.3781

[8] B. Watillon, R. Kettmann, P. Boxus and A. Burny: Plant Mol. Biol., Vol.23 (1993), p.501

[9] R. Tang, J. Jia and L. Li: Acta phytophysiologica Sininca, Vol.23 (1997), p.337

[10] Z. Liu, C.C. Taub and C.R. Mcclung: Plant Physiol., Vol.112 (1996), p.43

[11] N. Ukaji, C. Kuwabara, D. Takezawa, K. Arakawa, S. Yoshida and S. Fujikawa: Plant Physiol., Vol.120 (1999), p.481

[12] T. Roitsch, M.E. Balibrea, M. Hofmann, R. Proels and A.K. Sinha: J. Exp. Botany, Vol.54 (2003), p.513

*Advanced Materials Research Vols. 175-176 (2011) pp 30-35*

*doi:10.4028/www.scientific.net/AMR.175-176.30*

# Differential Expression Analysis of Fat Body Proteome during Pupation in Silkworm (*Bombyx mori*)

Tingliang Wang[1,a], Zhiping Wu[1,3,b], Hailing Wang[1,c], Wenqian Liu[1,d],

Yanyan Liu[1,2,e], Jianzhong Tan [1,2, f *]

[1]Department of Horticulture, Soochow University, Suzhou Jiangsu, 215123 China

[2]Institute of Sericulture, Soochow University, Suzhou Jiangsu, 215123 China

[3]Jiangsu Huajia Silk Co., Wujiang Jiangsu, 215227 China

[a] wangtingliang0413@163.com, [b] wzhp05@126.com, [c] wanghailing2@126.com

[d]liu_wq@163.com, [e]sunnice105@163.com, [f]Corresponding author, szutjz@hotmail.com

**Key words:** Silkworm; Pupation; Fat body proteome; Two-dimensional electrophoresis; Mass spectrometry.

**Abstract.** In order to investigate the differential expression of proteins related to pupation in silkworm, the fat body proteins were extracted from larvae of 5$^{th}$ day of 5$^{th}$ instar, un-pupated larvae and pupae of pupating day of multivoltine variety "da zao". The optimized IPG-IEF/SDS-PAGE (2-DE) was used to analyze the differential expression of proteome in different developmental stage during pupation. The results showed that 66 proteins exhibited a more than two-fold differential expression, in which 43 proteins were down-regulated while 23 proteins were up-regulated. Additionally, 14 proteins with stage-specific expression characteristics were also observed. From 25 proteins with three-fold differential expression, 12 proteins were identified by MALDI-TOF/TOF MS, such as actin, calponin-like protein, NADH, beta-tubulin, receptor for activated protein kinase C, IMP cyclohydrolase, tropomyosin, antichymotrypsin precursor and 30K protein precursor *etc*. These results suggest that the differentially expressed proteins (enzymes) are related to the regulation of silkworm metamorphosis or sex differentiation, which provides a new experimental basis for better understanding the physiological functions and the mechanism of gene expression in silkworm fat body.

## Introduction

Fat body is one of the most important metabolism organs of silkworm, and it is both the center of sugar, fat and protein metabolism and the target tissue of several hormones such as neurohormone, ecdysone and juvenile hormone. Therefore, it is essential for growth and development of silkworm [1], and also the important object of silk biological, physiological and biochemical research in silkworm. As the achievement of whole genomic analysis of silkworm, some reports on the functional gene expressions of silkworm fat body have been published [2-6]. In this paper, differential proteome of fat body in different pupation phases was analyzed by two-dimensional electrophoresis (2-DE) and mass spectrum, which provide a new experimental basis for further investigation of physiological function and gene expression of fat body in silkworm.

## Materials and methods

**Material.** A multivoltine variety of silkworm, P50 was used as the experimental materials, and reared by batching of male and female from the stage of $5^{th}$ instar larvae. The fat body was isolated from the larvae of $5^{th}$ day of $5^{th}$ instar larvae (L5), un-pupated larvae of silking end (LE) and pupae of pupating day (P0), and stored in -70℃.

**Preparation of the samples of fat body proteins.** The fat body tissues were powdered with liquid nitrogen, and grinded in the buffer solution Ⅱ(6 mol·$L^{-1}$ urea, 2 mol·$L^{-1}$ thiourea, 2% CHAPS, 15 mmol·$L^{-1}$ DTT). After centrifugation at 14000 rpm 30 minutes at 4℃, supernatant was collected. After repeating the above step, 3 times volume of pre-cooled acetone was added and deposited at -20℃ overnight. The protein depositions were suspended by sample buffer solution (6 mol·$L^{-1}$ urea, 2 mol·$L^{-1}$ thiourea, 2% CHAPS, 15 mmol·$L^{-1}$ DTT, 0.5% IPG buffer), and used for SDS-PAGE (1-DE) and IPG-IEF/SDS-PAGE (2-DE) respectively.

**IPG-IEF/SDS-PAGE of the fat body proteins.** Isoelectric focusing (IEF) was performed using IPG strips with nonlinear pH range of 3-10, 17cm. The IPG strips were rehydrated with 350 μL of rehydration buffer (6 mol·$L^{-1}$ urea, 2mol·$L^{-1}$ thiourea, 2%CHAPS, 2%IPG Buffer, 15mmol·$L^{-1}$DTT, 0.002% bromophenol blue) containing 600μg protein. The following process was conducted according to reference[7].

**Analysis of 2-DE images.** 2-DE gels were scanned by Image Scanner. Protein spots were detected, matched, and analyzed for 3-dimention image by the analysis software of Image Master 2D Platinum 5.0 (GE Healthcare).

**In-gel digestion and MS analysis.** The differential expressed protein spots selected from 2-DE gels were analyzed with MALDI-TOF/TOF MS (4800 Plus MALDI TOF/TOFTM, ABI) after treatment with in-gel digestion (Trypsin digestion, 20h), extracting for enzymolysis liquid and desalting. According to MS/MS data analysis, MS/MS Ion Search of NCBInr was searched by Matrix Science software in order to identify the protein components in which the error of peptide and MS/MS was 100ppm and 0.8Da and others were analyzed using universal rule and standards.

## Results

**SDS-PAGE analysis of differential proteome in silkworm fat body during pupation.** According to the SDS-PAGE images, the characteristic of protein expression in fat body showed some similarities between male and female silkworm from $5^{th}$ day of $5^{th}$ instar to pupating day. The expression level of several protein compositions decreased as growing up compared to those of $5^{th}$ day of $5^{th}$ instar (Fig.1 as indicating by arrow with the full line), however, up-regulation of the 30k protein components were detected (Fig.1 as shown by the dashed line), especially, the expression level of storage proteins, SP (aryl type storage protein ) showed a significant increase in the female larvae during the un-pupated larvae and pupae of pupating day, which significantly differ from the changing trend of hemolymph proteins in the same stage[7].

It suggests that the storage protein SP is secreted into the hemolymph after being synthesized in fat body, and accumulates in the fat body in the middle and later stages of $5^{th}$ instar larvae, whereas almost all 30k protein components are secreted into the hemolymph at the same time. The secretion and accumulation against concentration gradient relied on the mechanism of transport proteins located on the outer membrane of the fat body, which is one of the characteristic of material metabolism for silkworm from nutritional physiology to reproductive physiology stage.

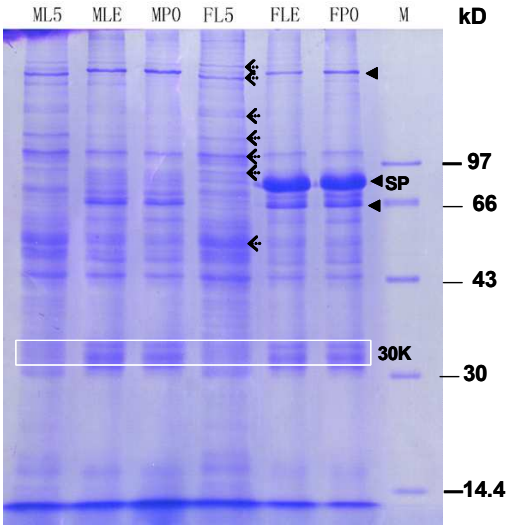


←: proteins increased with development; ⇐: proteins decreased with development;
M: protein marker; SP: storage protein of arylphorin; 30K: storage protein with 30 kDa; FL5/ML5: the 5th day of 5th instar larvae; FLE/MLE: un-pupated larvae of silking end; FP0/MP0: pupating day (female/male).

Fig. 1 SDS-PAGE of differential expressed proteins from fat body of silkworm during pupation

**IPG-IEF/SDS-PAGE analysis of differential proteome in silkworm fat body during pupation.** On the basis of optimized 2-DE technology, the 2-DE analysis of fat body proteome was performed by using larvae of 5th day of 5th instar, un-pupated larvae and pupating pupae as materials respectively. 2-DE gel results showed that the fat body proteins were separated well (Fig. 2) Similar distribution pattern of protein spots was observed in un-pupated larvae of silking end and pupating day, but both showed great difference from larvae of 5th day of 5th instar, suggesting that silkworm larvae in the middle stage of 5th instar undergo organ dissociation or reconstruction related to pupation metamorphosis development.

Also, according to the comparative analysis of 2-DE maps, 14 stage-specifically expressed protein components were found, and they could be classified into 4 expression types (Fig. 2) (Ⅰ) protein spots without expression in larvae of 5th day of the 5th instar, but with expression or up-regulated expression in pre and post pupation, such as F33, F34, F35, F36, M34, M35, M36, M37 and M38; (Ⅱ) protein spot F37 only expressed in larvae; (Ⅲ) protein spots expressed both in the 5th instar larvae and un-pupated larvae except on the pupating day, such as spots F38, F39 and M40; (Ⅳ) only expressed in the short times in un-pupated larvae for example, the spot M39. The differential expression of these stage-specific proteins were supposed to be associated with molecular regulation of pupation metamorphosis development.

Furthermore, by analysis with 2-DE ImageMaster software, 32 and 34 spots were detected to express differentially more than twice in the 2-DE maps of fat body proteins in male and female silkworms respectively at the different development stages, in which 43 protein spots were down-regulated while 23 were up-regulated. According to change trend of expression level, several types were determined as follow (Fig. 3) (Ⅰ) decrease all the time (spot F1 and M2); (Ⅱ) decrease first and then increase, totally decrease (spot F17 and M17); (Ⅲ) decrease first and then increase, totally increase (spot F21); (Ⅳ) increase all the time (spot F24 and M26); (Ⅴ) increase first and then decrease, totally increase (spot F28 and M32); (Ⅵ) increase first and then decrease, totally decrease (spot F31).

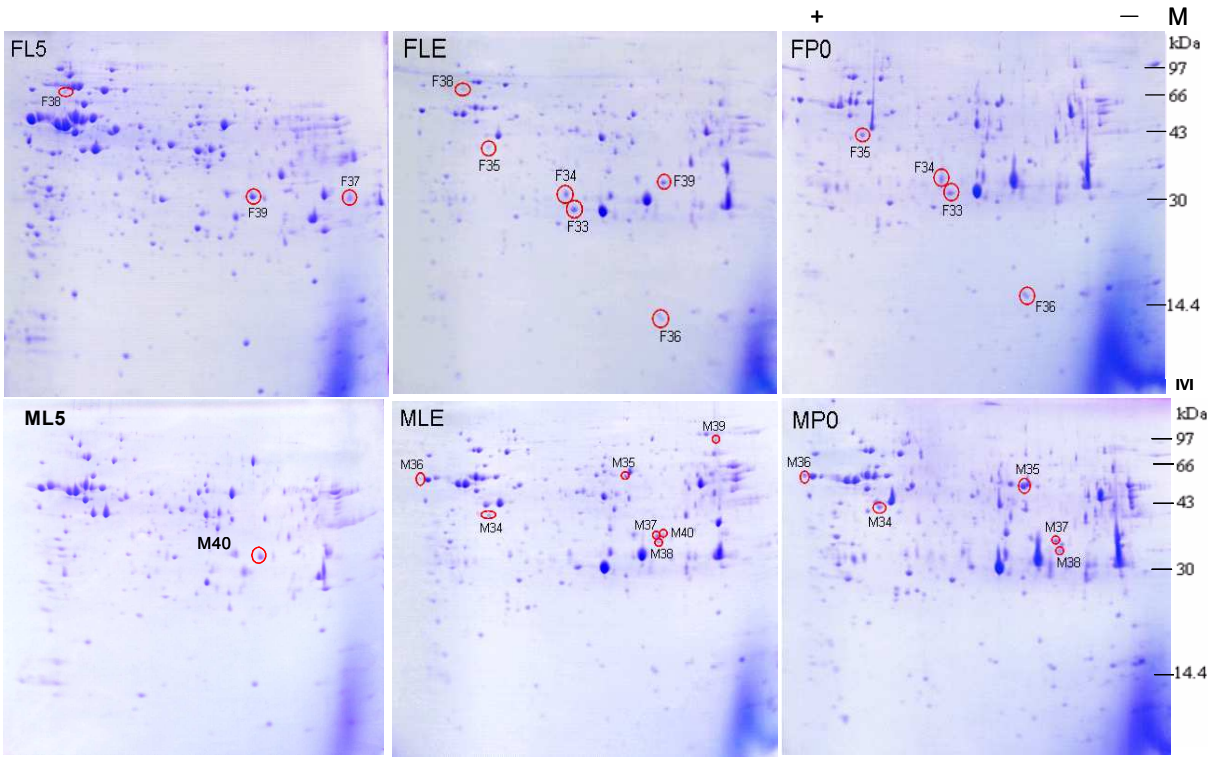


Spot O: stage-special expressed proteins

Fig. 2 2-DE of differential expressed proteins from silkworm fat body during pupation

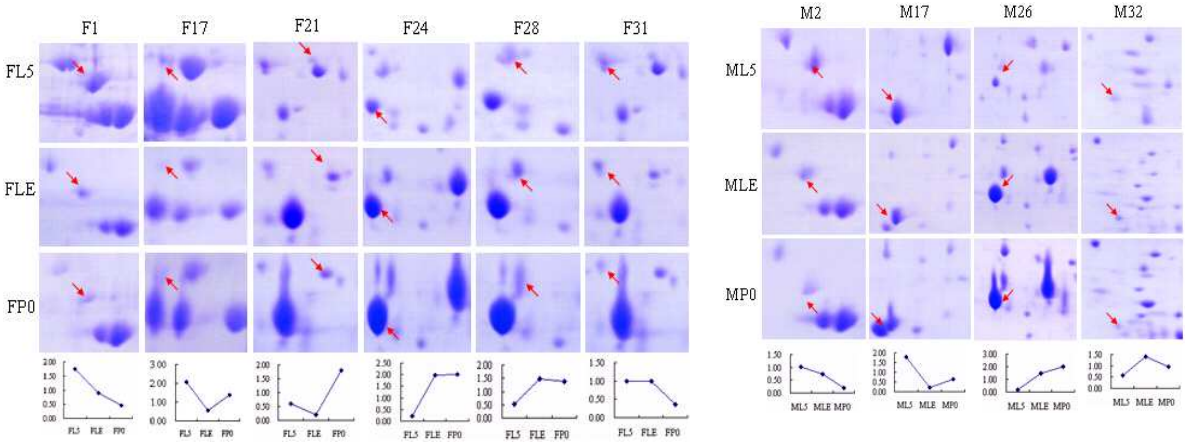


Fig. 3 The types of differential expression of fat body proteins during pupation in female silkworm

**Identification of differential proteins in silkworm fat body during pupation.** According to the above analysis of 2-DE images of fat body proteins, 25 differential expressed protein spots were selected for in-gel digestion and then MALDI-TOF/TOF MS analysis, and 10 proteins were successfully identified, such as actin, calponin-like protein, 75 kD subunit NADH, beta-tubulin, receptor for activated protein kinase C, IMP cyclohydrolase, tropomyosin, antichymotrypsin precursor, calponin-like protein, 30K protein precursor and 30K lipoprotein precursor *etc*. Combining with comparative analysis of 2-DE images, antichymotrypsin precursor, 30K protein precursor and 30K lipoprotein precursor had same changing trend in the male and female silkworm, which suggested that these proteins had more direct relationship with nutritional physiology of metamorphosis development in silkworm.

## Discussion

Abundant information related to metamorphosis development has been obtained from fat body of silkworm, which are excellent target tissues for investigating the metamorphosis development and molecular mechanism in insects. In the current study, based on SDS-PAGE analysis of fat body proteome, the optimized technology of IPG-IEF/SDS-PAGE was used to analyze protein expression pattern of fat body from the male and female silkworm in different developmental stage, and the clear images of 2-DE were obtained. 66 differential expressed protein spots were detected, in which 43 proteins were down-regulated while 23 proteins were up-regulated. Additionally, 14 protein components were found to have characteristic of stage-specific expression, and 12 differentially protein components were identified, which provided experimental basis for better understanding the proteins and regulation of gene expression related to metamorphosis development in silkworm.

It is generally accepted that antichymotrypsin precursor belonged to the serine proteinase inhibitor family, which is the important protein in the silkworm hemolymph and maintains dynamic balance with the fat body proteins. Antichymotrypsin also has important physiological function on metamorphosis development in larvae to pupa and pupa to moth [1,8]. In this study, antichymotrypsin precursor was detectable only in larvae of silking end and the expression level increased at the pupating day, but it could not be detected at the earlier stage of $5^{th}$ instar larvae in contrast to the former study. For example, it was thought that the concentration change of antichymotrypsin precursor CI-8 had two peaks in the fat body which appeared on the $4^{th}$ to $5^{th}$ day of $5^{th}$ instar and the $3^{th}$ day of pupation respectively[9]. This phenomenon is likely to be caused by the existence of several kinds of antichymotrypsin precursor in fat body.

Usually, 30K protein precursor is a group of small molecular weight glycoprotein and the main storage protein in the course of silkworm growth which synthesizes in the fat body at the beginning of $5^{th}$ instar larvae and disappears on the $3^{th}$ day of $5^{th}$ instar which mostly transports into the hemolymph, and then, 30K protein precursor transports back to fat body and stores in it during the development stage from the $5^{th}$ instar larvae to moth[10]. In this study, the decreasing and increasing changes of 30K protein precursor were different from which mentioned above, the rank order of expression level from high to low were the pupating day, un-pupated larvae of silking end and the $5^{th}$ day of $5^{th}$ instar larvae.

It was thought that 30K mRNA could hardly be detected in the fat body at the earlier stage of $5^{th}$ instar larvae [6], while its activity soared on the $3^{th}$ day of $5^{th}$ instar, reached maximum value on the $4^{th}$ day of $5^{th}$ instar and decreased gradually to disappear at pupation, which was different from our results and would be related to the gene regulation at the translation level of 30K protein. Therefore, the differential expressions of mRNAs and proteins in fat body need to be further studied in order to understand more about the expression characteristic of pupation related gene in silkworm.

## Acknowledgments

This work was supported by the Natural Science Foundation of National Hi-Tech Research and Development Project “863” (2006AA10A118). Also, it is a part of the postdoctoral project “Studies on the abduction technology and the regulation mechanism of trimolter silkworm, *Bombyx mori*” from the post-doctoral station on Textile Science and Technology in Suzhou University, China.

**References**

[1] Y. Wang: Insect physiology (China Agricultural Press, Beijing 2004)

[2] D. Cheng, Q. Xia, P. Zhao, Z. Wang, H. Xu, G. Li, C. Lu and Z. Xiang: Arch Insect Biochem. Physiol., Vol.61 (2006), p.10

[3] Y. Shen, D. Cheng, X. Zha, Q. Xia and Z. Xiang: Acta Sericologica Sinica, Vol.30 (2004), p.24

[4] T. Cheng, P. Zhao, C. Liu, P. Xu, Z. Gao, Q. Xia and Z. Xiang: Genomics, Vol.87 (2006), p.356

[5] Y. Xu, J. Xu and H. Kawasaki: Acta Sericologica Sinica, Vol.26 (2000), p.239

[6] Y. Hou, P. Zhao, H. Liu, Y. Zou, J. Guan and Q. Xia: Chinese Journal of Biotechnology, Vol.13 (2007), p.867

[7] Y. Liu, X. Chi, J. Tan, X. Fang, X. Kan, B. Zheng and H. Hisashi: Acta Sericologica Sinica, Vol.34 (2008), p.676

[8] Z. Xiang, J. Huang, J. Xia and C. Lu: Biology of sericulture (China Forestry Publishing House, Beijing 2005)

[9] Z. Qiu, Z. Zhang, X. Ye and J. He: Biotechnology Bulletin, Vol.1 (2002), p.26

[10] P. Tang, B. Li, W. Shen, J. Chen and W. Wang: Entomological Knowledge, Vol.44 (2007), p.826

*Advanced Materials Research Vols. 175-176 (2011) pp 36-40*

*doi:10.4028/www.scientific.net/AMR.175-176.36*

# Determination of DNJ of Mulberry Latex and Evaluation of the Hypoglycemic Effect on Mice

Heyu Zhang [1, a] Wei Chen [2,b] Taichu Wang [3,c] Jinzhu Liu [1,d]

[1]College of Life Science Anhui Agricultural University, Hefei, Anhui, China

[2]College of Light-Textile Engineering and Art Anhui Agricultural University, Hefei, Anhui, China

[3]Sericultural Institute Anhui Agricultural Academy of Science, Hefei, Anhui, China

[a] zhyheyu@163.com [b] lucy-zi@163.com [c] wangtaichu123@hotmail.com

[d] jinzhu2005@sohu.com

**Keywords:** Mulberry; Latex; α-Glucosidase Inhibition.

**Abstract.** Mulberry trees (*Morus* spp. Moraceae) are used for rearing the silkworm. *Moraceae* plants are characterized by the presence of latex, and mulberry trees exude latex when their stem, leaf or root were damaged. We found in the present study that mulberry latex contains very high concentrations of DNJ (0.63% wet weight, 4.5% dry weight), the DNJ content of latex varied with different part of tree and collecting time. The study also evaluated the antihyperglycemic effects of mulberry latex on streptozotocin induced diabetic mice. Diabetic mice were treated with mulberry latex or acarbose with food for 21 days. The results indicated that postprandial blood glucose and fasting-blood glucose level of mice were lowed, mulberry latex displayed a significant reduction ( $P \leq 0.05$) in blood glucose. This finding suggested that mulberry latex have high value for herbal medicine as hypoglycemic function.

## Introduction

Latex is widely found among plant species; 12,000-35,000 species have been reported to exude it [1,2]. Mulberry trees (*Morus* spp. *Moraceae*) leaves have been used for rearing an important economic insect, the silkworm (*Bombyx mori*) for thousands of years. *Moraceae* plants are characterized by the presence of latex, and mulberry trees also exude latex when their leaves are damaged. Mulberry alkaloids, a potent glucosidase inhibitor, However, content in mulberry leaf were as low as about 0.1% (100 mg/100 g of dry product). Mulberry latex contains very high concentrations of alkaloidal sugar-mimic glycosidase inhibitors, such as 1-deoxynojirimycin (DNJ), the overall concentrations of these inhibitors in latex reached 1.5-2.5% (8-18% dry weight) [3].

Diabetes mellitus is defined as a condition in which the body does not produce enough insulin. This causes glucose to accumulate in the blood, often leading to various complications. The major goal in the treatment of diabetes mellitus is keeping both short-term and long-term blood glucose levels within acceptable limits to reduce the risk of long term complications. Although optimizing both fasting-blood glucose and postprandial glucose levels is important in achieving near-normal glucose levels, it has been reported that postprandial glucose levels could be a better marker of glycemic control than fasting blood glucose levels [4]. Since DNJ is believed to be the most bioactive substance (*a*-glucosidase inhibitor), dietary mulberry DNJ might be beneficial for suppressing abnormally high blood glucose levels, thereby helping prevent diabetes mellitus [5]. We believe that *a*–glucosidase inhibitory activity is correlated to DNJ content in mulberry latex. In

this study, DNJ content determination of mulberry latex in different time and different part, the hypoglycemic effect of latex on streptozotocin induced diabetic mice, the relationship between DNJ content and *a* -glucosidase inhibitory activity are discussed.

## Materials and methods

**Chemicals.** Standard DNJ was purchased from Sigma (St. Louis, MO). Acetonitrile, ethanol and distilled water were obtained from Sangon Biotech (Shanghai, China). All other reagents used were of analytical grade.

**Mulberry latex.** Mulberry latex was collected from Anhui agricultural university experimental garden and Anhui Agricultural Academy of Science species garden. Latex was collected by cutting the bark of mulberry branch and trunk. Latex exuded from the cut bark was collected in ice-cooled test tubes, lyophilized, and kept at -20°C. Lyophilized latex powder was dissolved in water in the original concentration, and this solution was the latex used in bioassays.

**Determination of DNJ with HPLC.** A Reverse-phase high-performance liquid chromatography with UV detection (RP-HPLC-UV) method for the determination of DNJ content in mulberry latex after Pre-column derivatization with 9-methyl chloride methyl fluorine (FMOC-Cl) was developed. Mulberry latex was extracted with 70% ethanol, derivatized with FMOC-Cl in borate Potassium buffer solution (pH=8.5).SHI-MADZU Shim-Pack VP-ODS (250×4.6mm, 5um) column was used. The absorbance of the effluent was monitored at 254 nm. The mobile phase consisted of solvent A (acetonitrile/0.1% aqueous acetic acid, 1:1, v/v) and solvent B (methanol).

**Animal.** Kunming male mice obtained from Anhui Medical University (Hefei Anhui China). Mice were maintained under controlled environmental conditions (temperature 23 ± 2°C, relative humidity 55 ± 10%,) and consumed food and water ad libitum. Kunming mice rendered diabetic by a single intraperitoneal (i.p.) injection of 60 mg/kg of streptozotocin (STZ) freshly prepared in 0.1 M of citrate buffer (pH 4.5). Control group were injected with buffer alone. The mice were distributed into 5 groups (ten mice each group) as follows: (Ⅰ) control group, (Ⅱ) diabetic control group, (Ⅲ) diabetic group treated with 0.25ml/kg/day of mulberry latex (Ⅳ) diabetic group treated with 0.50 ml/kg/day of mulberry latex, and (Ⅴ) diabetic group treated with 4 mg/kg/day of acarbose.

In postprandial blood glucose test, the mice fasted for 12 h, were used. Control rats were orally administered sucrose (2.0 g/kg), treated mice were orally administered the sucrose and mulberry latex, tail blood glucose levels were determined 0, 30, 60,120 min. In fasting- blood glucose test, fasting-blood glucose was estimated every week. Serum glucose was measured using an enzymatic method with a test kit from One- Touch Ultra$^{TMT}$ (Johnson and Johnson USA).

## Results

**The determination of DNJ content in mulberry latex with HPLC.** Fig. 1A presents a HPLC separation of DNJ standard solution, 1 peak appeared at a retention time of 3.7 min and was identified as DNJ-FMOC through internal standard method. Fig. 1B presents HPLC separation of Mulberry latex DNJ samples, it showed that the method is credible and it can be used as an effective method in determining the DNJ content in Mulberry latex, other organizations of Mulberry. Table 1 presents DNJ concentrations in the mulberry latex obtained from different parts and

different time, the DNJ content were closely related to the seasonal variation and the region of mulberry branches. Latex taken from the middle part of the branches in the July was enriched in DNJ, A similar tendency was found in the other cultivars. The DNJ content in latex was lowest at bottom of branches in January. Considering the results (Table1), we selected middle branches of M. multicaulis .var.nongsang14 for large-scale production of DNJ-enriched latex in July. The DNJ of latex is about 10 times higher than that of latex of bottom branches in January.

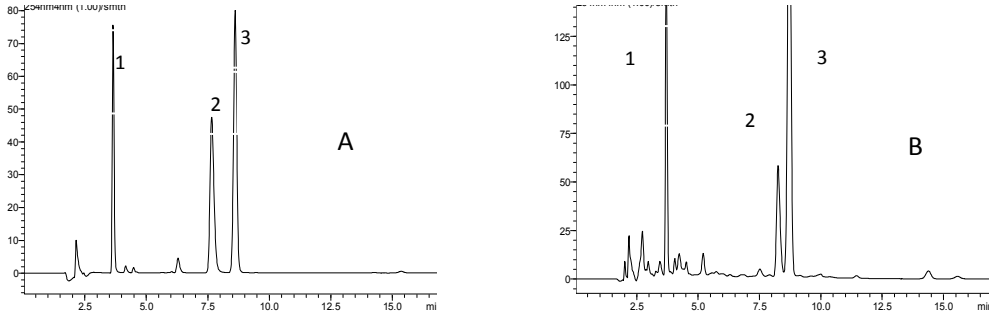


Fig. 1 C analysis of DNJ in mulberry latex (A) HPLC separation of DNJ standard solution (B) HPLC separation of Mulberry latex DNJ samples (M. multicaulis .var.nongsang14)

Note：1 DNJ-FMOC，2 Gly-FMOC，3 FMOC-OH

Table 1. DNJ content in mulberry latex from different parts and different time

| | April (mg/g) | July (mg/g) | October (mg/g) | January (mg/g) |
|---|---|---|---|---|
| Top branches | 3.853 | 5.813 | 1.013 | 0.667 |
| Middle branches | 4.131 | 6.338 | 1.359 | 1.035 |
| Bottom branches | 1.646 | 1.638 | 0.660 | 0.483 |

Note: M. multicaulis .var.nongsang14, the latex were collected from the top, middle and bottom parts of branches. (wet weight)

**Effects of mulberry latex on postprandial blood glucose of diabetic mice.** Using the mulberry latex collected from middle branches in July, The experiment was conducted to investigate the change in postprandial blood glucose and the fasting blood glucose level. Based on the Table1, the DNJ administered by mice (0.50 ml/kg/day) was calculated as 3.2mg/kg/day.

Blood glucose concentrations of mice were significantly elevated after the administration of sucrose. Table 2 shows that mice blood glucose concentrations of Group (Ⅲ) and Group (Ⅳ) were reduced and blood glucose concentrations tended to be delayed compared to diabetic control group. The peak height of the postprandial blood glucose was markedly decreased by oral administration of mulberry latex.

**Effects of mulberry latex on fasting-blood glucose of diabetic mice.** Table2 shows the changes in fasting blood glucose level over 3 weeks. Control mice did not show any significant variation in the blood glucose throughout the experimental period. Diabetic control mice induced by STZ led high elevation of blood glucose levels, diabetic group treated with 0.25ml/kg/day mulberry latex, diabetic group treated with 0.50 ml/kg/day mulberry latex almost reached the Positive drug group (treated with 4 mg/kg/day of acarbose), ( $P < 0.05$). Thus, the latex of mulberry tree showed that it has a significant effect on lowing blood glucose.

Table 2. Effects of mulberry latex on postprandial blood glucose of STZ induced diabetic mice

| groups | postprandial blood glucose after drug administration （mmol/L） | | | |
|---|---|---|---|---|
| | 0 min | 30 min | 60 min | 120 min |
| Control | 8.26 ±0.45 | 15.24±1.12 | 10.23±0.61 | 8.84±0.32 |
| Diabetic control | 16.78±1.25 | 21.44±2.45 | 19.10±2.34 | 17.56±1.34 |
| Group (Ⅲ) | 16.24±1.56 | 19.56±1.57* | 18.40±1.56* | 14.68±1.05* |
| Group (Ⅳ) | 17.14±0.98 | 18.19±1.04* | 17.59±0.24* | 13.90±1.76* |
| Positive drug control | 16.25±1.44 | 18.74±0.89* | 17.54±1.45* | 13.58±1.88* |

Note: Group (Ⅲ) diabetic group treated with 0.25ml/kg/day of mulberry latex. Group (Ⅳ) diabetic group treated with 0.50 ml/kg/day of mulberry latex. Positive drug control group diabetic group treated with 4 mg/kg/day of acarbose. After fasting for 12h, the mice administered mulberry latex, followed by of sucrose in water. Blood samples were collected before intake and 30, 60, 120 min after the administration. An asterisk indicates $P < 0.05$ vs the diabetic control.

Table 3. Effects of mulberry latex on fasting-blood glucose of STZ induced diabetic mice

| groups | before treatment fasting-blood glucose （mmol/L） | 7 days after treatment fasting-blood glucose （mmol/L） | 14 days after treatment fasting-blood glucose （mmol/L） | 21 days after treatment fasting-blood glucose （mmol/L） |
|---|---|---|---|---|
| Control | 8.34 ±0.89 | 8.64 ±1.12 | 8.59 ±0.61 | 8.48 ±0.32 |
| Diabetic control | 16.34±1.65 | 19.43±2.45 | 21.56±2.34 | 20.56±1.34 |
| Group (Ⅲ) | 17.15±2.44 | 13.34±1.57* | 12.68±1.56* | 13.68±1.05* |
| Group (Ⅳ) | 16.63±1.56 | 15.56±3.04* | 14.59±0.94* | 13.59±1.76* |
| Positive drug control | 16.06±2.59 | 11.75±0.89* | 12.54±1.45* | 13.58±1.88* |

Note: Group (Ⅲ) diabetic group treated with 0.25ml/kg/day of mulberry latex , Group (Ⅳ) group diabetic group treated with 0.50 ml/kg/day of mulberry latex, positive drug control group diabetic group treated with 4 mg/kg/day of acarbose. An asterisk indicates $P < 0.05$ vs the diabetic control.

## Discussion

A number of substances, proteins, carbohydrate, lipid, resin, alkaloid and other chemicals with no known biological functions have been found in plant latex [6]. We found in the present study mulberry latex contains high concentrations of DNJ (0.63% wet weight, 4.5% dry weight). The DNJ content of mulberry leaf, bud, root, fruit, branch, phloem and xylem was determined in previous studies, such as root bark (0.18% dry weight), fruits (0.11% dry weight), and leaves (0.14% dry weight) of mulberry [7]. Kotaro Konno [3] found that surprisingly high concentrations of alkaloids exist in mulberry latex and that it is easy to purify them in a simple method. In this study, we first demonstrated that latex taken from middle region branches in summer has more DNJ. The reason may be related to the biosynthesis and transport of DNJ in mulberry. In Toshiy Kimura study [5], they demonstrated that young mulberry leaves taken from the top part of the branches in summer are rich in DNJ, They speculated that the young mulberry leaves have high enzyme activity. Mulberry latex exist in non-articulate laticiferous vessel, laticiferous vessel as plant secretory tissue can produce many kinds of substance, especially secondary metabolites. Due to the laticiferous vessel distributing all organs of tree and latex has high concentrations alkaloid, so we guess the some kinds alkaloid as DNJ of mulberry produced or stored in laticiferous vessel.

Our results indicate that postprandial blood glucose responses at 30-60 min after sucrose

administration were significantly decreased by the oral administration of mulberry latex. Since DNJ is structurally similar to glucose, the intestinal absorption of DNJ can be regulated via a glucose transporter at the small intestinal brush-border [8]. The relationship between 1-deoxynojirimycin content and *a*-glucosidase inhibitory activity has been reported [9]. The fasting-blood glucose hypoglycemic effect of mulberry latex observed in this study look alike the observations made by other researchers studying mulberry extracts [10]. Mohammadi [11] reported that fasting blood glucose levels in a diabetic group treated with mulberry reduced by 50%; in the present investigation, treatment with 0.5ml/kg/day of mulberry latex could lower the blood glucose level to that of Positive drug control group.

Since DNJ is believed to be the most bioactive agent, dietary mulberry DNJ might be beneficial for suppressing abnormally high blood glucose levels. Some papers have confirmed that the DNJ contents in mulberry leaves are very low. Since the estimated effective dose (more than 10mg of DNJ/60 kg human) can not be provided by oral administration of mulberry leaves [5], development of DNJ-enriched products is highly desired. Our results indicate that plant latexes could be both good targets to discover novel medicines and good materials to start purifications. Although it is difficult to collect the latex from mulberry tree now, latex could be a potential treasury of bioactive substances useful as medicines if the convenient and successive method .of obtaining latex was found.

**Acknowledgements**

Financial support for this work was provided by the sericulture industry technology in China

**References**

[1] B. L. Karina Lucas, T. Marcela and A. A. Aristéa: Botany Vol. 87 (2) (2009), p.202

[2] A. Anurag Agrawal, K. Kotaro Latex: Annual Review of Ecology, Evolution, and Systematics Vol. 40 (2009), p.311

[3] K. Kotaro, O. Hiroshi, N. Masatoshi, K. Tateishi and C. Hirayama: Proc Natal Acad Sci U S A. Vol. 103 (5) (2006), p.1337

[4] L. Monnier, C. Colette , C. Cauble and A. Avignon: Diabetes Care Vol. 25 (2002), p.737

[5] T. Kimura, K. Nakagawa and H. Kubota: Journal Agriculture Food Chemistry Vol. 55, (14) ( 2007), p.5869

[6] N. Wasano, K. Konno , M. Nakamura, C. Hirayama, M. Hattori and K. Tateishi: Phytochemistry Vol. 70 (4) (2009), p.880

[7] W.Q. Liu, X. R. Zhu: Bulletin of Sericulture Vol.37 (4) (2006), p.31

[8] J. M. Park, H. Y. Bong and H. I. Jeong: Nutrition Research and Practice Vol. 3 (4) (2009), p. 272

[9] K. Yatsunami, M. Ichida and S. Onodera: J Nat Med Vol. 62 (2008), p.63

[10] C. Kuriyama, O. Kamiyama, K. Ikeda and F. Sanae: Bioorganic & Medicinal Chemistry Vol. 16 (2008), p.7330

[11] M. Jamshid, N. PrakashR: Indian Journal of Pharmacology Vol. 40 (1)(2008),p.15

*Advanced Materials Research Vols. 175-176 (2011) pp 41-45*

*doi:10.4028/www.scientific.net/AMR.175-176.41*

# Studies on the Joint Impact of Mulberry Cultivation and Sericulture Enterprise as a Scheme for Border Area Development Programme in Kashmir, India

Manzoor Ahmad Malik, Afifa Shaheen Kamili, Ghulam Nabi Malik,

Abdul Majeed Sofi, Irfan Lateef Khan, Nisar Ahmad Ganie,

Firdous Ahmad Malik, Awquib Sabhat and Syed Farhat Iqbal Qadri

Division of Sericulture, Sher-e- Kashmir University of Agricultural Sciences & Technology of Kashmir, Mirgund, Post Box No. 674, GPO Srinagar -190 001 (J&K) India

Email: manzoor_auqib@yahoo.ca

**Key Words:** Silkworm; Mulberry Cultivation;Silk; Temperate climate.

**Abstract.** With the development of new technologies in silkworm rearing though sericulture has now emerged as a main profession and a major cash crop for the rural people of the India in tropical areas but in temperate belt like Kashmir the constraints faced by the sericulture farmers/silkworm rearers are more and these are responsible for yield gaps which have to be considered seriously and accordingly the extension services need to be modulated and implemented. Exploitable yield gaps in Border areas are often caused by various factors including physical, biological, socio-economic and institutional constraints which can be effectively improved through participatory and holistic approaches. Kashmir is a univoltine area where for generations only one crop in spring season is taken between May and June. Spring (May – June, 2009) data of Kandi Kupwara J&K India (Border area) revealed varying cocoon yields from 7 to 13 kgs dry cocoons per 100 DFLS with cocoon price varying from Rs. 172-430 per kg. These facts and figures prove that these silkworm rearers by realizing the potential of sericulture (a new culture in a Border area) increased their income substantially from Rs. 720 to Rs.5590/100DFLS. It was also found that sericulture productivity can be further increased by planting improved varieties of mulberry as it has been observed that where, very good quality mulberry leaf and inputs are available, the sericulture productivity is reasonably good. The present communication, therefore, discusses the extension strategies and new technologies to improve the essential knowledge and skills to the sericulture farmers to improve the yield and profitability of sericulture.

## Introduction

Sericulture is an eco-friendly agro-based labour intensive rural cottage industry providing subsidiary employment and supplementing the income of rural farmers especially the economically weaker section of the society. The industrial production of raw silk and fabric employs a large number of semi literate and semi skilled poor workers throughout the year. Thus a large portion of the cost incurred in the conversion of soil to silk reaches poor workers involved in the value addition at each stage like cocoon production, silk reeling, fabric production, dying and printing. Sericulture industry is, therefore, discretely helping in building an egalitarian society in highly populous countries like India and china[1].

Sericulture occupies the place of pride in the rural economy by being only cash crop that guarantees attractive returns in a short period of time. In recent years, though India has taken strides in sericulture development by introduction of innovations [2]. Sericulture also has an important

place in the economy of Jammu & Kashmir as more than 23,000 families are generating their employment through this avocation. Jammu and Kashmir State is basically an agrarian economy. Agriculture occupies predominant position in terms of dependence for livelihood and employment. Though we have a salubrious climate, a predominately agriculture economy, a dense population giving us ample man-power which are willing and able to work it economically, socio religious traditions favouring the use of silk fabrics and a growing domestic and export market, but like other cottage industries sericulture too has been languishing. With large number of our village population deriving the greater part of their income from sericulture in hilly and far flung areas and not having other identified areas like horticulture sector to absorb and employ huge chunk of population in the state, faster growth in sericulture is necessary to provide boost to their incomes. Rising income in sericulture will help redress the rural-urban imbalance. Therefore, a new approach in sericulture is necessary in view of the fact that as an important activity allied to agriculture, it can strengthen the productivity base of agriculture economy in such areas where other activities to provide livelihood are minimal.

Sustenance of any technology depends on the knowledge and adoption level of the technology by the farmers which is influenced by many factors. Tough the Government agencies organize many extension programmes and training courses, involvement of the farmers is the basic criteria for popularizing any technology. In spite of availability of many improved techniques in host plant management and as well as silkworm rearing, majority of the silkworm rearers of Kashmir valley are still inclined to follow their traditional practices. After inclusion of sericulture in the illustrative list of schemes for Border Area Development programme in India in general and Jammu and Kashmir State in particular a sericulture project entitled, “Studies on the Joint impact of mulberry cultivation and sericulture enterprise as a scheme for Border Area Development programme” was formulated which envisaged introduction of improved methods of sericulture among Border people for alleviating their socio economic status as socio economic conditions of the farmers not only influence the knowledge and adoption level but also cocoon productivity. However, no such innovations have been introduced in any Border district of Jammu and Kashmir, even though the cocoon production exists in Border districts. Adoption of new technologies in silk worm rearing has remained an enigma at farmers level in Border villages of kashmir. Hence, the present study attempts to evaluate the awareness and adoption pattern of improved technologies among Border Silkworm rearers of Kupwara, Jammu & Kashmir State in cocoon production.

## Materials and methods

The study was conducted in Kupwara district during May to June -2009. To provide Border people with gainful employment 21 house holds spread over five villages were identified in consultation with Sericulture Development Department, Kashmir for effective implementation of the programme and were divided into three groups as given below:

*Group A*: House holds which undergo disinfection, have mulberry leaf, conduct Tray rearing and use Plastic mountages for spinning cocoons.

*Group B*: House holds which undergo disinfection, have mulberry leaf, conduct floor rearing and use grass mountages for spinning of cocoons.

*Group C*: House holds which undergo disinfection have no mulberry leaf (depend on road side plantation) conduct floor rearing and use paddy grass (Oryza sativa) or mulberry twigs for spinning of cocoons.

The data were collected during 2009 spring (Commercial) Crop. Twenty One silkworm rearers were randomly selected and provided with 21 ounces of silkworm eggs and divided in above groups A, B and C each comprising of seven silkworm rearers for collecting the information required for the study. In this study, data was recorded on silkworm seed distributed, green /dry cocoons harvested, rate per kilogram of cocoons and gross income generated.

**Results and discussion**

For successful sericulture adoption of recommended sericultural practices is essential. Chawkie reared Silkworms of cross breed corresponding to 7 ounces of Silkworm seed were distributed among seven randomly selected Silkworm rearers (per rearer one ounce) in group A, B and C as indicated in Tables 1-3.

Table 1. Group A: House holds which undergo disinfection have mulberry leaf, conduct tray rearing and use plastic mountages for spinning cocoons.

| S.No. | Seed Distributed | Green Cocoons harvested (Kg) | Dry Cocoons harvested (Kg) | Rate /Kg (Rs) | Total Income generated /Farmer (Rs) |
|---|---|---|---|---|---|
| 1 | 01 | 39.000 | 13.000 | 430.00 | 5590.00 |
| 2 | 01 | 30.000 | 10.000 | 330.00 | 3300.00 |
| 3 | 01 | 30.000 | 10.000 | 310.00 | 3100.00 |
| 4 | 01 | 30.000 | 10.000 | 300.00 | 3000.00 |
| 5 | 01 | 19.980 | 6.660 | 290.00 | 1931.40 |
| 6 | 01 | 30.000 | 10.000 | 275.00 | 2750.00 |
| 7 | 01 | 30.000 | 10.000 | 273.00 | 2730.00 |
| Total | 07 | 208.980 | 69.660 | - | 22,401.40 |
| Mean | - | 29.854 | 9.951 | 315.429 | 3200 |
| SE± | - | 2.077 | 0.692 | 20.522 | 431.107 |

Table 2. Group B: House holds which undergo disinfection have leaf, conduct floor rearing and use grass mountages for spinning cocoons.

| S.No. | Seed Distributed | Green Cocoons harvested (Kg) | Dry Cocoons harvested (Kg) | Rate /Kg (Rs) | Total Income generated /Farmer (Rs) |
|---|---|---|---|---|---|
| 1 | 01 | 24.000 | 8.000 | 270.00 | 2160.00 |
| 2 | 01 | 27.000 | 9.000 | 265.00 | 2385.00 |
| 3 | 01 | 24.000 | 8.000 | 262.00 | 2096.00 |
| 4 | 01 | 30.000 | 10.000 | 260.00 | 2600.00 |
| 5 | 01 | 39.000 | 13.000 | 260.00 | 3380.00 |
| 6 | 01 | 39.000 | 13.000 | 240.00 | 3120.00 |
| 7 | 01 | 30.000 | 10.000 | 230.00 | 2300.00 |
| Total | 07 | 213.000 | 71.000 | - | 18041.00 |
| Mean | - | 30.429 | 10.143 | 255.286 | 2577 |
| SE± | - | 2.399 | 0.799 | 5.506 | 186.383 |

The cocoon yield of adopted farmers ranged from 6.660 to 13.000 kgs dry in group A farmers 8.000 to 13.000 kgs dry in group B farmers while it was 3.000 to 8.000 kgs dry in group C farmers. The rate per kg of dry cocoons ranged from Rs. 273.00 to Rs.430.00 in group A, Rs. 230.00 to Rs. 270.00 in group B while it was Rs. 172.00 to Rs.210.00 in group C. Total income generated from spring crop (May to June) ranged from 1931.00 to Rs. 5590.00 per ounce of Silkworm seed per farmer in group A Rs. 2160.00 to Rs.3380.00 in group B and Rs. 720.00 to Rs. 1680.00 in group C.

Table 3. Group C : House holds which undergo disinfection, conduct floor rearing, have no leaf and use paddy grass or mulberry wigs for spinning cocoons.

| S.No. | Seed Distributed | Green Cocoons harvested (Kg) | Dry Cocoons harvested (Kg) | Rate /Kg (Rs) | Total Income generated /Farmer (Rs) |
|---|---|---|---|---|---|
| 1 | 01 | 15.000 | 5.000 | 200.00 | 1000.00 |
| 2 | 01 | 24.000 | 8.000 | 210.00 | 1680.00 |
| 3 | 01 | 9.000 | 3.000 | 210.00 | 630.00 |
| 4 | 01 | 12.000 | 4.000 | 190.00 | 760.00 |
| 5 | 01 | 18.000 | 6.000 | 185.00 | 1110.00 |
| 6 | 01 | 12.000 | 4.000 | 180.00 | 720.00 |
| 7 | 01 | 18.000 | 6.000 | 172.00 | 1032.00 |
| Total | 07 | 108.000 | 36.000 | - | 6932.00 |
| Mean | - | 15.429 | 5.143 | 192.429 | 990 |
| SE± | - | 1.900 | 0.633 | 5.579 | 133.431 |

Although the quantity of dry cocoons was slightly more 71.00 kgs in group B conducting floor earing than in group A 69.66 Kgs but the rate per Kg of Cocoons was more in group A adopting tray rearing with plastic mountages for spinning and ranged from Rs. 273.00 to Rs. 430.00 per kg per farmer in comparison to Rs. 230.00 to RS.270.00 per kg per farmer in group B and both are significant to group C with Rs. 172.00 to Rs. 210.00 per kg per farmer Table 4. Further, the total income generated from spring crop was more in group A with Rs. 22,401.40 followed by group B with Rs. 18041.00 and group C with Rs. 6932.00 indicating impact of technology adoption. The reason for low level of adoption of these improved practices was highly associated with lack of awareness. It has also been reported that lack of knowledge is the primitive factor for non-adoption of improved package of practices [3,4]. Similarly productivity in Sericulture (a new culture in Border area) also revealed that the scope of increasing productivity was mainly due to impact of improved technologies especially efficient use of inputs which is also in conformity with the studies of [5-7]. Information gathered revealed that Sericulture productivity in Border villages of Jammu & Kashmir State can be further increased by planting improved varieties of mulberry as it has been observed in groups A & B that owing to good quality mulberry leaf availability with the Sericulturists, cocoon productivity is reasonably good in comparison to group C which are dependent on road side plantation for leaf supply. Hence the quality and productivity improvement seem to be twin approaches for better profitability in Sericulture and will help to boost up the much needed productivity of mulberry silk to a great extent in Border villages and indicate similar trend as reported in studies conducted by Mohandas et al. [8], in Bangalore rural district.

Table 4. Average green Cocoon yield and rate / kg of cocoons.

| **Group** | **Yield (Kg)** | **Rate / Kg (Rs.)** |
|---|---|---|
| A | 29.854** | 315.429** |
| B | 30.429** | 255.286** |
| C | 15.429 | 192.429 |
| CD @ (5%) | 6.346 | 37.685 |

**Significant p=0.05

**Acknowledgement**

The authors thankfully acknowledge the financial support provided by the authorities of Life Sciences Research Board, Govt. of India for the said project and the necessary facilities rendered by the authorities of Sher-e-Kashmir University of Agricultural Sciences and Technology of Kashmir, Shalimar, Srinagar India for carrying out the research/extension work.

**References**

[1] S. Lakshmanan, B. Mallikarjuna, R. Gannapathi Rao, H. Jayaram and R.G. Geetadavi: *Indian J.Seric*.Vol. 37 (1) (1998), p.44

[2] S.S. Dolli, H.K. Kalappa, R.K. Subramaniam, Chikkanna, N.R Singhvi, A.K. Sen, M.N.S. Lyengar, and R.K. Datta: *Indian Silk* Vol. 31 (10)(1993), p.35

[3] N. R. Singhivi, M. K. Sethu Rao, Y.R. Madhava Rao, M.N.S. Lyengar, and R.K. Datta: *Indian J. Seric*.,Vol. 33 (2) (1994), p.48

[4] T. Puttaswamy: Knowledge, adoptionand attitude of small farmers towards mixed farming in Sira and Anekal taluks. M.sc. (Agriculture)Thesis, University of Agricultural Sciences, Bangalore, India (1977)

[5] R.C. Panda: Indian J. Agri. Econ.Vol. 51(3) (1996), p. 355

[6] K. Singh and J.D. Yadav: Gaps and Constraints in Wheat productivity – A system analysis, Agricultural Situation in India – XI, p. 627 (1989)

[7] S.B. Dandin, and P. Kumaresan: *Indian Silk* June, (2003), p. 5

[8] T.P. Mohandas B. Ramarao, A.K. Sikdar, and H. Jayaram, Adoption rate of validated Sericulture technologies and its impact on Cocoon productivity-a case study. Proc. Of Natl, Semi on Trop Sericulture, Dec 28-30, University of Agricultural Sciences, Bangalore, India, p.140 (1999)

*Advanced Materials Research Vols. 175-176 (2011) pp 46-50*
*© (2011) Trans Tech Publications, Switzerland*
*doi:10.4028/www.scientific.net/AMR.175-176.46*

# Cloning and Transcriptional Expression of *CYP6AE22*-A Member of Cytochrome P450 Family from *Bombyx mandarina*

Yanhong Wang [1,2,a] Bing Li [1,2,b] Dong Wang [1,2,c] Huaqiang Zhao [1,2,d]
Zhengguo Wei [1,2,e] Weide Shen [1,2,f]

[1]School of Basic Medicine and Biological Sciences, Soochow University, Suzhou, 215123, China

[2]The National Engineering Laboratory of Modern Silk, Soochow University,Suzhou, 215123, China

[a]wangyh2004@163.com, [b]sdlibing@hotmail.com, [c]dongdong1642@sina.com
[d]hqzhao33@tom.com, [e]szwei1969@hotmail.com, [f]Corresponding author, shenwd@suda.edu.cn

**Key words:** *Bombyx mandarina*; Cytochrome P450; *CYP6AE22*; Semi-quantitative RT-PCR.

**Abstract** The cytochrome P450-dependent monooxygenases play an extremely important role in metabolic system involved in the catabolism and anabolism of xenobiotics and endogenous compounds. According to the predicted P450 sequences from the genome of *Bombyx mori*, a pair of primers was designed and a novel gene named *CYP6AE22* was successfully cloned from the midgut mRNA of *Bombyx mandarina* by RT-PCR (GenBank accession number: FJ843077). Sequence analysis revealed that this gene contains a 1551 bp ORF, encoding a protein of 516 amino acids. The predicted molecular weight and isoelectric point of this protein was 60 kD and 9.0, respectively. The results of semi-quantitative RT-PCR showed that this gene was highly expressed in fat body and brain. And the expression level could be increased by induction with cypermethrin. Treatment with 5ng/uL cypermethrin could increase the expression level in midgut and fat body of the larvae of 1.5 fold and 2.5 fold, respectively. It is inferred that *CYP6AE22* gene may be involved in detoxification of insecticide in *Bombyx mandarina*.

## Introduction

Cytochrome P450-dependent microsomal monooxygenases represent the single most important enzyme system involved in the detoxification of xenobiotics and have been detected in virtually all organisms examined from bacteria to mammals[1]. Cytochrome P450 monooxygenase-mediated detoxication is an important mechanism by which insects and mites become resistant to pesticides [2-4]. Some CYP enzymes metabolize and/or detoxify exogenous substances like drugs and esticides [5]. Members of the CYP6 and CYP9 are known to be involved in insecticide resistance in some insects such as *Musca domestica L.* [6], *Heliothis virescens* (Fabricius) [7], *Culex quinquefasciatus* Say [8], *Anopheles minimus* (Theobald) [9], *Anopheles gambiae* (Giles) [10], and *Drosophila melanogaster* (Meig.) [11].

The wild silkworm, *Bombyx mandarina, is* believed to be the ancestor of *Bombyx mori* [12]. *Bombyx mandarina*, was very similar to *Bombyx mori* in morphological and physiological characteristics [13-14]. Due to long-term natural selection, there was a difference of resistance to insecticides between the two species [15]. *Bombyx mori* had a weak resistance to insecticide, and its production was reduced by more than 30% annually because of insecticide poisoning in china. On the other hand, being one of the major pests in mulberry fields, *Bombyx mandarina* showed increasing resistance to insecticides owing to their wide use.

There were many studies about the relations between CYP450 and insect resistance. Cytochrome

P450 represents an inducible enzyme system, and increased amounts of specific P450 isozymes are observed after exposure of organisms to a variety of organic chemicals [1]. Several major classes of environmental contaminants induce the cytochrome P450 system [16]. Cytochrome P450 enzymes are inducible through a mechanism that is controlled at the transcriptional level [17].In this study, we designed a pair of primers according to the predicted P450 sequences from the genome of Bombyx *mori*, cloned a cDNA, named *CYP6AE22*, and study its transcriptional level in five tissues: brain, blood, silk gland, midgut and fat body. Also, we study its transcriptional level in midgut and fat body after induced by cypermethrin. The result provided the references for studying resistance of *Bombyx mandarina* and other Lepidoptera insects.

## Materials and methods

**Insects and tissue collection.** The larvae of *Bombyx mandarina* (Suzhou strain), maintained in our laboratory, were reared on mulberry leaves under a 12-h light/12-h dark photoperiod.

Choose 5 $^{th}$ instar 3d larvae (600±50 mg), the brain, midgut, fat body, silk gland and blood were dissected out and stored at -70°C.

For testing the induced result, cypermethrin was diluted into acetone, and the concentration was 5 ng/μL. Used drop method, and dropped each larva 1μL cypermethrin on the region between head and chest. The control treat used acetone. 24 h later ,the midgut and fat body were dissected out and stored at -70°C.

**RNA extraction and cDNA synthesis.** Total RNAs were extracted from tissue of control and induced *Bombyx mandarina* larvae using RNAiso reagent (TaKaRa) according to the manufacturer's instructions. First-strand cDNA synthesis was performed using M-MLV RTase cDNA Synthesis Kit (TaKaRa) according to the manufacturer's instructions.

**Gene cloning.** The following *CYP6AE22* gene-specific primers were used for cloning cDNA, 6AE-F(TTGTACTCCAATCGATCGTTGGTGAATT-3'), 6AE-R(5'-TACAACTGGTGTTCCGGT CTCTTCA-3'). The conditions were: 94 °C, 30 s; 56 °C, 30 s; 72 °C, 1 min 45 s. Then test by 1.2% agarose gel electrophoresis, and compared using Tanon Gel Analysis Software.

**Reverse transcription (RT)-PCR analysis.** *B. mori actin*-3 cDNA was used as an internal standard to normalize the templates in a preliminary PCR experiment. After template adjustment, PCRs were performed to detect relative levels of *CYP6AE22* cDNAs using the primers BDL-F(5'-CCTGAACATTTTCCGAACCCG-3') and DL-R(5'-CTCTTTGCTGCCATCTTCAC -3'). The thermal cycling conditions for *actin*-3 were: 94 °C, 30 s; 60 °C, 30 s; 72 °C, 30 s. The thermal cycling conditions for *CYP6AE22* were: 94 °C, 30 s; 57 °C, 30 s; 72 °C, 30 s. After separation by 1.2% agarose gel electrophoresis, intensities of the PCR products were quantified and compared using Tanon Gel Analysis Software.

## Results

***Bombyx mandarina CYP6AE22* Cloning.** The first-chained cDNA was synthesized by reverse transcription of mRNA from the midgut of *Bombyx mandarina*. A pair of degenerate primer transcript was used to amplify the template by RT-PCR.A 1551 bp fragment was obtained, after restriction mapping with *pst* I and sequencing analysis, the correctness of the gene cloning was confirmed, and named *CYP6AE22*, GenBank accession number: FJ843077(Fig. 1).

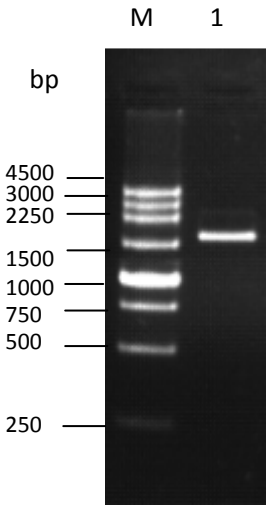


M. 250 bp Marker 1. Product of RT-PCR

Fig. 1 Cloning of *CYP6AE22* from *Bombyx mandarina*

**Tissue expression of *CYP6AE22* from *Bombyx mandarina.*** Using RT-PCR tested the transcriptinal level of *CYP6AE22* in brain, blood, silk gland, midgut and fat body The result showed that, the transcriptional level were different in tissues tested, and it highly expressed in brain and fat body and midgut(Fig. 2).

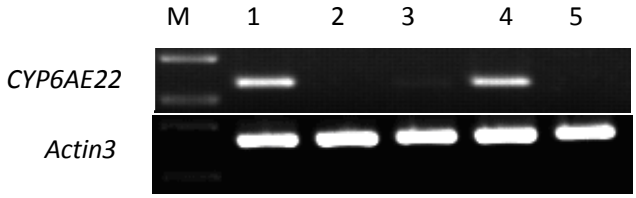


M. 250 bp DNA marker; 1.brain; 2. Silk gland; 3. Midgut; 4. Fat body; 5. Blood

Fig. 2 The expression profile of *CYP6AE22* from *Bombyx mandarina* by Semi-quantitative RT-PCR

**Transcriptional expression of *CYP6AE22* after induced by cypermethrin.** The transcriptional level of *CYP6AE22* was changed after induced by cypermethrin. The result showed that the express level of *CYP6AE22* of cypermethrin induced larva in midgut and fat body were higher than that of control larva as 1.5 fold and 2.5 fold, respectively (Fig. 3).

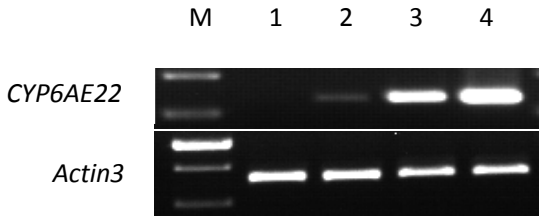


M. 250 bp DNA Marker; 1.midgut control; 2.midgut induced by cypermethrin;3.fat body control; 4.fatbody induced by cypermethrin.

Fig.3 The expression profile of *CYP6AE22* from *Bombyx mandarina* after induced by cypermethrin.

**Discussion**

In insects, CYP genes mostly belonging to microsomal CYP4, CYP6, CYP9 and mitochondrial CYP12 families, have frequently been associated with detoxification processes giving tolerance to insecticides [1] or plant toxins [18]. It has often been mentioned that insecticide detoxification by P450s is via increased level resulting from their elevated expression [2, 19]. Elevated levels or overexpression of P450s has been reported in some pyrethroid-resistant insects. For example, increased mRNA level of *CYP6AA2* has been observed in *Anopheles minimus* deltamethrin resistant strain [20]; *CYP6F1* [21] of *Culex pipiens pallens* have also demonstrated an overexpression in deltamethrin-resistant strain; *CYP6B7* [22] in fenvalerate-resistant strain of *Helicoverpa armigera*; and *CYP6Z1* [23] in permethrin-resistant *Anopheles gambiae*.

It is commonly acknowledged that CYP6 family members have close relationship with the resistance to insecticide in the known superfamilies of insect P450 [24]. In this paper, we studied the transcriptional expression profile of *CYP6AE22* of *Bombyx mandarina* larval in different tissues and the transcriptional expression profile after induced by cypermethrin. The result showed that, the transcriptional level was different in tissues tested, and it highly expressed in brain, fat body and midgut. Also, the express level of *CYP6AE22* of cypermethrin induced larva in midgut and fat body were higher than that of control larva as 1.5 fold and 2.5 fold, respectively. And the results indicated that *CYP6AE22* may play roles in the resistance to cypermethrin of *Bombyx mandarina*, and this also can give us some indications to study the resistance to pesticide of other Lepidoptera insects, but the relations between transcriptional expression and resistance still needed more study.

**Acknowledgments**

Financial support for this work was provided by the foundation of post scientist in National Sericultural System (nycytx-27-gw307).

**References**

[1] G. Scott: Insect. Biochem. Mol. Biol, Vol. 29.(1999), p. 757

[2] Feyereisen: Annu. Rev. Entomol, Vol. 44 (1999), p. 507

[3] N. Stumpf and R. Nauen; Pestic. Biochem.Physiol, Vol. 72 (2002), p. 111

[4] S. Kasai: J. Pestic. Sci,Vol 29 (2004), pp. 234

[5] D.R. Nelson, L. Koymans, T. Kamataki, J.J. Stegeman, R. Feyreisen,D.J. Waxman, M.R. Waterman, O. Gotoh, M.J. Coon, R.W. Estabrook,I.C. Gunsalus and D.W. Nebert: Pharmacogenetics, Vol. 6 (1996), p. 1

[6] T. Tomita and J.G. Scott: Insect Biochem. Molec, Vol 25 (1995), p. 275

[7] R.L. Rose, D. Goh, D.M. Thompson, K.D. Verma, D.G. Heckel, L.J.Gahan, R.M. Roe and E. Hodgson: Insect Mol.Biol, Vol. 27 (1997), p. 605

[8] S. Kasai, I.S. Weerashinghe, T. Shono and M. Yamakawa: Insect Biochem. Molec, Vol. 30 (2000), p. 163

[9] P. Rongnoparut, S. Boonsuepsakul, T. Chareonviriyaphap and N.Thanomsing: J. Vector Ecol, Vol. 8 (2003), p. 150

[10] Nikou, H. Ranson and J. Hemingway: Gene, Vol. 318 (2003), p. 91

[11] G. Le GoV, S. Boundy, P.J. Daborn, J.L. Yen, L. Sofer, R. Lind, C.Sabourault, L. Madi-Ravazzi and R.H. Vrench-Constant: Insect Biochem. Molec, Vol. 33 (2003), p. 701

[12] Y. Banno, T. Nakamura, E. Nagashima, H. Fujii and H. Doira: Genome, Vol. 47(2004), p. 96

[13] B.L. Astaurov, M.D. Golysheva and I.S. Rovinskaya: Cytology, Vol. 1(1959), p. 327

[14] Yoshitake: Journal of Sericological Sciences of Japan, Vol. 37(1968), p. 83

[15] W.D. Shen, B .Li, P. Ji, Z. Wei, Y. Chen and G. Pang: Science of Sericulture, Vol. 29(2003), p. 375

[16] D.J. Hoffman, B.A. Rattne, Jr,GA. Burton and Jr,J. Cairns: Handbook of Ecotoxicology (Lewis Publishers,Boca Raton1995)

[17] Batar, M.A. Schalk, A. Pierrel, F.D. Zimmerlin and D. Werck-Reichhart: Plant. Physiol, Vol. 113(1997), p. 951

[18] M.R. Berenbaum: J. Chem. Ecol, Vol. 28(2002), p. 873

[19] D.W. Nebert and F.J. Gonzales: Annu. Rev. Biochem, Vol. 56 (1987), p. 945

[20] P. Rongnoparut, S. Boonsuepsakul, T. Chareoviriyaphap and N.Thanomsing: J. Vector Ecol, Vol. 28 (2003), p. 150

[21] M.Q. Gong, Y. Gu, X.B. Hu, Y. Sun, L. Ma, X.L. Li, L.X. Sun, J. Sun,J. Qian and CL. Zhu: Biochim. Biophys. Sinica, Vol. 37 (2005), p. 317

[22] C. Ranasinghe and A.A. Hobbs: Insect Biochem. Mol. Biol, Vol. 28 (1998), p. 571

[23] D. Nikou, H. Ranson and J. Hemingway: Gene, Vol. 318 (2003), p. 91

[24] M.B. Cohen, J.F. Koener and R. Feyereisen: Gene, Vol. 146 (1994), p. 267

*Advanced Materials Research Vols. 175-176 (2011) pp 51-55*

*doi:10.4028/www.scientific.net/AMR.175-176.51*

# Full Length cDNA Cloning and Expression characteristics of *ace* Gene from Wild Silkworm, *Bombyx mandarina*

Bing Li[1,2,a], Yan-Hong Wang[2,b], Ju-Mei Wang[2,c], Wei-De Shen[1,2,d]

[1]National Engineering Laboratory for Modern Silk, Soochow University, Jiangsu 215123, China.

[2]School of Basic Medicine and Biological Sciences, Soochow University, Jiangsu 215123, China.
[a] Lib@suda.edu.cn, [b]wangyh2004@163.com, [c]13771764026@139.com, [d] Corresponding author , shenwd@suda.edu.cn

**Keywords:** *Bombyx mandarina*; acetylcholinesterase gene; Cloning; Gene expression.

**Abstract.** Acetylcholinesterase (AChE), which contains two subfamilies, *ace*1 and *ace*2 in insects, was identified to be the target of organophosphorous and carbamate insecticides. To research the sequences and tissues expressions of two *ace*s, full length cDNAs encoding two *ace* genes were cloned, designated as *Bmm-ace*1 and *Bmm-ace*2 from larvae of the *Bombyx mandarina*. The amino acid sequence of *Bmm-ace*1 shared 99.71 % homology with its homolog, *Bm-ace*1, in silkworm, *Bombyx mori*, with two mutations (G664S and S307P), and the amino acid sequence of *Bmm-ace*2 shared 99.37 % homology with *Bm-ace*2, in *B. mori* , with four mutations (M18I, N233S, I310V and G621S). Tissue expression analysis showed that *ace*1 gene expressed only in the brains and fat bodies of *B. mandarina,* while *ace*2 genes expressed in all the tissues tested. *ace*1 and *ace*2 expressed highly in brains and fat bodies. The present results are significant to the study of resistance evolution of *Lepidorptera* as well as the understanding of the mechanism of pesticide resistance of insects.

## Introduction

The wild silkworm, *Bombyx mandarina*, was very similar to silkworm, *Bombyx mori* in morphological and physiological characteristics[1-3]. From the close relationship between the two species, it was generally believed that *B. mandarina* was the original type of the *B. mori* [4]. Due to long-term natural selection, there was a different resistance to insecticides between the two species [5]. *B. mori* had weak resistance to insecticide, and its production was reduced by more than 30% annually because of insecticide poisoning. On the other hand, being one of the major pests in mulberry fields, *B. mandarina* showed increasing resistance to insecticide owing to its wide use.

Acetylcholinesterase (AchE[2] EC 3.1.1.7) which was encoded by acetylcholinesterase gene (*ace*) can terminate neurotransmission in postsynaptic membrane by hydrolysis of neurotransmitter, Acetylcholine (ACh) [6]. Organophosphate insecticide was currently one of the major insecticides used in farming, and AChE was one of the principal targets of insecticides. The organophosphate and carbamate insecticides inhibited AChE, resulting in the accumulation of ACh in postsynaptic membrane, and then excess ACh caused desensitization of AChR, inducing confusion of ACh signaling [7].

Insect AChE gene was firstly cloned from *Drosophila melanogaster*[8]. Alterations in the structure of AChE were the main reasons for its insensitivity to organophosphate insecticides. According to researches into resistant strains of *D. melanogaster*, there were five mutations in AChE including F115S, I119V, I119T, G303A and F368Y, each of which could cause AChE insensitivity to organophosphate insecticides, thus increasing mutants' resistance[9]. Moreover,

based on researches into resistant strains of *Bactrocera oleae*[10], *Anopheles gambiae* [11], *Aedes aegypti* [12], mutations in AChE, namely, G488S, G119S and G105S were found, respectively.

Recently, the cDNAs of two acetylcholinesterase genes in *B. mori* were cloned and analyzed [13-14]. There were presently no reports regarding the *ace* genes of *B. mandarina*. In order to explore the mechanisms underlying the difference in resistance to organophosphate insecticide between *B. mori* and *B. mandarina*, in this study, full-length cDNAs of *Bmm-ace*1 and *Bmm-ace*2 *of B. mandarina* were cloned. Furthermore, expression of the genes in different tissues and stages was also studied.

## Materials and methods

**Insects.** The larvae of *B. mandarina* (Suzhou strain), maintained in our laboratory, were reared on mulberry leaves under a 12-h light/12-h dark photoperiod.

**Chemicals.** $T_4$ DNA Ligase, plasmid extraction kit and gel Extraction Kit were the products of Shanghai Shenergy Biocolor Bioscience and Technology Company. DNA molecular weight marker, restriction enzymes, reaction buffers and other routine chemical reagents were all purchased from TAKARA Biotechonolgy (Dalian) Co., Ltd. Primers were synthesized by Shanghai Sangon Biological Techonology and Services Co., Ltd. The reagent of phoxim was purchased from Sigma-Aldrich Company.

**Extraction of total RNA and RT-PCR.** The larvae of *B. mandarina* on the third day of $5^{th}$ instar were dissected, and their respective hemolymph, brain, midgut, fat bodies, silk gland and the whole body of each newly molted B. mandarina were selected. Total RNAs were extracted from these samples, respectively, by using TRIzol according to instructions of the manufacturer (TAKARA Biotechonolgy (Dalian) Co., Ltd), and then stored at -70°C for use. RT-PCR was carried out by using M-MLV RTase cDNA Synthesis Kit according to instructions of the manufacturer (TAKARA Biotechonolgy (Dalian) Co., Ltd). Primers, Type P1 (5'-TTG TGG GTG TAG GTG CCA GCG ACG GTA T-3') and Type M1 (5'- ACT TAT ATG GTG TAT TTG AAC AGT GCT GTG CCT GTA-3'), were designed according to sequences 26 bp upstream of and 2029 bp downstream of ATG of *ace*1 of *B. mori* (GenBank Accession No. DQ186605), respectively, and PCR cycling conditions were as follows: 94 °C for 3 min; 35 cycles of 98 °C for 20 s, 68 °C for 3 min 30 sec; and a final extension at 72 °C for 10 min. Primers, *ace*2 P2 (5'- GAA TCA CAA TGA TCA ACT ACG GCA AGA TT-3' ) and *ace*2 M2 (5'- TAC AAA GCA ATA GTG ATT GCC AAA GTG GTG-3'), were designed according to sequences 8 bp upstream of and 1 869 bp downstream of *ace*2 of *B. mori* L. (Accession No. DQ115792 ), respectively, and PCR cycling conditions were as follows: 94 °C for 3 min; 35 cycles of 94 °C for 35 sec, 63 °C for 40 sec, 72 °C for 150 sec; and a final extension at 72 °C for 10 min. With the cDNA of brain tissue of *B. mandarina* as template, RT-PCR was carried out.

**The RACE for full length cDNA cloning.** According to the sequencing result of *Bmm-ace*1*,* the following primers for 5' RACE were designed at the 5' of *Bmm-ace*1: Ache1-RT: 5'- (P) TCG CTC GTG ATT AG -3'; AChE1-S1: 5'- ACC AAG ACT CGA AGA CCA CG -3'; AChE1-A1: 5′- CGT GGT GCC TCG CCC GGT GC -3'; AChE1-S2: 5'- GAG AAC CAA GTA TGA GGA GAG -3'; AChe1-A2: 5'- GCT CGT GCG GAC CGG CAA GG -3'. According to the sequencing result of *Bmm-ace*2*,* the following primers for 5' RACE were designed at the 5' of *Bmm-ace*2: AChe2-RT: 5'- (P) TTC GCA AAC GGG AT -3'; AChe2-S1: 5'- CGG TCT CAT CAA AGG ATA CGC -3'; AChe2A1: 5'- GTA GTT TGT GTT GTA GAT GTT GTG G -3'; AChe2-S2: 5'- ACT GTA ATG GGA CGC GAG GT -3'; AChe2-A2: 5'- CAA AAG TAC CGG ATA TGA GC -3'. 5'-RACE was performed according to instructions of TAKARA 5'-Full RACE Core Set.

The 3' anchored oligo-dT primer used in the synthesis of the first-strand cDNA in 3' RACE was 3′Race-dT(5'- ACG CTA CAC GAC TCA CTA ATG GGC (T)12 N -3'), and anchored primer was

3'Race-M (5'- ACG CTA CAC GAC TCA CTA ATG GGC TT -3'). For *Bmm-ace*1, the gene specific primer in the first round was None3 race1 (5'- CAG CAA ACG CTT AAT GAG ATA TTG GGC -3') and the nested specific primer in the second round was None3 race2 (5'- TAA TGG CTG CTA CCA ATA AAC CAG AGC -3'). For *Bmm-ace*2, the gene specific primer in the first round was the 3' race 1 (5'- TCT GGG GAG AAT GGA TGG GTG T -3') and the nested specific primer was the 3' race 2 (5'- CCT CCC TGT AAC CCT TCT CAC CAC -3').

**Tissues and development stages expression of *ace* from *B. mandarina.*** The following primers for *Actin*-3 were designed: *Actin*-3 P1 (5'- AAC ACC CCG TCC TGC TCA CTG -3') and *Actin*-3 P2 (5'- GGG CGA GAC GTG TGA TTT CCT -3'). According to *Bmm-ace*1 and *Bmm-ace*2 sequences, the following primers across introns were designed: 814 ace P1 (5'- CCG ACG GAT ATT TGA ACC A -3'), 814 ace P2 (5'- GTG TAG TAA TGA GGC GAA GAC C -3'), 814 ace1P1 (5'- ATG GTC GGA GAC TAT CAT TTC ACT -3') and 814 ace1 P2 (5'- GCG GCT CTG GTT TAT TGG T -3'). The cDNAs of hemolymph, brain tissue, midgut, fat body, silk gland and the whole body of each stage of *B. mandarina* were used as templates and normalized by *Actin*-3 gene, and then the expression of *ace*1 and *ace*2 was studied in these tissues of *B. mandarina*. PCR cycling conditions for *Actin*-3 were as follows: 94 °C for 2 min; 22 cycles of 94 °C for 30 sec, 60 °C for 30 sec, 72 °C for 30 sec; and a final extension at 72 °C for 10 min. PCR cycling conditions for *ace*1 were as follows: 94 °C for 2 min; 28 cycles of 94 °C for 30 sec, 52.9 °C for 30 sec, 72 °C for 30 sec; and a final extension at 72 °C for 10 min. PCR cycling conditions for *ace*2 were as follows: 94 °C for 2 min; 28 cycles of 94 °C for 30 sec, 51.1 °C for 30 sec, 72 °C for 30 sec; and a final extension at 72 °C for 10 min.

## Results

**Cloning of full-length *Bmm-ace*1 and *Bmm-ace*2 cDNAs.** With the total RNA of brain tissue of *B. mandarina* as template, two fragments with the length of 2 078 bp and 1 917 bp were amplified by RT-PCR, respectively. Two fragments of 336 bp and 333 bp for the 5' UTR of the genes *Bmm-ace*1 and *Bmm-ace*2 containing the overlapping sequence were amplified in 5' RACE. In the same way, the fragments with 144 bp *ace*1 and 225 bp *ace*2 containing the overlapping sequence were obtained in 3'RACE. The full-length fragments of the genes of *Bmm-ace*1 and *Bmm-ace*2 were obtained. The *Bmm-ace*1 gene contains a 2 052 bp ORF, 231 bp and 140 bp of 5' UTR and 3'UTR, respectively, while the *Bmm-ace*2 gene contains a 1 917 bp ORF, 333 bp and 225 bp of 5' UTR and 3'UTR.

Comparison of amino acid sequences encoded by *Bmm-ace*1 and *Bm-ace*1 (EU328261) showed that there were 681 identical amino acid residues of 683, with 2 mutations, S307P and G664S. By comparing *Bmm-ace*2 and *Bm-ace*2 (EU328262) amino acid sequences, the four mutations including M18I, N233S, I310V and G621S634 were found in the amino acid residues.

**Gene expression in tissues and development stages.** By RT-PCR assay, the results showed that *Bmm-ace*1 was highly expressed in brain and fat bodies. However, the former was with minor expression while the latter without detectable expression in midgut. *Bmm-ace*2 was expressed in the five tissues tested with high expression in brain and fat bodies. The expression of *Bmm-ace*1and *Bmm-ace*2 decreased gradually from 1$^{st}$ instar to 5$^{th}$ instar stage, and *Bmm-ace*1 decreased greatly than *Bmm-ace*2.

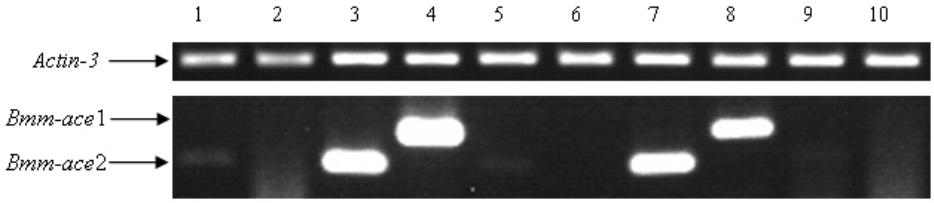


Fig. 1 Expression distribution of *aces* in different tissues of *B. mandarina*
1-2: hemolymph 3-4: brain 5-6: midgut 7-8:fat body 9-10:silk gland

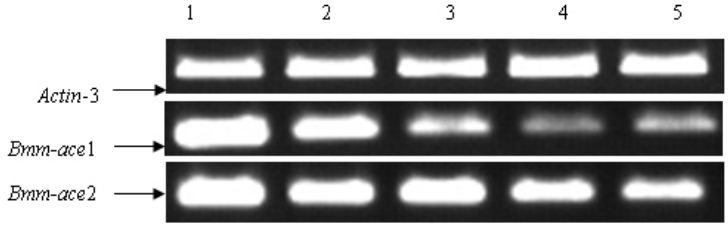


Fig. 2 Expression analysis of *ace*s in different instars of *B. mandarina*
1-Newly-hatched *B. mandarina*; 2-2nd instar newly molted *B. mandarina*; 3-3rd instar newly molted *B. mandarina*; 4-4th instar newly molted *B. mandarina*; 5-5th instar newly molted *B. mandarina*

## Discussion

*B. mandarina* was long regarded as a pest in mulberry fields. However, with the development of the research on functional genomics of *B. mori* in recent years, importance had been attached to *B. mandarina* in that genes of *B. mandarina* were used to compare with their homologs in *B. mori.* In this study, we firstly obtained full-length sequences of two *ace* genes from *B. mandarina* by using RACE, according to the homology genes in other *Lepidopteran* insects (Seino *et al*., 2007; Hall and Spierer, 1986; Gao and Zhu, 2002).

Compared with their respective homologs, *Bm-ace*1 and *Bm-ace*2, the genes of *Bmm-ace*1 and *Bmm-ace*2 cloned in this study had some corresponding amino acid mutations. Two mutations (G664S and S307P) occurred in the *ace*1 gene, and four mutations (M18I, N233S, I310V and G621S) occurred in the *ace*2 gene. Especially, two mutations (G-to-S and I-to-V) of the *ace*2 gene might be closely related to organophosphate insecticide resistance as mentioned in the introduction. However, the speculation should be verified by comparing the differences of organophosphate insecticide metabolism between *B. mori* and *B. mandarina.*

## Acknowledgments

This work was supported by the National Special Public Sector Research (nyhyzx07-020) and the Project SYN201009 Supported by Science and Technology Planning Project of Suzhou.

## References:

[1] B. L. Astaurov, M. D. Golysheva and I. S. Rovinskaya: Cytology Vol. 1(1959), p. 327

[2] Q. Xia, Z. Zhou and C. Lu: Science Vol. 306 (2004), p. 1937

[3] Yoshitake N J. Sericult. Sci. Jpn. Vol. 37 (1968), p. 83

[4] Y. Banno , T. Nakamura and E. Nagashima: Genome. Vol. 47 (2004), p. 96

[5] W.D. Shen, B. Li and P. Ji. Science of Sericulture. 29 (2003), p. 375

[6] D. Fournier, A. Mutero: Comparative Biochemistry and Physiology Part C: Pharmacology, Toxicology and Endocrinology Volume 108, Issue 1, May (1994), p. 19

[7] G. Voss, F. Matsumura: Nature Vol. 202 (1964), p. 319

[8] L. M. Hall, P. Spierer: EMBO J Vol. 5 (1986), p. 2949

[9] A. Mutero, M. Pralavorio and J.M. Bride: Proc. Natl. Acad. Sci. USA. 91 (1994), p. 5922

[10] J.G. Vontas, M.J. Hejazi and N.J. Hawkes: Insect Mol. Biol. Vol. 11(2002), p. 329

[11] M. Weill, G. Lutfalla and E. Morgensen: Nature Vol. 423 (2003), p. 137

[12] R.H. Ffrench-constant, B. Pittendrigh and A. Vaughan: Insecticide Resistance: From Mechanisms to Management. UK: CABI publishing, (1998), p. 9

[13] A. Seino, T. Kazuma and A. J. Tan: Pesticide Biochemistry and Physiology Vol. 88 (2007), p. 921

[14] J. Y. Shang, Y. M. Shao and G. J. Lang, Insect Science Vol. 14 (6) (2007), p. 443

*Advanced Materials Research Vols. 175-176 (2011) pp 56-60*

*doi:10.4028/www.scientific.net/AMR.175-176.56*

# Expression Profiles of Glutathione S-transferase Genes in *Bombyx mori* Exposed to NaF

Guodong Zhao[1,2,a], Yiling Zhang[1,2,b], Ruixian Wang[1,2,c], Sisi Zhao[1,2,d], Ran Peng[1,2,e], Baojin Su[1,2,f], Bing Li[1,2,g], Yuhua Chen[1,2,h], Weide Shen[1,2,i], Zhengguo Wei[1,2,j]

[1] National Engineering Laboratory for Modern Silk, Soochow University, Suzhou, 215123, China

[2] School of Basic Medicine and Biological Sciences, Soochow University, Suzhou, 215123, China

[a]zgd-66@163.com, [b]zhangyiling008@126.com, [c]wrx19860312@163.com, [d]zhaosisi2006@yahoo.com.cn, [e]ohpenny2008@163.com, [f]subaojin@126.com, [g]sdlibing@hotmail.com, [h]chenyh1973@hotmail.com, [i]shenwd@suda.edu.cn, [j]Corresponding author, szwei2002@126.com

**Keywords:** *Bombyx mori*; *BmGST* genes; Quantified transcription level; Tissue-specific expression; Induced expression.

**Abstract.** In order to explore the roles of *Bombyx mori* glutathione S-transferase gene (*BmGST*) in detoxification and resistance to insecticides, we used real-time PCR method to detect the transcription levels of five *BmGST* genes in different tissues of the 5th instar larvae feeding on sodium fluoride treated mulberry leaves. The detection results were normalized by using 3 internal reference genes. The results indicated that the transcription levels of *BmGSTs* were different in various tissues. Transcription of *BmGST* genes could be induced by NaF, The normalized data with the above 3 internal reference genes indicated that, it is very important to choose adequate internal reference genes so as to ensure the reliability of the detection results.

## Introduction

Living organisms are very sensitive to chemicals such as insecticides and chemokines, and need intricate defensive mechanisms to defend them from the effects of such noxious substances [1]. The Glutathione S-transferases (GSTs) are a large family of multifunctional enzymes, many of which play an important role in detoxification[2]. The insect GSTs are classified into Delta, Epsilon, Omega, Theta, Sigma, and Zeta classes, as well as a number that are unclassified [3].

About 70% of agricultural insect pests are lepidopteran species. The silkworm (*Bombyx mori*) is both an important economic species and a model lepidopteran insect, and is therefore an ideal candidate for the study of detoxification processes in lepidoptera. Yamamoto has cloned and identified a sigma-class GST from the silkworm [4]. Yu has identified BmGSTs and analyzed their genomic organization [5]. Some studies have indicated that glycometabolism and the activities of several kinds of enzymes can be affected by insecticides and fluoride [6-7]. However, the mechanism of sodium fluoride (NaF) induced *BmGST* expression remains unclear.

## Materials and methods

***Bombyx mori* and their dissection.** The larvae (strain Haoyue) were reared on mulberry leaves at 25±1°C at a relative humidity of 60-75%. 2 h, 4 h, 8 h, 12 h, 24 h and 48 h after feeding with sodium fluoride, the larvae were dissected.

**Sample preparation.** Total RNA was simultaneously extracted from various tissues of *B. mori* larvae using TRNzol-A$^+$ Total RNA Reagent according to the manufacturer's instructions. The RNA portion was treated with DNase I, and the total RNA was used as a template to synthesize the cDNA chain by reverse transcription.

**Primers for real-time PCR.** The primer pairs corresponding to *BmGSTs* and three internal reference genes are listed in Table 1.

Table 1 Primer pairs for Real-time PCR

| Target gene | Primer Sequence | Tm of primer（°C） | length of product |
|---|---|---|---|
| *Actin*3 | F: 5′-CGGCTACTCGTTCACTACC-3′ | 59.72 | 147 bp |
| | R: 5′-CCGTCGGGAAGTTCGTAAG-3′ | 59.72 | |
| *GAPDH* | F: 5′-TGTTGAGGGCTTGATGAC-3′ | 55.02 | 150 bp |
| | R: 5′-ACCTTACCCACAGCTTTG-3′ | 55.02 | |
| 28S rRNA | F: 5′-CCCAGTGCTCTGAATGTCAAC-3′ | 59.97 | 150 bp |
| | R: 5′-AGATAGGGACAGTGGGAATCTC-3′ | 60.07 | |
| *BmGSTe*2 | F: 5′-ATCTGGTGATTGCCGATAGC-3′ | 57.80 | 150 bp |
| | R: 5′-TGGGGAATAGAATGGTCGC-3′ | 57.56 | |
| *BmGSTe*5 | F: 5′-GCGGCGAGAAAGAAATACG-3′ | 57.56 | 139 bp |
| | R: 5′-CTGATGGAAGTAACGCAGCAA-3′ | 58.01 | |
| *BmGSTo*3 | F: 5′-CTCCGACACTGTCAATGAGGA-3′ | 59.97 | 145 bp |
| | R: 5′-CTCGAACCAAGGCCATATCAT-3′ | 58.01 | |
| *BmGSTz*2 | F: 5′-CGGTCTGAAGAAACATTTGGG-3′ | 58.01 | 129 bp |
| | R: 5′-TGATCTCCGATGCAGTAAGC-3′ | 57.80 | |
| *BmGSTs*1 | F: 5′-GACATGGGGTGATTTCGTG-3′ | 57.56 | 136 bp |
| | R: 5′-AGCCTTCACTTTGGGCTGT-3′ | 57.56 | |

**Real-time PCR protocol.** Real-time PCR was performed in a DNA Engine Option 2 thermal cycler (MJ Research) using the SYBR Premix Ex Taq Kit (TaKaRa). The reaction volume was 20 μl. The qPCR protocol consisted of an initial denaturation at 95°C for 1 min followed by 50 cycles: 95°C for 5 s, 55°C for 10 s, and 72°C for 10 s.

**Real-time qPCR data analysis.** Based on the standard curve method, the threshold cycle (Ct) model was adopted for relative quantification in this study [8].The data of RT-PCR were processed with Sequence detection software version 1.3.1, and were regulated according to the method of Schefe [9].

## Results

**Tissue-specific expression of BmGST genes.** The *BmGSTe*5 gene was mainly expressed in the midgut. The *BmGSTs*1 gene was distributed mainly in the fat body, where its expression level was very high. And the other 3 *BmGST* genes were distributed in all the tissues, where their expression levels were different.

The data above indicated that the expression profiles of *BmGST* genes were similarly in the Malpighian tubule and fatbody while 3 genes were used as the internal reference, respectively. In the midgut, due to the strong Glucose metabolism, the normalized data with the *GAPDH* gene was not credible. Similarly, due to the high expression of *Actin*3 and a large number of synthetic of silk protein in the silk gland, the normalized data with the *Actin*3 and 28S rRNA genes was not credible.

Table 2 The transcription levels of *BmGST* genes in various tissues of *Bombyx mori*

| Gene name | Internal Reference | Relative quantity | | | |
|---|---|---|---|---|---|
| | | Silk gland | Malpighian tubule | Fat body | Midgut |
| *BmGSTe*2 | *Actin*3 | 95.65±0.87 | 113.73±1.12 | 76.69±1.21 | 985.53±5.85 |
| | *GAPDH* | 514.56±2.33 | 250.80±1.35 | 116.33±2.06 | 1 903.47±21.08 |
| | 28S rRNA | 142.43±1.02 | 947.65±6.43 | 66.77±2.58 | 497.92±3.33 |
| *BmGSTe*5 | *Actin*3 | 17.65±0.02 | 0.65±0.02 | 24.03±0.72 | 1 921.94±15.68 |
| | *GAPDH* | 94.93±0.67 | 1.44±0.04 | 36.44±0.68 | 3 711.98±6.73 |
| | 28S rRNA | 26.28±0.11 | 5.44±0.38 | 20.92±0.83 | 971.03±3.75 |
| *BmGSTo*3 | *Actin*3 | 284.50±1.92 | 548.19±2.35 | 131.17±0.41 | 632.36±1.92 |
| | *GAPDH* | 1 530.47±5.85 | 1 208.87±9.56 | 198.96±2.92 | 1 221.32±2.11 |
| | 28S rRNA | 423.65±1.97 | 4 567.65±9.99 | 114.20±10.31 | 319.49±1.58 |
| *BmGSTz*2 | *Actin*3 | 20.46±0.15 | 9.77±0.86 | 9.62±0.05 | 21.18±0.33 |
| | *GAPDH* | 110.04±1.32 | 21.55±0.92 | 14.59±0.07 | 40.91±1.82 |
| | 28S rRNA | 30.46±0.33 | 81.43±2.24 | 8.37±0.58 | 10.70±0.15 |
| *BmGSTs*1 | *Actin*3 | 458.53±2.01 | 211.47±1.45 | 214 167.34±71.02 | 4 597.76±7.31 |
| | *GAPDH* | 2 466.72±8.57 | 466.32±3.60 | 324 840.74±23.83 | 8 879.97±9.68 |
| | 28S rRNA | 682.81±2.30 | 1 761.98±8.52 | 18 644.75±97.57 | 2 322.93±4.32 |

**The affect of NaF on the transcription levels of *BmGST* genes in different tissues of fifth instar larvae.** In the Malpighian tubule of larvae fed with NaF treated mulberry leaves, the *BmGSTe*2 gene showed expression profile with significant induction 2 to 4 h after feeding, peaking at 4 h and declining thereafter (Fig. 1). The main gene in the fat body was *BmGSTe*2 where its expression level was very high.

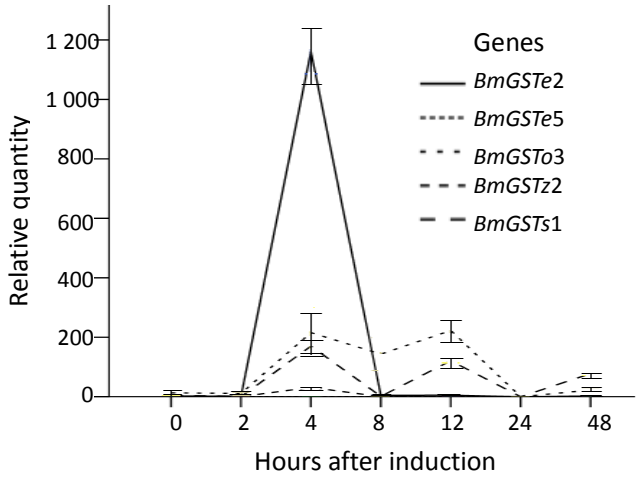


Fig. 1 The affect of NaF on the transcription levels of *BmGST* genes in Malpighian tubule

As shown in Table 3, In the fat body of larvae fed with NaF treated mulberry leaves, the five *BmGST* genes showed similar expression profiles, with significant induction 12 to 24 h after feeding, peaking at 24 h and declining thereafter. The transcription levels of *BmGSTs*1 and *BmGSTo*3 genes were very high, suggesting that they play important metabolic roles in the fat body.

Table 3 The affect of NaF on the transcription levels of *BmGST* genes in the fat body

| Genes | The time after induction | | | | | | |
|---|---|---|---|---|---|---|---|
| | 0 h | 2 h | 4 h | 8 h | 12 h | 24 h | 48 h |
| *BmGSTe2* | 66.77±2.58 | 2.91±0.08 | 10.70±0.24 | 8.51±2.05 | 29.77±1.67 | 517.37±4.92 | 75.13±3.72 |
| *BmGSTe5* | 20.92±0.83 | 30.41±5.32 | 76.21±3.25 | 17.93±4.81 | 109.70±8.46 | 1 456.01±9.31 | 657.67±7.57 |
| *BmGSTo3* | 114.20±10.31 | 112.41±9.13 | 4 726.48±21.33 | 2 358.73±19.35 | 3 824.31±18.42 | 17 238.01±76.63 | 754.55±5.82 |
| *BmGSTz2* | 8.37±0.58 | 6.56±0.89 | 37.57±2.38 | 18.77±3.18 | 16.82±1.92 | 523.44±4.33 | 68.98±2.31 |
| *BmGSTs*1 | 18 644.75±97.57 | 2 238.54±85.45 | 21 392.91±93.33 | 9 489.99±32.76 | 16 227.56±99.35 | 145 728.82±151.69 | 24 849.42±87.92 |

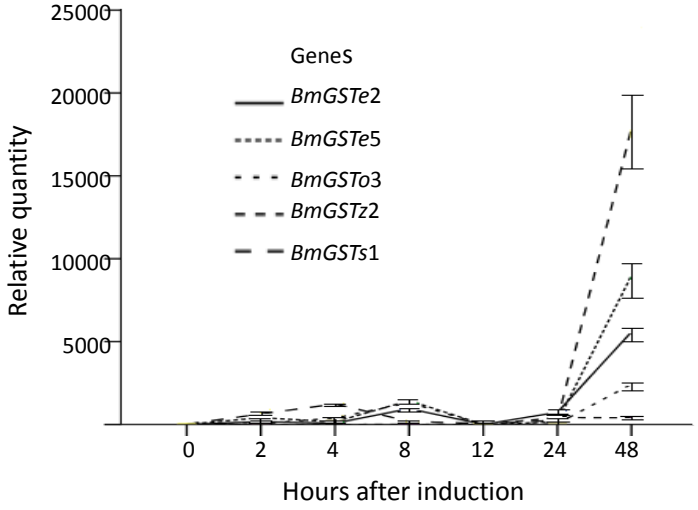


Fig. 2 The affect of NaF on the transcription levels of *BmGST* genes in the midgut

As shown in Fig. 2, in the midgut of larvae fed with NaF treated mulberry leaves, the 5 *BmGST* genes showed similar expression profiles, with significant induction 24 to 48 h after feeding, but we did not get the samples and analyze 48 h after feeding, so we need further experiment.

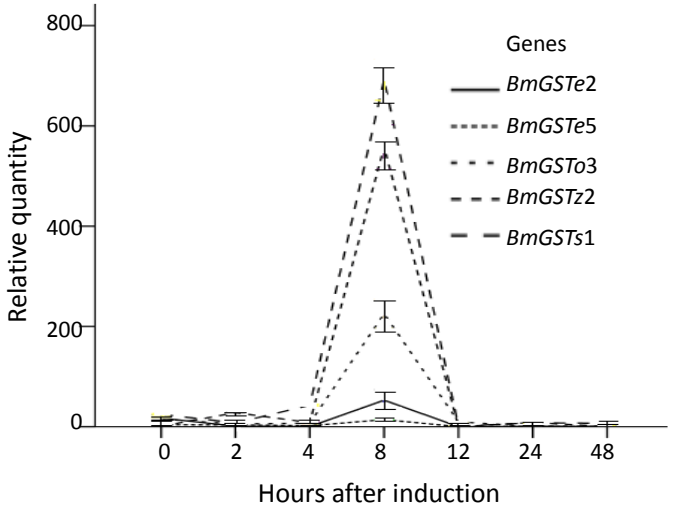


Fig. 3 The affect of NaF on the transcription levels of *BmGST* genes in the silk gland

In the silk gland of larvae fed with NaF treated mulberry leaves, the 5 *BmGST* genes showed the expression profiles, with significant induction 4 to 8 h after feeding, peaking at 8 h and declining thereafter (Fig. 3). The transcription levels of *BmGSTs*1 and *BmGSTz*2 genes were very high, suggesting that they play an important metabolic role in the silk gland.

## Discussion

The results of this study show that *BmGSTs*1 gene expressed mainly in the fat body, and the *BmGSTe*5 gene was distributed mainly in the midgut where its expression level was very high. Findings are in line with previous studies by Q.Y.Yu [5]. The expression of *BmGST* genes are the highest in the midgut and fat body, suggesting their involvement in detoxification of sodium fluoride.

Currently the normalization with a single internal reference is not very accurate[10]. The house keeping genes as internal references show different expression profiles in different tissues and growth stages. In this study, the detection results were normalized by using 3 internal reference genes, and we choose a suitable internal reference relatively to determine the transcription levels in any tissue, this is a new attempt, we can find some more suitable internal reference genes by analyzing more data and exploring more reasonable methods.

## Acknowledgements

This work was supported by a grant from the National High Technology Research and Development Program of China (No. 2006AA10A118).

## References

[1] I. Kostaropoulos, A.I. Papadopoulos, A. Metaxakis: Insect. Biochem. Mol. Biol.Vol. 31.(2001), p. 313

[2] D. Sheehan, G. Meade, V.M. Foley: J. Bio. Chem. Vol. 360, (2001), p. 1

[3] G. Chelvanayagam, M.W. Parker and P.G. Board: Chem. Biol. Interact Vol. 133, (2001), p. 256

[4] K. Yamamoto, P.B. Zhang, Y. Banno: Appl. Entomol. Vol. 130, (2006), p. 515

[5] Q.Y. Yu, C. Lu, B. Li: Insect. Biochem. Mol. Bio Vol. 1.38 (2008), p. 1158

[6] Y.Y. Chen, Y.C. Wu: Sericologia. Vol. 34, (1994), p. 627

[7] Y.G. Miao, L.J. Jiang, D. Bharathi: Fluoride Vol. 37, (2004), p. 117

[8] K.J. Livak, T.D. Schmittgen: Methods Vol. 25 (2001), p. 402

[9] J.H. Schefe, K.E. Lehmann, I.R. Buschmann: J. Mol. Med. Vol. 84, (2006), p. 901

[10] B.K. Jacques, W. R. Rain, A.G. Belinda: Lab Investigation Vol. 85, (2005), p. 154

*Advanced Materials Research Vols. 175-176 (2011) pp 61-66*

*doi:10.4028/www.scientific.net/AMR.175-176.61*

# Expression Profiles of P450 4 Family Genes in Larval Fatbody and Midgut of *Bombyx mori* Exposed to Rutin

Ruina Gao[1,2,a], Ting Zhang[1,2,b], Sisi Zhao[1,2,c], Bing Li[1,2,3,d], Yuhua Chen[1,2,3,e], Weide Shen[1,2,3,f], Zhengguo Wei[1,2,3,g]

[1] The State Engineering Laboratory of Modern Silk, Suzhou 215123, China

[2] Pre-clinical Medical and Biological Science College, Soochow University, Suzhou 215123, China

[3] Institute of Sericulture, Soochow University, Suzhou 215123, China

[a]gaoruina2008@163.com, [b]eward1986@163.com, [c]zhaosisi2006@yahoo.com.cn, [d]sdlibing@hotmail.com, [e]chenyh1973@hotmail.com, [f]shenwd@suda.edu.cn, [g]Corresponding author, szwei2002@126.com

**Keywords:** silkworm; CYP; rutin; dual-spike-in qPCR; expression level.

**Abstract.** The present study was undertaken to clarify the change of induction of *CYP4M5* and *CYP4M9* expression level by rutin. In this study, we used dual-spike-in qPCR to examine expression profiles of the silkworm Bombyx mori *CYP4M5* and *CYP4M9* genes in the larval midgut and fatbody after exposure to rutin. In organization-course study, rutin at middle concentration ($5\times10^{-2}$ng/μL) caused significant upregulation of *CYP4M5* and *CYP4M9* genes at early time point (2h) in fatbody, higher concentration ($5\times10^{-1}$ng/μL) did secondly, while lower concentration ($5\times10^{-3}$ng/μL) caused little change. In the midgut of silkworm, rutin in all concentrations didn't affect the expression of the two genes. These findings showed that induction of *CYP4M5* and *CYP4M9* expression level by rutin are concentration depended and tissue-specific.Collectively, *CYP4M5* and *CYP4M9* genes may have some relationships with metabolism of rutin in silkworm.

## Introduction

It is well known that multigene families encoding cytochrome P450, glutathione S-transferase (GST) and esterase enable animals to avoid xenobiotic challenges from the environment, such as toxic plants or microbial chemicals encountered in food, drugs, pesticides or organic pollutants[1]. Recent identification of the P450 genes and several other molecules involved in metabolic of the resistance in other insets [2]had opened a door to a better understanding of expression regulation silkworm *CYP4M5* and *CYP4M9* genes exposed to exogenous inducer.

Secondary metabolites are generated during normal physiological metabolism in plant, such as rutin, alkaloids, flavonoids, saponins II, coumaricelements and other volatile substances and so on. P450 genes family enable insects to avoid xenobiotic challenges from the environment[3]. Gao Xi-Wu *et al.* [4] have studied the activity of detoxification enzymes and some target enzymes in *Helicoverpa armigera* in vivo after exposed to quercetin. In *Bombyx mori*, Wang Dong [5]has reported that the expression of *CYP4M5* and *CYP4M9* genes were repressed in first larval after exposed to rutin and quercetin by RT-PCR.

We studied the expression of *CYP4M5* and *CYP4M9* in the fatbody and midgut of *Bombyx mori* after exposure to secondary metabolites(rutin) using dual-spike-in qPCR in this study.

## Materials and methods

**Silkworms.** Larvae of the silkworm, *Bombyx mori*, used in this study were DAZAO and were supplied by the Sericultural Research Institute, Suzhou University. Silkworms were reared on fresh mulberry leaves at 26°C and 60%-75% RH.

**Rutin exposure and tissue collection.** Rutin(Sigma) dissolved in boiling water was applied to three concentrations rutin solutions($5\times10^{-1}$ng/μL, $5\times10^{-2}$ng/μL, $5\times10^{-3}$ng/μL) in which leaves were immersed for 5s and allowed to dry naturally, before being fed to second day, fifth instar silkworms. Two hours later, the silk worms were allowed to feed on untreated mulberry leaves. A control group was treated with $ddH_2O$. The larvae were dissected at 0h, 2h, 4h, 8h, 12h, 24h, 48h, 72h and then the tissues of midgut and fatbody were collected after washed three times in excess cold PBS buffer and stored at -80°C. Each treatment was applied in triplicate. Three replicates of five pooled silkworm individuals were used for each sample.

**RNA and DNA extraction.** Total RNA and DNA were simultaneously extracted from various tissues of *Bomybx mori* larvae using TRNzol-$A^+$ Total RNA Reagent (Tiangen Biotech) according to the manufacturer's instructions. DNA within RNA samples was digested with RNase-free DNase I.

**Reverse transcription.** The total RNA was used as a template to synthesize the primary complementary DNA (cDNA) chain by reverse transcription, following the manufacturer's instructions (TaKaRa).

**Exogenous RNA and DNA references.** In this study, in vitro transcribed *IFP2* mRNA, and plasmid pPigT7 (4 983 bp) were used as the spike references for sample RNA and sample DNA, respectively.

**Primer design.** The same primer pair was used when determining the mRNA level and DNA copy number of a certain gene and listed in Table 1.

Table 1 Primer pairs for Real-time PCR

| Target gene | Primer sequence | Tm of primer(°C) | length of product(bp) | Tm of product (°C) |
|---|---|---|---|---|
| *CYP4M5* | F:5'-tatgaaatacccgccggttcg-3'<br>R:5'-ggtatgtatgcgtacggatgtc-3' | 59.97<br>60.07 | 146 | 82 |
| *CYP4M9* | F:5'-tcgccgtcaatacataagaggg-3'<br>R:5'-ccatctcgttctgcctttagc-3' | 60.07<br>59.97 | 138 | 80 |
| *IFP2* | F:5'-ctgtgcacggtagttgtc-3'<br>R:5'-tcagtacttccggtatctcg-3' | 57.30<br>57.80 | 144 | 80 |

Note. Tm, melting temperature; F, forward; R, reverse.

**Quantitative real-time RT-PCR.** Real-time PCR was performed using the SYBR Premix Ex Taq Kit (TaKaRa). The reaction volume was 20 μL. The qPCR protocol consisted of an initial denaturation at 95°C for 1 min followed by 45 cycles: 95°C for 15 s, 60°C for 31 s, and Dissociation Stage.

**Real-time qPCR data analysis.** Based on the dual-spike-in qPCR method, the transcription level per gene copy of a target mRNA can be calculated from the Ct for the mRNA (cDNA) and DNA templates, and the slope of the qPCR curve. The slope of the qPCR curve for a certain gene can be estimated from the standard curve and are listed in Table 2.

Table 2 The slope of standard curve for each gene

| Target gene | *IFP2* | *CYP4M5* | *CYP4M9* |
|---|---|---|---|
| *a* value | -3.6882 | -3.1813 | -3.2932 |

## Results

**Rutin-induced transcription of *CYP4M5* and *CYP4M9* genes in fatbody.** We measured the transcription levels of *CYP4M5* (Fig. 1 A, B) and *CYP4M9* (Fig. 1 C, D) genes in fatbody of *Bombyx mori* treated with rutin by dual-spike-in qPCR. Rutin caused upregulation of the two genes mRNA at higher concentrations ($5\times10^{-1}$ng/μL, $5\times10^{-2}$ng/μL), and *CYP4M5* showed greater upregulation than *CYP4M9*. While we observed no significant effect on these genes at lower concentration solution ($5\times10^{-3}$ng/μL) . A significant increase in expression of *CYP4M5* and *CYP4M9* genes were observed at 2h, 4h after exposure to $5\times10^{-2}$ng/μL rutin and the maximum reached to 1282.3, 39.8 respectively. The expression levels of *CYP4M5* and *CYP4M9* genes were reached maximum (53.27, 5.4) at 48 h, 24h respectively after exposure to $5\times10^{-1}$ng/μL rutin .

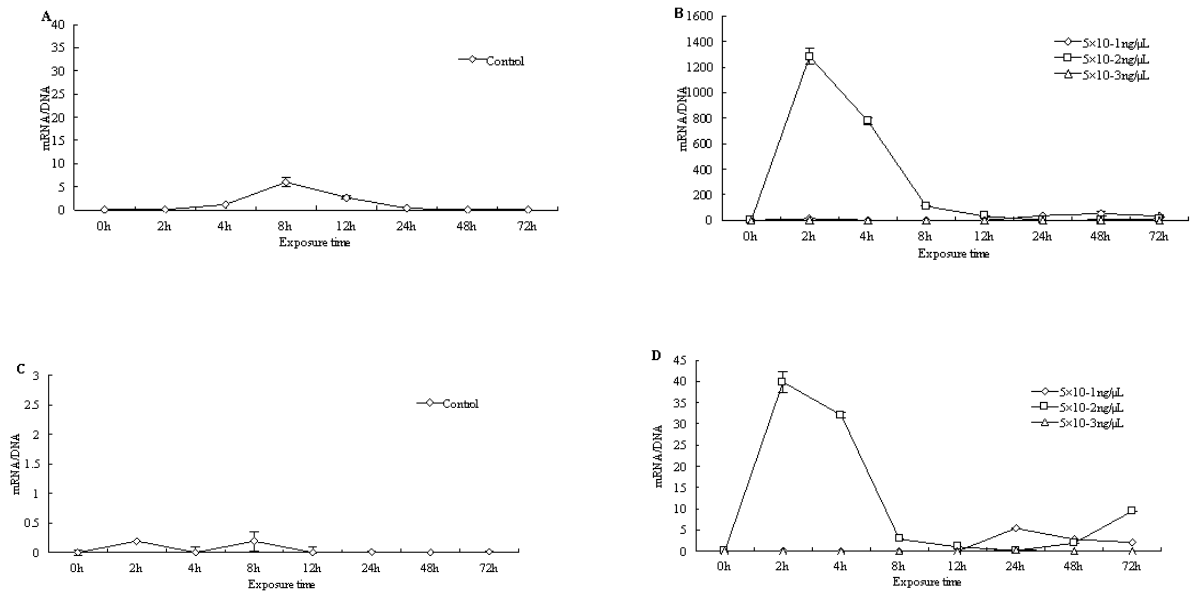


Fig. 1 Expression profile of *CYP4M5* (A,B)and *CYP4M9* (C,D)in *B. mori* larvae fatbody exposed to rutin .The larvae on the second day of the fifth instar were exposed to rutin of three concentrations. Each treatment was applied in triplicate. CYP mRNA expression values were normalized relative to *IFP2* expression shown as mean ± SE (n = 3).

**Rutin-induced transcription of *CYP4M5* and *CYP4M9* genes in midgut.** As showed in Fig.2, the expression levels of *CYP4M5* (Fig. 2 A, B) and *CYP4M9* (Fig. 2 C, D) genes in the midgut had a significant upregulation at 24h, 48h after exposure to $5\times10^{-2}$ng/μL rutin.*CYP4M9* showed greater upregulation than *CYP4M5*, and maximum reached to 36.54, 27.24 respectively. There were no significant effect on these genes at higer concentration solution ($5\times10^{-1}$ng/μL) and lower concentration solution ($5\times10^{-3}$ng/μL).

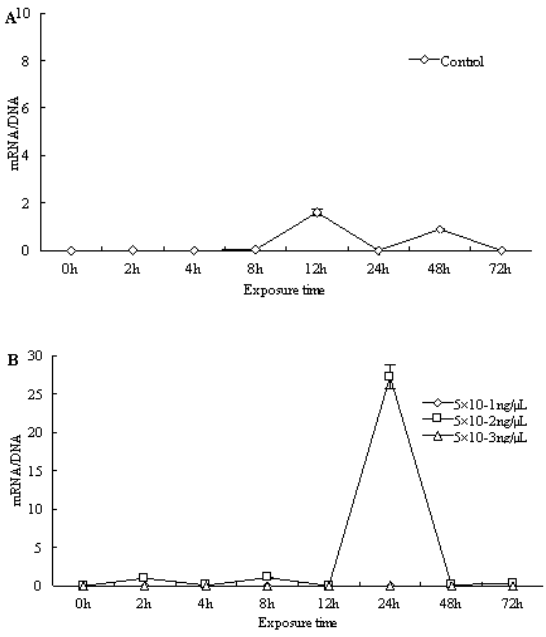

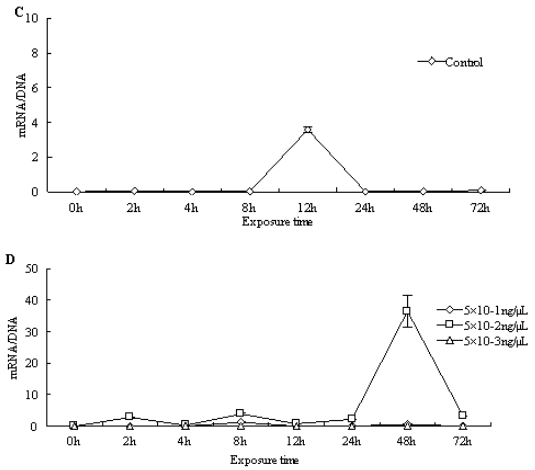


Fig. 2 Expression profile of *CYP4M5* (A,B)and *CYP4M9* (C,D)in *B. mori* larvae midgut exposed to rutin .The larvae on the second day of the fifth instar were exposed to rutin of three concentrations. Each treatment was applied in triplicate. CYP mRNA expression values were normalized relative to *IFP2* expression shown as mean ± SE (n = 3).

## Discussion

It was reported that deltamethrin was shown to increase the level of *CYP4G11* in *Helicoverpa*[6]. In addition, the rate of transcription of the *CYP4E2* gene is regulated by DDT in DDT resistant strain of *Drosophila*[7]. The silkworm, *Bombyx mori* has been recognized as an economically important animal for silk production, and one of the most important model insects for Lepidoptera genetics and molecular biology [8]. It is therefore an ideal species in which to study the role of P450 in biological processes with resistance. Our study provided evidences that rutin is primarily responsible for the regulation of *CYP4M5* and *CYP4M9* expression in *Bombyx mori*. At the same time, these results suggest that the silkworm larval expression of *CYP4M5* varied from that of *CYP4M9*, which may be related to gene structure, the sensitivity of the gene to inducer, relevant regulatory elements or other regulatory factors.

Datas improve us to understanding of the expression, regulation and function of P450 proteins in *Bombyx mori* midgut and fatbody. Investigation of the species difference and of the underlying molecular mechanisms of the differential regulation of P450 genes is necessary for a deeper understanding of the regulation of insect development. Further research on the regulatory elements and factors relevant to *CYP4M5* and *CYP4M9* gene expression will be interesting.

## Acknowledgements

Financial support for this work was provided by the National High Technology Research and Development Program of China (No. 2006AA10A118). Thanks are also due to to Dr. Changde Lu, Shanghai Institute for Biological Sciences, Chinese Academy of Sciences, for his kind gift of the plasmid pPigT7 .

**References**

[1] Y. Zhang, Z.G. Wei, Y.Y. Li, Y.H. Chen, W.D. Shen and C.D. Lu: Anal Biochem Vol. 394 (2009), p. 202

[2] A.C. Lu, Z.G. Wei, B. Li and W.D. Shen: Journal of Anhui Agricultural ScienceVol. 37 (12) (2009), p. 5400

[3] D. Sheehan, G. Meade, V.M. Foley and C.A. Dowd: Biochem J Vol. 360 (2001), p.1

[4] P. Cheng, Y.G. Cao, M.Q. Gong: .Journal of Pathogen Biology Vol. 4(1)(2009), p.62

[5] J. Zhao, W.J. Yang, W.H. Zhu: Chinese Bulletin of Life Sciences Vol. 11(3)(1999), p. 127

[6] X.W. Gao, X.L. Dong, Y. Zhao: Chinese Journal of Pesticide Science Vol. 1(3) (1999), p. 56

[7] D. Wang: Identification and Functional Studies of Cytochrome P450 and Carboxylesterase Family Genes from the Silkworm, Bombyx mori (University doctoral dissertation, Suzhou 2009).

[8] B. Pit tendrigh, K. Aronstein, E. Zinkovsky: Insect Biochem Mol Biol Vol. 27 (6) (1997), p. 507

[9] M. Amichost, A. Brun, Cuamy: Paris: John Linney Eurotext (1994) p. 689

[10] Z. Wang, X. Zha, N. He, Z. Xiang, Q. Xia: Molecular cloning and expression analysis of Bmrbp1, the *Bombyx mori* homologue of the Drosophila gene rbp1. Mol Biol Rep. doi:10.1007/s11033-009-9768-z

*Advanced Materials Research Vols. 175-176 (2011) pp 67-71*

*doi:10.4028/www.scientific.net/AMR.175-176.67*

# Standardization of Reference Genes in Silkworm, *Bombyx mori*

Ran Peng[1,2,a] , Baojin Su[1,2,b], Guodong Zhao[1,2,c], Xing Ji [1,2], Sisi Zhao[1,2], Ting Zhang[1,2], Ruina Gao[1,2], Ruixian Wang[1,2], Weide Shen[1,2,3*], Zhengguo Wei[1,2,3*]

[1] The State Engineering Laboratory of Modern Silk, Suzhou Jiangsu, China; [2] Pre-clinical Medical and Biological Science College, Soochow University, Suzhou Jiangsu, China;

[3] Institutes of Sericulture, Soochow University, Suzhou Jiangsu 215123, China;

Corresponding authors: Weide Shen, Zhengguo Wei.
E-mail: ohpenny2008@163.com; szwei2002@126.com

**Keywords:** qRT-PCR; reference gene;standardization; *Bombyx mori.*

**Abstract.** The *Bombyx mori* serves as model organism among the *Lepidoptera* insects. In the post-genomic era, in order to study gene function, the profiling of mRNA transcription has become a popular research field. Real-time quantitative RT-PCR (qRT-PCR) has become established as the sensitive method for detecting the expression level of low abundance mRNA, and it usually chooses one or several reference genes to standardize the expression level of target gene. Since the changes in amplification of reference gene can reflect the changes of RNA production, quality or cDNA synthesis efficiency. So choosing an appropriate reference gene can reduce the differences between tested samples. Based on the comparison of Standardization of three frequently-used reference genes (*GAPDH, Actin-3, 28srRNA*), and decide which is the best way to study gene expression level in silkworm, *Bombyx mori*.

## Introduction

Real-time quantitative RT-PCR (qRT-PCR) has become established as the method of choice for high-throughput and accurate expression profiling of selected genes [1]. For an exact comparison of mRNA transcription in different samples or tissues, it is crucial to choose the appropriate reference gene. Ideally the housekeeping gene should not be regulated or influenced by the experimental procedure. Prominent genes were glyceraldehydes 3-phosphatedehydrogenase (GAPDH), β-actin (Act), and 18S and 28S rRNAs. These proteins are essential for the maintenance of cell function; it is generally assumed that they are constitutively expressed at similar levels in all cell types and tissues [2].However, it has been reported that these genes as well as alternatives, like rRNA genes, are unsuitable references, because their transcriptions are significantly regulated in various experimental settings and variable in different tissues [3]. Moreover, several reports indicate that the expression of these housekeeping genes varies across tissues and cell types, during cell proliferation and development [4]. For instance, GAPDH mRNA level is widely altered in cultured cells in response to various stimuli, including hypoxia, insulin, dexamethasone, mitogens and epidermal growth factor (EGF) as well as in virally transformed or oncogene-transfected fibroblasts [5,6].

In silkworm *Bombyx mori,* the commonly used reference gene is *Actin-3*. However, to our best understanding, no reports have investigated the variation in expression of reference genes during development and aging. To make our gene quantification measurement more accurate at the mRNA

level, it is necessary to identify genes which are expressed relatively stable during different developmental stages in silkworm B.mori. In the present study, we compared the level of expression of three common housekeeping genes *Actin-3*, *GAPDH* and *28srRNA* in three different tissues fat body, mid-gut and malpighian tube in silkworm, *Bombyx mori*.

**Materials and methods**

**Samples preparation.** Silkworms of Dazao, a Chinese silkworm strain, provided by the Sericulture Institute of Soochow University, were reared on mulberry leaves under stable 12h light and 12h dark photoperiod at 25 ± 1°C and 80% ± 5% RH. Insects were dissected and the fat body, mid-gut and Malpighian tube tube tissues were separated each day (24 h period) of 5th instar larvae.

**Exogenous RNA and DNA references.** In this work, an exogenous RNA was used as the spike reference for sample RNA, and an exogenous DNA that contains the gene of the exogenous RNA was used as the spike reference for sample DNA. The mixture of exogenous RNA and DNA references with a certain ratio was added to the sample homogenate prior to the simultaneous extraction of RNA and DNA, so that the exogenous RNA reference underwent the same process as the sample RNA and the exogenous DNA reference underwent the same process as the sample DNA [6].

**RNA isolation and cDNA cloning.** Total RNA and DNA were simultaneously extracted from various tissues of B. mori larvae using TRNzol-A+ Total RNA Reagent following the manufacturer's instructions. After the RNA portion was treated with RNase-free DNase I, the total RNA was used as template to synthesize the primary complementary DNA (cDNA) chain by reverse transcription following the manufacturer's instructions. The reaction was carried out at 37°C for 1 h in a final volume of 20 μL with 4 μL of 5× reaction buffer, 1 μg of total RNA, 0.5 mM of each deoxynucleoside triphosphate (dNTP), 25 U of RNasin (40 U/μL), 1 μL of 50 μM (dN) 6, 2 μL of 10 μM oligo(dT15), and 200 U of M-MuLV reverse transcriptase (200 U/μL). The DNA portion was treated with phenol/chloroform and ethanol precipitation

**Real-time PCR.** The primer pairs corresponding to target genes are listed in Table 1. Real-time PCR was performed in a DNA Engine Option 2 thermal cycler (MJ Research) using the SYBR Premix Ex Taq Kit (TaKaRa). The reaction volume was 20 μL. The qPCR protocol consisted of an initial denaturation at 95°C for 1 min and then 50 cycles: 95°C for 5 s, 55°C for 10 s, and 72°C for 10 s. The temperature for collecting fluorescence data was 3°C below the melting temperature of each amplified segment.

Table 1 Primer pairs for Real-time PCR and slopes of qPCR curves for genes

| Gene | Primer Sequence（5'-3'） | Function | a Value |
|---|---|---|---|
| *IFP*-2 | F: CTGTGCACGGTAGTTGTC<br>R: TCAGTACTTCCGGTATCTCG | Lepidopteran transposon | -3.6882 |
| *Actin-3* | F: CGGCTACTCGTTCACTACC<br>R: CCGTCGGGAAGTTCGTAAG | Cytoskeleton | -3.1147 |
| 28s rRNA | F: CCCAGTGCTCTGAATGTCAAC<br>R: AGATAGGGACAGTGGGAATCTC | Ribosome subunit | -3.617 |
| *GAPDH* | F: TGTTGAGGGCTTGATGAC<br>R: ACCTTACCCACAGCTTTG | Glycolysis enzyme | -3.1607 |

Based on the standard curve method, the threshold cycle (Ct) model was adopted for the relative quantification in this work. The slope of the qPCR curve for a certain gene can be estimated from the standard curve from serially diluted aliquots of any sample. The slopes of the qPCR curves for the genes are listed in Table 1. Thus, the transcription level per gene copy of a target mRNA can be calculated from the Ct for mRNA (cDNA) and DNA templates and the slope of the qPCR curve.

## Results

Quantitative real-time PCR was used to measure the RNA transcription level of various housekeeping genes in 3 different silkworm tissues: fat body, mid-gut and Malpighian tube. To compare the different RNA transcription levels the Ct values were compared directly. The Ct is defined as the number of cycles needed for the fluorescence signal to reach a specific threshold level of detection and is inversely correlated with the amount of template nucleic acid present in the reaction [7].

**Expression profiles of *Actin-3, GAPDH* and *28srRNA* gene in three different tissues.** In fat body, all three genes have a high expression level on the 4th day of 5th instar larvae, *28srRNA* get the peak point (A). In mid-gut, the expression level of *Actin-3* and *GAPDH* in 5th instar larvae is relatively stable, *28srRNA* reach the peak expression on the 2nd, 3rd, 4th day of 5th instar larvae (B). In Malpighian tube, all of the three genes have a high expression level on the 2nd day of 5th instar larvae , *28srRNA* get the peak point, the expression level of *GAPDH* is relatively flat (C).

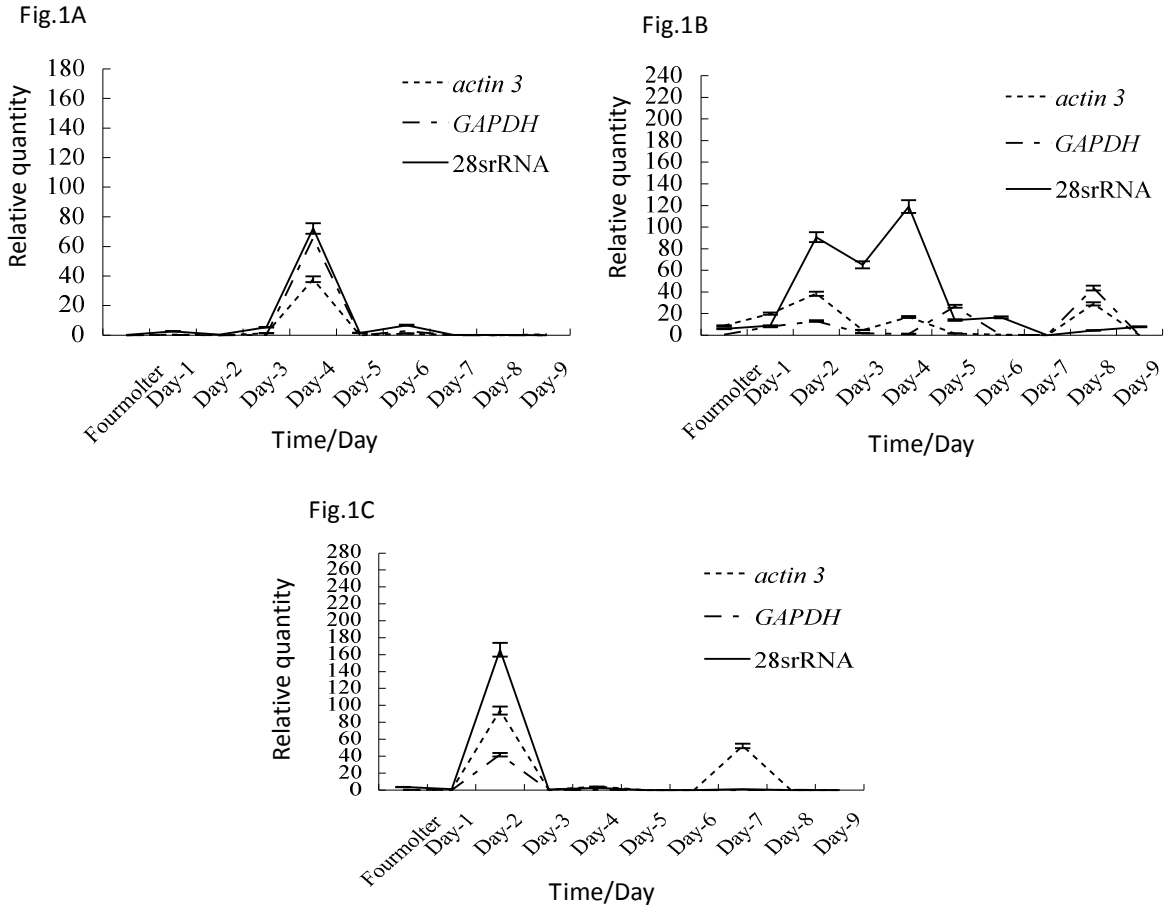


Fig. 1 Transcription levels of *Actin-3, GAPDH* and 28srRNA gene in fat body (A), mit-gut (B) and malpighian tube (C) tissue from fourmolter to the 9$^{th}$ day of 5$^{th}$ instar larvae.

**Steady expression profiles**

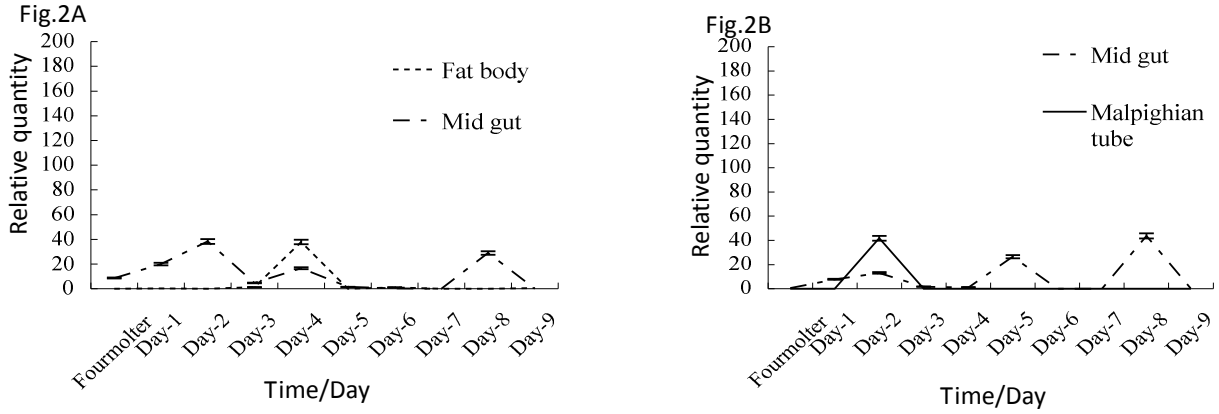


Fig.2 Transcription levels of *Actin-3* gene in fat body and mid-gut tissue (A) and *GAPDH* gene in mid-gut and Malpighian tube tissue (B) from fourmolter to the 9$^{th}$ day of 5$^{th}$ instar larvae.

Expression profiles of *Actin-3* gene in fat body and mid-gut tissues are both steady (Fig.2A). Expression profiles of *GAPDH* gene in mid-gut and Malpighian tube tissues are both steady (Fig.2B).

**Discussion**

Measurement of three frequently-used reference genes (*GAPDH, Actin-3* and 28srRNA) transcript abundance was originally selected as a normalizer for other expressions because it encodes for a protein with a housekeeping function, *Actin-3* as an actin cytoskeleton gene is a major cytoplasmic structural protein which can control the formation of microtubules, *GAPDH* genes mainly participate in energy metabolism, *GAPDH* is an important glycolytic enzyme that catalyzes the oxidative phosphorylation of glyceraldehyde-3-phosphate to 1,3-diphosphoglycerate. It is a glycolytic intermediate and is therefore expected to be present in all cells and exhibit minimal modulation [8]. 28S constitute of ribosomal RNA, is an rRNA, mainly involved in protein synthesis. They are therefore not always representative of the overall cellular mRNA population. Significant changes in the levels of particular mRNAs may not be accompanied by the same change, or even any change, in rRNAs. The overall protein synthesis level during the Fifth instar silkworm is downward trend, protein synthesis level are high during the early age of 5th instar larvae, then declined. There are some problems these three traditional reference genes commonly use as a standard. Additionally, overall stability of expression levels of *28srRNA* gene is inferior to *Actin-3* and *GAPDH* gene.

In these situations, this led us to consider the probability that, *Actin-3, GAPDH*, *28srRNA* are not always the ideal or even suitable normalizers. Although housekeeping gene expression have been reported to vary considerably, no systematic survey has properly determined the errors related to the common practice of using only one control gene, nor presented an adequate way of working around this problem. Gene transcription studies using quantitative real-time PCR should start with the selection of an appropriate reference gene, which is useful for the individual experimental setting. Correct choice of reference genes, depends on the cells or tissues under study, the researchers should look for their experimental system for stable expression of the reference gene-specific. whatever you decide to use as a standard or standards should be validated for your tissue - If possible, you should be able to show that it does not change significantly in expression when your cells or tissues are subjected to the experimental variables you plan to use. Therefore, the good

choice of an appropriate reference gene should accommodate for each type of cells and any experimental conditions. In a given set of samples or experimental conditions, the parallel determination of two or more housekeeping genes in the amount of help to find any systematic error. We agree with other authors that more than one gene should be used as a reference gene to obtain the most reliable results in gene transcription analysis [1, 9].

**Acknowledgements**

This work was supported by a grant from the National High Technology Research and Development Program of China (No. 2006AA10A118). Thanks are also due to to Dr. Changde Lu, Shanghai Institute for Biological Sciences, Chinese Academy of Sciences, for his kind gift of the plasmid pPigT7.

**References**

[1] J. Vandesompele, K.D. Preter, F. Pattyn: J. Genomebiology research Vol. 3 (7) (2002), p. 0034.1

[2] D. Goidin: J. Analytical Biochemistry Vol. 295 (2001), p. 17

[3] A. Radonic, S. Thulke, I.M. Mackay: J. Biochem Biophys Res Commun Vol.313 (4) (2004), p.856

[4] W. J. De Leeuw, P. E. Slagboom, and J. Vijg: J. Nucleic Acids Research Vol.17 (1989), p. 10137

[5] E. Spanakis: J. Nucleic Acids Research Vol. 21 (1993), p. 3809

[6] A. Oikarinen, J. Makela, T. Vuorio and E. Vuorio. J. Biochimica et Biophysica Acta Vol. 1089 (1991), p. 40

[7] Y. Zhang, Z.G. Wei, Y.Y. Li: J. Analytical Biochemistry Vol. 394 (2009), p. 202

[8] N.J. Walker, Tech. Sight: Science, Vol. 296 (2002), p. 557

[9] K.K. Graven, H.W. Farber: J. Laboratory and Clinical Medicine Vol. 132 (1998), p.456

[10] S.A. Bustin: J. Molecular Endocrinology Vol. 29 (2002), p.23

*Advanced Materials Research Vols. 175-176 (2011) pp 72-75*

*doi:10.4028/www.scientific.net/AMR.175-176.72*

# Study on the Biomass Utilization from Various Genetic Resources of Mulberry

Hiromitsu Nakanishi[1, a], Subaru Okimi[2, b], Makiko Watanabe[2, c], Midori Takasaki[1, d] and Hajime Konishi[1, 2, e]

[1] Satellite Venture Business Laboratory, Shinshu University, 3-15-1 Tokida, Ueda, Nagano 386-8567, Japan

[2] Faculty of Textile Science and Technology, Shinshu University, 3-15-1 Tokida, Ueda, Nagano 386-8567, Japan

[a]h_nakani@shinshu-u.ac.jp, [b]10fa409f@shinshu-u.ac.jp, [c]wmakiko@shinshu-u.ac.jp, [d]mitakas@shinshu-u.ac.jp, [e]konishi@shinshu-u.ac.jp

**Keywords:** mulberry;genetic resource; biomass; bioethanol.

**Abstract.** Mulberry (*Molus alba* L. and other plants of the genus *Morus*) has been cultivated in many Asian countries such as China, Korea, Japan and Thailand, and their leaves are used to feed silkworms (*Bombyx mori* L.). Additionally, the leaves are rich in alkaloid components including 1-deoxynojirimycin (1-DNJ) which is known as one of the most potent glucosidase inhibitors. Dietary mulberry 1-DNJ has been hypothesized to be beneficial for suppression of an abnormally high blood glucose level. In this study, we investigated the high 1-DNJ concentration cultivars from among over 500 various cultivars growing in the field at Experimental Farm of Shinshu University, to utilize the mulberry biomass in addition to feed silkworms. We extracted 1-DNJ from thirty-five varieties of mulberry leaves, and we determined the amount of 1-DNJ. As a result, some cultivars were found to contain a high DNJ concentration compared with Ichinose which is a standard cultivar.

## Introduction

Mulberry plants are distributed widely in Asian countries and the growth rate of them is high compared with general trees. The cultivation of the mulberry is easy on the field of hilly and mountainous area, thus the productivity of the mulberry is high and it is suitable for bioethanol resource. Mulberry leaves have been used historically as feed for silkworms and have been consumed as a tea or a health food for human. Improving effective use of the mulberry by appending value will enhance value as farm products.

An active component of *Morus* leaves, 1-deoxynojirimycin (1-DNJ), is known to be a strong intestinal α-glucosidase inhibitor [1]. 1-DNJ is a glucose analogue with an NH group substituting the oxygen atom of the pyranose ring (Fig. 1). 1-DNJ has been hypothesized to be beneficial suppression of abnormally high blood glucose levels by suppressing intestinal α-glucosidase activity, thus preventing the development of diabetes [2]. On the other hand, the mulberry leaves are highly toxic to caterpillars other than the silkworm *Bombyx mori*, because of the ingredients of the 1-DNJ and other alkaloidal sugar mimic glycosidase inhibitors [3]. The silkworm has evolved

adaptive enzymes to circumvent the toxic effects of such sugar mimic alkaloids to be able to feed on mulberry leaves [4].

Thus, 1-DNJ from the mulberry is utilized not only to improve symptom of diabetes mellitus but also to avoid caterpillars as repellent. However, 1-DNJ content of general mulberry cultivars are included only in about 0.1-1.0 %. It is necessary to find the cultivar that contains high 1-DNJ to use the mulberry effectively. Therefore, in this study, we investigated the high 1-DNJ concentration cultivars from among over 500 various cultivars growing in the field at Experimental Farm of Shinshu University.

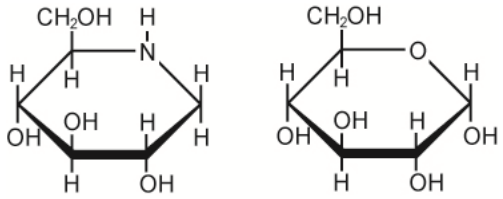


Fig. 1 Chemical structure of 1-DNJ (left) and D-glucose (right)

## Materials and Methods

**Plant Materials.** Thirty-five varieties of mulberry leaves (Yukishirazu, Takai wase, Ichinose, Enashiguwa, Kairyou nezumigaeshi, Ichibei, Tago wase, Inaguwa, Ueda wase, Kairyou ichinose, Chikuma ooha, Nagano ooha, Nezumigaeshi, Ficus, Textile No. 303; 307; 311; 312; 314; 317; 322; 335; 401; 402; 404; 406; 416; 442; 443; 445; K51; K61, Keguwa 1, Keguwa 2, and T3), were collected in October 16, 2009, from grown in the field at Experimental Farm of Faculty of Textile Science and Technology, Shinshu University (Ueda, Nagano, Japan). The leaves were dried at room temperature and crushed into powder, and then stored in at desiccator until use.

**Quantification of 1-DNJ from Mulberry leaves.** Mulberry 1-DNJ was determined using HILIC-MS as previously reported by [5] with some modifications. The HILIC-MS system consisted of Shimadzu LC-10AD pump (Tokyo, Japan), DGU-14AM degasser, CTO-10A column oven, SIL-10AD auto injector, and LCMS-2010 electrospray ionization mass spectrometer (ESI-MS). A TSK gel Amide-80 column (2.0 mm x 150 mm; Tosoh, Tokyo, Japan) was used. The mobile phase was a mixture of acetonitrile and 6.5 mmol/L ammonium acetate, pH 5.5 (72:28, v/v). The flow rate was adjusted to 0.2 mL/min, and column temperature was maintained at 40 °C. ESI-MS was carried out in a positive ion measurement mode. The mass spectra of 1-DNJ was detected at a retention time of 9.2 min in the single-ion monitoring (SIM) at *m/z* 164.0 $[M + H]^+$.

The powder of mulberry leaves (0.05 g) were mixed with 1.0 mL of a mixture of acetonitrile and water (50:50, v/v, containing 6.5 mmol/L ammonium acetate, pH 5.5) in a microtube. After sonication for 1 hour, the mixture was centrifuged at 15,000*g* for 10 min. The supernatant was filtered through a PTFE filter (0.45μm pore size). The DNJ concentration in the leaves was calculated using the calibration curve equation of standard 1-DNJ.

## Results and Discussions

**Determination of the 1-DNJ level from thirty-five mulberry cultivars.** This research study aimed to obtain a high concentration cultivar from thirty-five varieties of mulberry leaves. First, to determine the 1-DNJ amounts, we extracted 1-DNJ from mulberry leaves with water, ethanol, methanol and acetonitrile. As a result, a mixture of acetonitrile and water (50:50, v/v) containing

6.5 mmol/L ammonium acetate (pH 5.5) was high extraction efficiency among our conditions. Next, we measured the amount of 1-DNJ from thirty-five varieties of mulberry leaves (Fig. 2), and the cultivars with high 1-DNJ content were found compared with Ichinose which is a standard cultivar. For example, diploid cultivar of Ueda wase, and triploid cultivar of Textile No.307, 322 and 317, and tetraploid cultivar of Textile No. 442 were contained a high 1-DNJ level about 5.2-10.3 times compared with Ichinose. However, 1- DNJ content changes by the season [2]. In this study, we collected thirty-five varieties of mulberry leaves in October when 1-DNJ content is a decreasing season. We must look more carefully into the cultivar with a high 1- DNJ content by collecting the mulberry leaves at summer when 1- DNJ content is high in the expert year.

**The relationship between 1-DNJ amounts and ploidy cultivars.** To know the inheritance pattern concerning 1-DNJ biosyntheses, 1- DNJ contents were compared in the genetic relationship of the ploidy cultivars (Fig. 3). Tetraploid cultivar of Textile No. 416 and 442 that derived Ichinose were increased the 1-DNJ content. This result suggests that Ichinose contains the genetic factor in the positive regulation of 1-DNJ content. On the other hand, tetraploid cultivar of Textile No. 404 and 445 that derived Enashiguwa were decreased the 1-DNJ content. This result suggests that Enashiguwa contains the genetic factor in the negative regulation of 1-DNJ content. The genetic locus that decides the amount of 1- DNJ could be expected to examine the genetic relationship and 1-DNJ content from many cultivars. In addition, it becomes possible to breed the cultivar with high 1-DNJ content and adaptation environment.

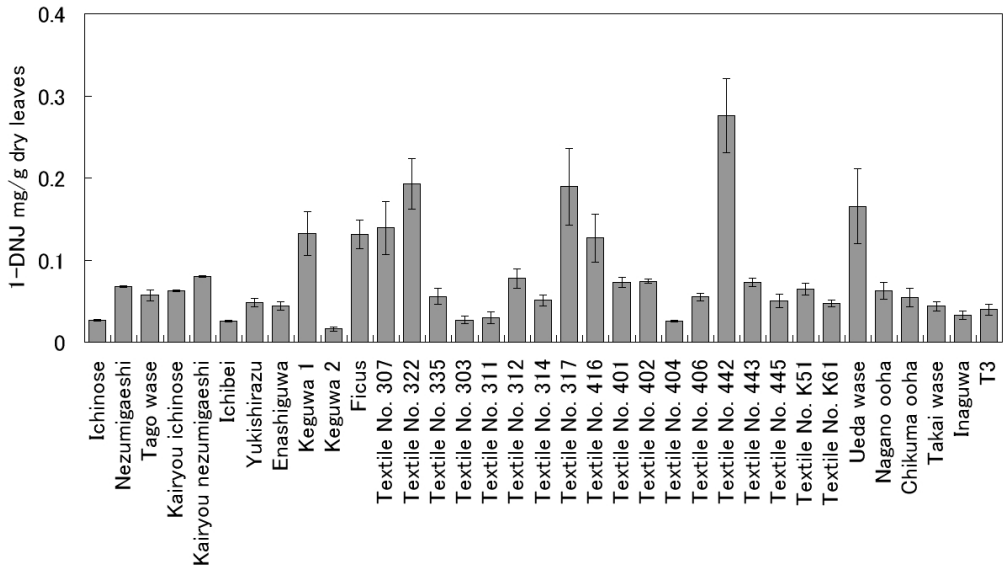


Fig. 2 1-DNJ amount of various genetic resource of mulberry
The data present the mean ± SD (n = 3).

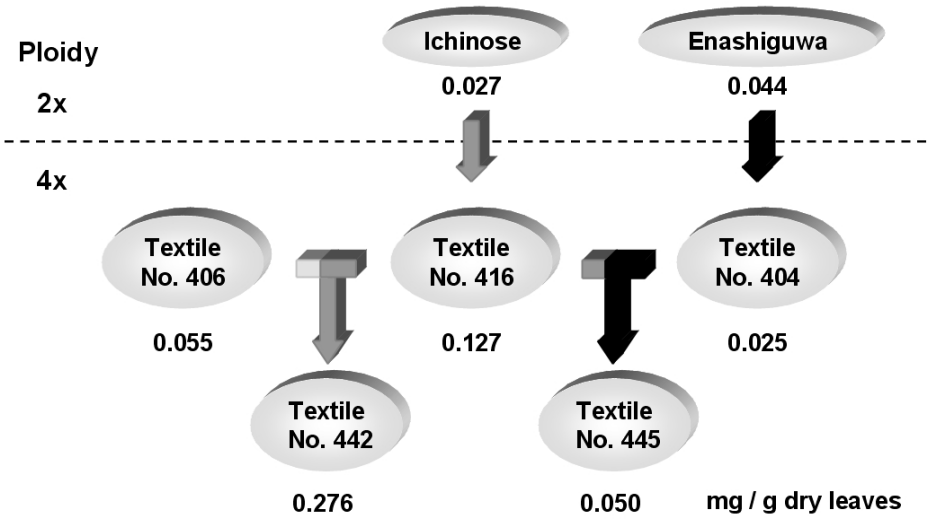


Fig. 3 Genetic relationship of ploidy cultivars

The cultivar names are indicated in ellipses. 1-DNJ amounts are indicated under the ellipses as mg/g dry leaves. Tetraploid cultivar of Textile No. 416 and No. 404 were induced by colchicine treatment from Ichinose and Enashiguwa, respectively. Gray arrows indicate positive regulation of 1-DNJ amount and black arrows indicate negative regulation of 1-DNJ amount.

**Summary**

In this study, we found the high 1-DNJ content cultivars compared with Ichinose which is a standard cultivar. Comparative study of genetic relationship in ploidy cultivars indicated that the genetic factors are involved in the positive regulation of 1-DNJ content in Ichinose and the negative regulation of 1-DNJ content in Enashiguwa. The gene that takes part in biosyntheses of 1-DNJ would be found by examining the inheritance background of these cultivars, and it is possible to breed with improvement productivity.

**Acknowledgments**

We thank the Experimental Farm of Faculty of Textile Science and Technology, Shinshu University (Ueda, Nagano, Japan) for providing mulberry cultivars.

**References**

[1] N. Asano, H. Kizu, K. Oseki, E. Tomioka, K. Matsui, M. Okamoto, and M. Baba. J. Med. Chem., Vol. 38 (13)(1995), p. 2349

[2] T. Kimura, K. Nakagawa, H. Kubota, Y. Kojima, Y. Goto, K. Yamagishi, S. Oita, S. Oikawa, and T. Miyazawa. J. Agric. Food Chem., Vol. 55 (14) (2007), p. 5869

[3] K. Konno, H. Ono, M. Nakamura, K. Tateishi, C. Hirayama, Y. Tamura, M. Hattori, A. Koyama, and K. Kohno. Proc. Natl. Acad. Sci. USA., Vol. 103 (5)(2006), p. 1337

[4] T. Daimon, T. Taguchi, Y. Meng, S. Katsuma, K. Mita, and T. Shimada. J. Biol. Chem., Vol. 283 (22)(2008), p. 15271

[5] K. Nakagawa, H. Kubota, T. Kimura, S. Yamashita, T. Tsuzuki, S. Oikawa, and T. Miyazawa. J. Agric. Food Chem., Vol. 55(22)(2007), p. 8928

# Textile and Silk Materials

*Advanced Materials Research Vols. 175-176 (2011) pp 79-84*

*doi:10.4028/www.scientific.net/AMR.175-176.79*

# Preparation Of Transparent Water-insoluble Silk Fibroin Films

Minqing Luo [1,a], Cencen Zhang [1,b] Shenzhou Lu[1,2,c*]

[1]National Engineering Laboratory for Modern Silk, Soochow University, 199 Renai Road, Suzhou 215123, China

[2]College of Textile and Clothing Engineering, Soochow University, 178 East Ganjiang Road. Suzhou 215006, China

[a]ap0411223@163.com, [b]ruxin-bing0@yahoo.com.cn,

[c*]Corresponding author: lushenzhou@suda.edu.cn

**Keywords:** silk fibroin; structure; mechanical properties; light transmittance; cornea.

**Abstract.** The transparent water-insoluble silk fibroin(SF) films were casted from the mixture solution of silk fibroin and xylitol/mannitol. The structure, surface morphology, solubility, mechanical properties and light transmittance of the blend films were measured. FT-IR, X-ray diffraction retuslts indicated that the films were mainly composed of Silk I structure. SEM showed the blend films with xylitol were miscible, whereas the blend films with mannitol had phase-separated structure. There were lots of nanopores in the blend films in the wet state. The insoluble SF /xylitol films had excellent mechanical properties while the SF / mannitol films were brittle. The mechanical property of SF/alcohol blend films were consistent with the human cornea in wet state.When the contents of xylitol were 10% and 20%, the blend films had high light transmittance which were similar to human cornea. In summary, the SF /xylitol film containing 10% xylitol provides a great potential to act as repairing materials for cornea.

## Introduction

In the world, about 10 million people are suffering from vision loss due to corneal damage or disease, but the only available treatment is transplantation with human donor corneal tissue. The corneal tissue engineering technology has opened a new road to repair and reconstruct the cornea. The core of corneal tissue engineering is to establish the three-dimensional complex between corneal cells and biological materials with good biocompatibility. The ideal materials should have good biocompatibility, low immunity, appropriate biodegradability, excellent light transmission and suitable mechanical properties. Now collagen was extensively used for corneal tissue engineering as scaffold materials. However, the collagen has potential immunogenicity and poor mechanical properties. So it is necessary to find new materials for corneal tissue engineering scaffold.

Due to it's good biocompatibility, low immunogenicity and moderate biodegradation, the silk fibroin (SF) has been widely used in the field of biomedical materials. The silk membrane, having good mechanical properties and oxygen permeability in the wet state [1], has acted as the materials of wound dressings [2], and bone tissue engineering [3]. However, the pure silk film is soluble in water (which process). Some processes such as organic solvent treatment [4] and stretching treatment [5] have been used to solve the problem, but those treated were brittle, which limited the applications. Blending with epoxy [6] may damage the biocompatibility of silk fibroin membrane. In this paper, xylitol and mannitol were blended with silk fibroin to obtain water-insoluble membranes. Their application for cornea tissue engineering materials were studied.

## Material and methods

**Preparation of silk solutions.** Bombyx mori silkworm silk was boiled for 30 min in an aqueous solution of 0.02 M $Na_2CO_3$ and then rinsed thoroughly with deionized water for three times to extract the sericin. After drying the degummed silk fibres were dissolved in 9.3 M LiBr solution at 60℃ for 1 h. This solution was dialyzed against deionized water using a dialysis membrane (Membrane Filtration Products, Inc.) with a molecular weight cutoff 12,000 Da for 72 h. The solution was centrifuged to remove the small amount of silk aggregates that formed during the process. The final concentration of silk fibroin aqueous solution was 3.2 % (wt./v). This concentration was determined by weighing the residual solid of a known volume of solution after drying at 105 °C.

**Preparation of blend films.** The purified silk fibroin solution was then mixed with xylitol or mannitol at weight ratios of 1:10, 2:10, 3:10, 4:10, 5:10 and 6:10. The mixed solutions (50ml) were cast into a polyethylene dish (10×20×2 cm) and dried at at room temperate in fume hood.

**Structure of blend films.** X-ray diffraction (XRD) was performed using X'PERT PRO MPD (Panalytical Company) with CuKα radiation. The XRD patterns with the speed of 10°/min at 40 kv and 35mA were recorded in the region of 2θ from 5° to 45°. Fourier transform infrared (FTIR) spectra were obtained with a Nicolet 5700 Fourier transform infrared spectroscopy(Nicolet, America). The blend films were processed into powder, with diameters less than 80 μm. The FTIR spectra in the absorbance mode were obtained in the spectral regions of 400-4000$cm^{-1}$. The surface morphologies of the blended films were imaged using a S-4700(Hitachi, Japan) scanning electron microscopy (SEM) at an operating voltage of 15 kV.

**Water solubility of silk films.** The blend films were placed in the room with the constant temperature and humidity (25 ℃, RH = 65%) for 24h. Then samples about 0.1g were put in 10 ml tubes, with adding deionized water by the liquor ratio 1:100 and kept at 37ºC for 24 h. After the incubation, the silk films were removed from the solution, dried, weighed, and compared with the mass of original film to obtain residual mass (%).The remaining solution was subjected to UV absorbance measurement at 280 nm. The amount of dissolved silk was then compared with the total silk mass in the film to obtain the percentage of the film dissolved silk fibroin in water.

**Mechanical properties.** Mechanical properties of the blend films were evaluated using an Instron 3365 testing frame (Instron, Norwood, MA) with a 10 N capacity load cell at room temperature and humidity (25 ℃, RH = 65%). Blend films with dumble shape (49×8×0.1mm) were held between two clamps positioned at a distance of 28mm. The measurements carried out at the rate of 20mm/min. The tensile strength, elastic modulus and elongation at break were determined. At least N=6 samples were used in every condition. For dry state test, the samples were placed at room temperature and humidity for 24h. For wet state test, the samples were immersed in 0.9% NaCl solution for 24h before testing.

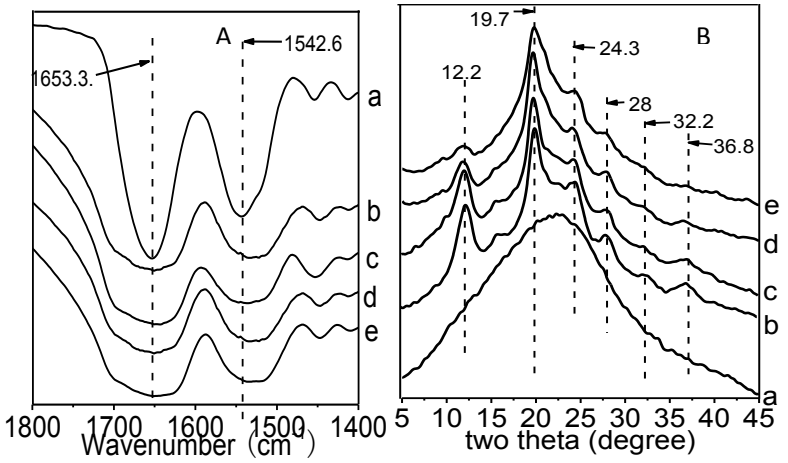


Fig. 1 Structure of blend films, (A) X-ray diffractogram of blend films;(B) IR spectra of blend films, a: Pure silk film, b:Xylitol/SF=30%(dry), c: Mannitol/SF=30%(dry), d:Xylitol/SF=30%(wet,), e: Mannitol/SF=30%(wet)

**Transmittance of blend films.** The transmittances of the films were Measured with an (BIO-TEK SYNERGY) at 492nm, 550 nm, 700nm at room temperature. Films were placed into 24-well plates. Every film tested for four times.

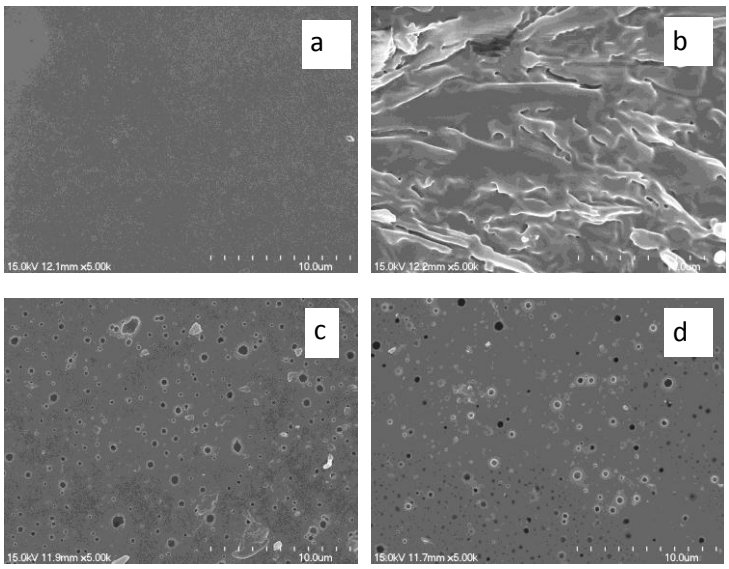


Fig. 2 SEM of blend films, polyhydric alcohol was 30 wt%, (a) Xylitol(dry), (b) Mannitol(dry), (c) Xylitol(wet), (d): Mannitol(wet)

## Results and discussion

**Structure characteristics.** It has been reported that silk fibroin has two kinds of crystalline modifications, ϒ-form (silk I, typeII ϒ-turn) and ϒ-form (silk II, anti-parallel ϒ-pleated sheet). In XRD spectra of silk fibroin, the main diffraction peaks of Silk I appeared at at 12. 2°(m s), 19. 7°( s), 24. 7°(m), 28. 2°(m), 32.3°(w), 36.8°(mw), 40.1°(mw), and those of Silk II appeared at 9. 1°(ms), 18. 9°(ms) , 20. 7°(vs) [7]. The pure silk film(Fig.1(A) a) was an amorphous structure, characterized by the presence of a broad peak in the scattering angle range, while the other samples(Fig. 1(A) b, c, d, e) exhibited silk I structure, corresponding to the diffraction peaks of silk I. No typical diffraction peaks of silk II were found for the blend films. The results indicated that xylitol and mannitol significant influence silk fibroin from amorphous structure to silk I structure and silk I structure was stable enough, without Silk II formation after immersing or drying.

Fig. 1(B) showed the FT-IR spectra of silk films in the range 1400-1800 $cm^{-1}$. The Fig. 1(B) shows that the structure of pure silk film is random coil due to the absorption bands of amide I be at 1654 $cm^{-1}$ and amide II at 1542 $cm^{-1}$ [8]. Fig. 1(B, b, c, d, e) shows that the absorption peaks of amide I and amide II became weak and broad after silk film mixed with xylitol and mannitol. The result indicated that there were hydrogen bonds between silk fibroin molecules and xylitol or mannitol. It's difficult to distinguish random coil from ϒ-form in the infrared spectrum, so there were not obvious peaks of ϒ-form in the other four curves (Fig. 1(B), b, c, d, e).

**SEM morphology.** Fig. 2(a) shows that the surface of 30% w/w xylitol/SF blend film was smooth and glassy while that of 30% w/w man-nitol/SF blend film (Fig. 2(b)) was a gra-nular appearance. The results indicated that xylitol was compatible with SF fibroin whereas mannitol was not compatible with SF fibroin. In the wet state (Fig. 2c, d), there are lots of nanopores on the surface of the blend films. This demonstrated that xylitol/mannitol act as pore formers.

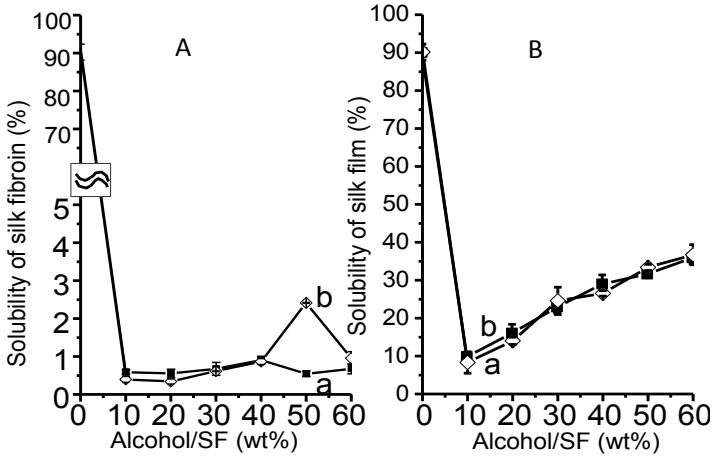


Fig. 3 Solubility of silk blend films ( A: Xylitol/SF B: Mannitol/SF)

**Solubility of silk blend films.** Dissolution of silk fibroin protein from the blend films was determined in water based on UV absorbance, since the silk fibroin protein has a significant content of tyrosines that absorb at 280 nm. Fig. 2 (A) shows that pure silk film was water soluble while blend films were insoluble (solubility ratio < 2%. The results indicated that xylitol or mannitol could improve the stability of silk fibroin in water, which may be due to the formation of cross-linking hydrogen bonds between silk fibroin molecules and xylitol or mannitol. The other reason may be the secondary structure changes of silk films from random coil to silk I after blend with xylitol or mannitol. The weight loss of the blend films similar to the content of polyhydric alcohols (Fig. 3, B). These may attribute to the -OH group which formed cross-linking hydrogen bonds with water were stronger than that with the silk fibroin molecules. The silk fibroin was stable and insoluble even after the xylitol or mannitol dissolved in water. The blend films can be used as biological material.

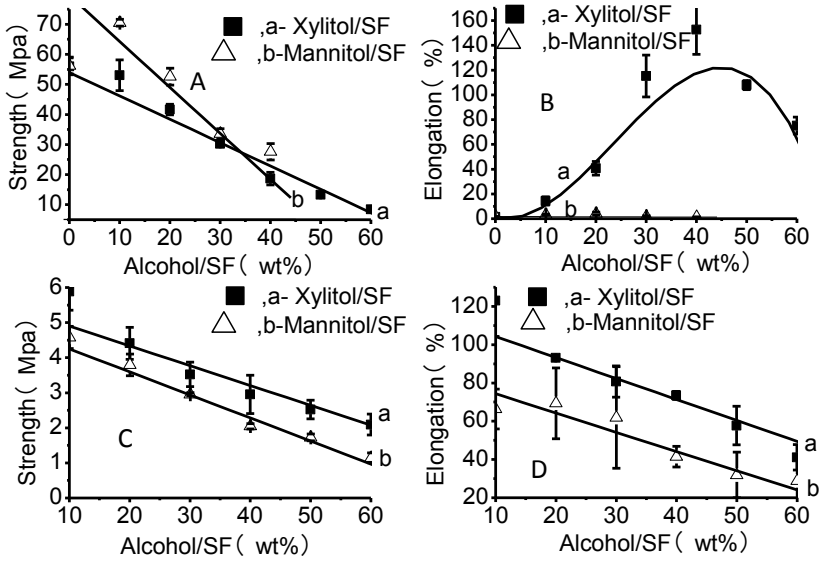


Fig.4 Mechanical properties of blend films(A, B: Dry state, C, D:Wet state). The blend films were too brittle to test when the content of mannitol exceed to 40 %(wt). The pure silk film in wet state did not test because of its solubility in water.

**Mechanical properties.** Generally,mechanical properties are very important to evaluate films performances for proper application. With the content of polyhydric alcohols increasing, the strengths of blend films deceased (Fig. 4 A). The phenomenon is due to xylitol and mannitol playing a role of plasticizers. The silk fibroin

macromolecules under the force was more easily to slip in the action of the plasticizers. Fig. 4(B) shows that the xylitol/SF blend films were flexility while the mannitol/SF films were brittle. The elongation of blend filmscontaing 40 wt% xylitol was over 150%, better than other samples. This indicated that xylitol significantly improved the flexibility of silk films.

In the wet state(Fig. 4 C,D), the strength and elongation decreased following the increase of polyhydric alcohol. The strength in wet state was much lower than that in dry state. The reason due to xylitol or mannitol dissolved in water under the wet condition and there were lots of nanopores on the surface of the films. The higher the content of polyhydric alcohol was, the more the holes were. All the wet blend films had excellent flexility. These may be related to the water, which played a good role of plasticizers. Therefore, the mechanical properties of silk blend films can be controlled by different content of polyhydric alcohols.

**The transmittance of the films.** Fig. 5 shows that the transmittance of the films decreased with the content of alcohol increasing. The blend films in dry state had good transmittance while dropped sharply in wet state, espacially for mannitol/SF films. The Xylitol/SF less than 40 wt% blend films had excellent light transmittance in water. Whereas the mannitol/SF blend films became turbid. The transmittance of the cornea increases with the increasing of wavelength.

In the range from 450 nm to 600 nm, the percentage transmission was found to increase from 80% to 94%. In the range from 600 nm up to 1000 nm, the percentage transmission was between

95% and 98% [10]. The transmittance of the xylitol/SF blend films with the content less than 20wt% were close to human corneas which could be applied to human tissue engineering.

The wet strength of human cornea is about 3.81 ± 0.41Mpa, and the wet elongation is 42.814% ±11.674% [9]. Fig.5 (C) (D) showed that the blend films with the content of xylitol or mannitol below 20% could meet these requirements.

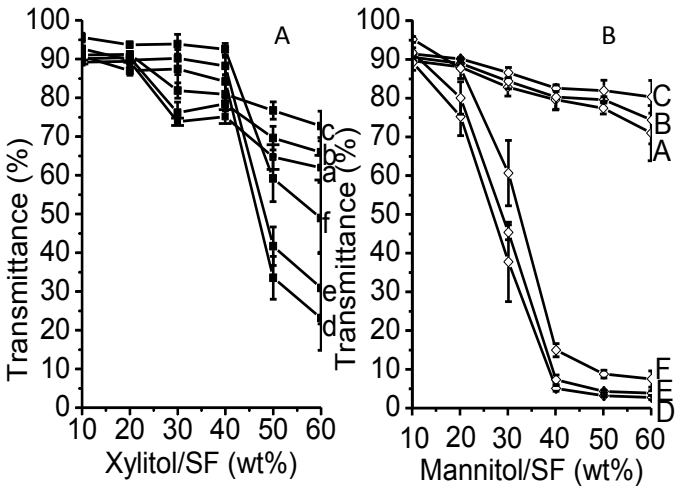


Fig. 5 (A)Transmittance of Xylitol/SF blend films, a,b,c:The transmittance of the dry blend films at 492nm, 550nm and 700nm; d,e,f: The transmittance of the wet blend films at 492nm,550nm, and 700nm; (B)Transmittance of Mannitol/SF blend films, A,B,C:The transmittance of the dry blend films at 492nm,550nm, and 700nm; D,E,F: The transmittance of the wet blend films at 492nm, 550nm, and 700nm. Before testing, wet samples were immersing in deionized water for24h and then placed in 24-well plates. Every well were filled with 1ml deionized water.

## Summary

(1) The secondry sturcture of silk fibroin changed from random coil to silk I after mixing with xylitol or mannitol. The water solubility of silk films blend with polyhydric alcohols were low to 2%, which could solved the problem of water-soluble of silk film.

(2) The xylitol/SF blend films had excellent mechanical properties while the inositol/SF blend films were brittle. The mechanical property of blend films content no more than 20 wt% inositol were consistent with the human cornea in wet state.

(3) When the content of xylitol from 10 wt% to 20wt %, the blend films had high light transmittance which were similar to human cornea.

Taking water solubility, mechanical properties and light transmittance into account, the silk film blend with 10 wt% xylitol provide a great potential to act as repairing materials for cornea.

## Acknowledgements

This work was supported by the National Key Basic Research Program (973 program, 2005CB623906), scientific and technological projects of Suzhou China (Grant No. SYJG0923) and Combination Projects of Industrialization, Teaching and Research of Jiangsu Province China(Grant No. BY2009127).

**References**

[1] G. Freddi, M. Romano, M. R.Massafra, et al : Appl Polym Sci. Vol.56(1995), p.1537

[2] B G Huang, D G Zhu, Z Y Wu , et al: Chinese Journal of Burns. Vol.14(1998), p. 270

[3] R Kino , T Ikoma , A Monkawa, et al.: Appl Polym Sci. Vol. 99 (2006), p. 2822

[4] M Tsukada, Y Gotoh , M Nagura ,et al: Polym Sci Part B: Polym Phy. Vol. 32(1994), p. 961

[5] H J JIN, D L KAPLAN: Nature. Vol. 424(2003), p. 1057

[6] S Z Lu, M Z Li, Y Liu: Polym Mater Sci& Eng.Vol. 19(2003), p. 104

[7] Z Y Wu, Z M Jin , L Q Xu: Science of Sericulture. Vol.19(1993), p. 105

[8] X Chen, W J Li , T Y Yu: Polym Sci Part B: Polymr phy. Vol. 35(1997), p. 2293

[9] Y J Zeng , J Yang , K Huang, et al: Biomechanics. Vol. 34(2001), p. 533

[10] E Beems, J V Best: Exp Eye Res. Vol. 50(1990), p. 393

*Advanced Materials Research Vols. 175-176 (2011) pp 85-89*

*doi:10.4028/www.scientific.net/AMR.175-176.85*

# Structure and mechanical property of silk fiber under gamma radiation

Wei-wei Yao[1,2, a], Zhi-wu Liu[1,2, b], Hong-gen Yi[1, c] and Jian-nan Wang[1, 2, d]

[1]National Engineering Laboratory for Modern Silk, University of Soochow, Suzhou, 215123, China

[2]College of Textile and Clothing Engineering, University of Soochow, Suzhou, 215021, China

[a]ywy_sd@sina.com, [b]yueliangIzw@163.com, [c]Yihg@suda.edu.cn , [d] Corresponding author: wangjn@suda.edu.cn

**Key words:** silk fiber; $Co^{60}$; molecular weight; secondary structure; mechanical property.

**Abstract.** An attempt to change the structure of silk fibers and their properties for the biological application was studied by utilizing gamma radiation in various $Co^{60}$ intensities (0 kGy, 30 kGy, 50 kGy, 100 kGy, 200 kGy, 500 kGy, 1000 kGy, 2000 kGy, 3000 kGy). With the increase of the gamma radiation intensity, SEM result shows that cracks and fragments were formed between microfibrils of the irradiated fiber significantly. Simultaneously SDS-PAGE results give the evidence that the molecular weight of the fibroin diminished. Furthermore, the breaking strength and elongation of irradiated fibers decreased gradually with the increasing $Co^{60}$ intensity. Although no significant changes of the molecular conformations were found by FTIR and X-ray diffraction, the effects on molecular interactions of the silk fibroin, such as peptide bonding, hydrogen bond and intermolecular bonding force, were obviously observed and enhanced gradually with the increase of gamma radiation intensity.

## Introduction

Silkworm silk such as *Bombyx mori* (*B. mori*) has been utilized in biomedicine for centuries due to its outstanding proterties, such as good biological safety, none of cytotoxicity, inactive inflammatory reaction and zero inherent toxicity. Many studies have revealed that *B. mori* silk fibroin can be made in various shapes (such as fibers, films, nets, mats, and sponges) and can support the adhesion, spreading and proliferation of many kinds of cells including keratinocytes, fibroblasts, vascular endothelial cells, epithelial cells, bone marrow stromal cells and neuroglia cells. In particular, stem cell-based tissue engineering has expanded the use of silk-based biomaterials for engineering a range of bone, ligament, cartilage, as well as connective tissues. But the controllable biodegradability of silk fibroin is still a key problem for the application in the field of tissue engineering [1-5].

Irradiance technique has been increasingly used for synthesis and improvement of polymers due to its low energy consumption and strong strength of penetration. Gamma radiation can cause the macromolecule chains to cross-link, graft, conjugate and degrade. Recently, few studies reported that the thermal stability and anti-crinkle of silk fabrics improved through grafting acrylonitrile and acrylamide by the gamma radiation [6, 7], and the biodegradability of silk fibers improved while the mechanical properties weakened after treatment with the gamma radiation [8, 9]. But the mechanism of action of gamma radiation on silk fibroin is still unclear. Especially, the application on silk modification has not been reported. In this paper, we studied the molecular structures and mechanical properties of silk fiber under $Co^{60}$-γ radiation, expecting to provide a pretreatment method for the improvement on the biodegradability of silk fibroin.

## Experimental

***Preparation of irradiated silk fiber.*** Raw silk fibers from *B. mori* were treated three times in 0.06 wt% $Na_2CO_3$ solution at 98-100 ºC for 30 min respectively to remove sericin. After drying, the degummed silk fibers were irradiated with 0 kGy, 30 kGy, 50 kGy, 100 kGy, 200 kGy, 500 kGy, 1000 kGy, 2000 kGy, 3000 kGy of $Co^{60}$-γ radiation.

***Fiber characterization.*** Microphotographs of irradiated silk fibers were obtained by scanning electron microscopy (HITACHI S-570, Japan). Molecular conformations and crystalline structures were performed on a Fourier transform infrared spectrometer (Niclet 5700, USA) and an X-ray diffractometer (D/MAX-IIIC, Holland) with a Cu Kα source. The diffraction intensity curves were obtained at a scanning rate of 2°/min and within the scanning region of 2θ=5°-40°. The breaking strength and breaking elongation of irradiated silk fibers were measured by an almighty materials tester (Instron3365, USA) under an elongation speed of 250 mm/min, a pre-stress of 0.5 cN/tex and a retaining length of 250 mm (repeat 10 times for each sample).

***Gel electrophoresis.*** 2g of gamma radiation treated *B. mori* silk fibers were dissolved in 20 ml of ternary solvent $CaCl_2 \cdot CH_3CH_2OH \cdot H_2O$ (mole ratio=1:2:8) at 70 ± 2 ºC with stirring. The mixed solution was dialyzed against deionized water with a molecular weight cutoff of 12-14 kDa at 4 ºC for 4 days (volume ratio of solution to regenerated cellulose tubular membrane was 1:3), and then filtered to get the silk fibroin solution. The concentration of silk fibroin solution was determined by drying and weighing. The samples of silk fibroin solutions (1.0%, m/v) were identified by SDS-PAGE run on 10% resolving gel under a voltage of 150 V. Gels were stained by Coomassie Blue staining.

## Results and discussion

**Microphotographs of irradiated silk fibers.** Fig. 1 shows the cross-section morphous of irradiated silk fibroin under the different intensity of gamma radiation. Obviously, the pores from the microphotographs increased gradually (Fig. 1b~f) compared with the control (Fig. 1a), clefts between microfiber lacertus and fragments formed when the radiation intensity up to 1000 kGy (Fig. 1e), and became more significantly when the radiation intensity up to 3000 kGy (Fig. 1f). It indicated that gamma radiation weakened the intermolecular force to result in rarefaction of silk fibers.

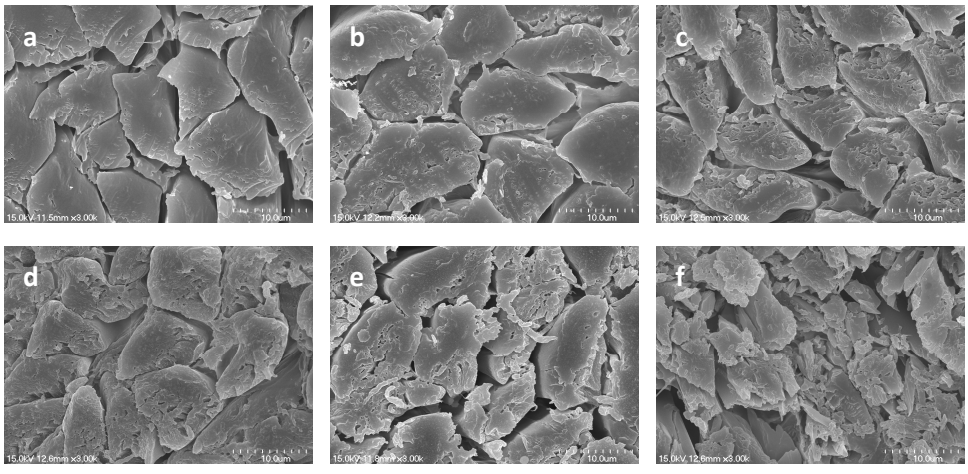


Fig. 1 microphotographs of silk fibers after treatment with $Co^{60}$-γ radiation
(a) 0 kGy, (b) 50 kGy, (c) 200 kGy, (d) 500 kGy, (e) 1000 kGy, (f) 3000 kGy

**Molecular conformation of irradiated silk fibers.** Fig. 2 shows that there was no remarkable change found in the secondary structure of silk fibers treated with the different intensity of gamma radiation. Molecular conformations were similar to each other that were mainly the silk I (around 1520, 1650 $cm^{-1}$), silk II (β-sheet, around 696, 1230 $cm^{-1}$) and random coil (around 648 $cm^{-1}$). The curves of XRD also show that the gamma radiation did not remarkably cause the crystalline structure change of silk fibers (Fig. 3). The notable characteristic bands around 9.3 °, 20.7 ° and a weak characteristic band around 24.1 ° were assigned to silk II and were all present in all fiber's samples.

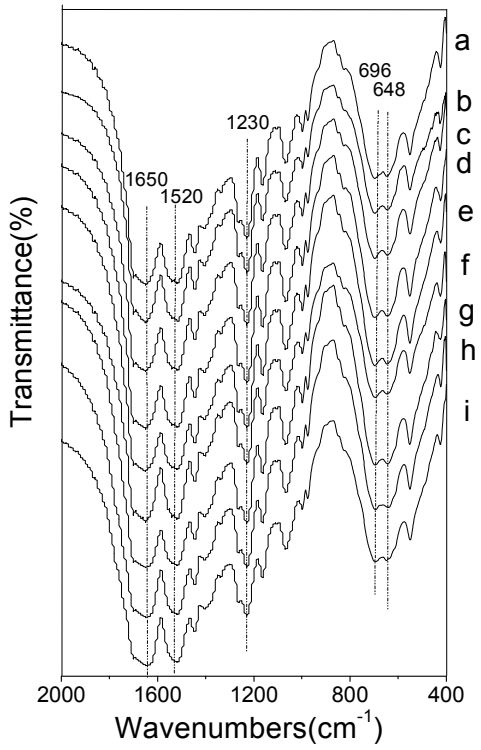


Fig. 2 FTIR of silk fibers after treatment with $Co^{60}$-γ radiation

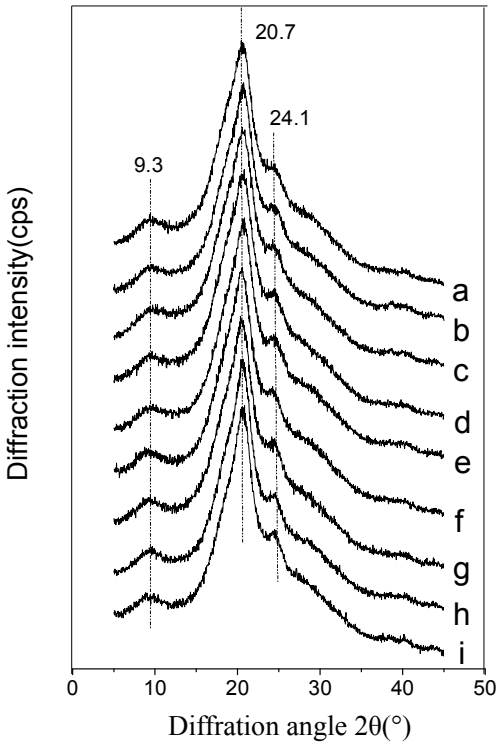


Fig. 3 XRD of silk fibers after treatment with $Co^{60}$-γ radiation

In fig. 2 and 3: (a)0 kGy, (b)30 kGy, (c)50 kGy, (d)100 kGy, (e)200 kGy, (f)500 kGy, (g)1000 kGy, (h)2000 kGy, (i)3000 kGy

**Mechanical property of irradiated silk fibers**. The breaking strength and elongation of silk fibers decreased with increasing gamma radiation intensity (Fig. 4). When up to 500 kGy, the breaking strength and elongation were reduced by 58% and 40%, respectively. When up to 1000 kGy, both of them almost disappeared. The results could be attributed to the weakness of peptide bonding, intermolecular bonding and molecular orientation in fibroin's peptide chain.

**SDS-PAGE electrophoresis analysis.** The solubility of irradiated silk fibers such as in $CaCl_2$ solution was improved, and the molecular weight of silk fibroin was lower compared with the untreated samples. Fig. 5 shows that the molecular weight of silk fibroin mainly distributed within the range of 30~85 kDa when irradiated by the intensity lower than 100 kGy (Fig. 5, line a~d). When over 100 kGy, high molecular weight of silk fibroin dissolved in $CaCl_2$ solution decreased remarkably and no obvious electrophoresis strip appeared in gel (Fig. 5, line e~h).

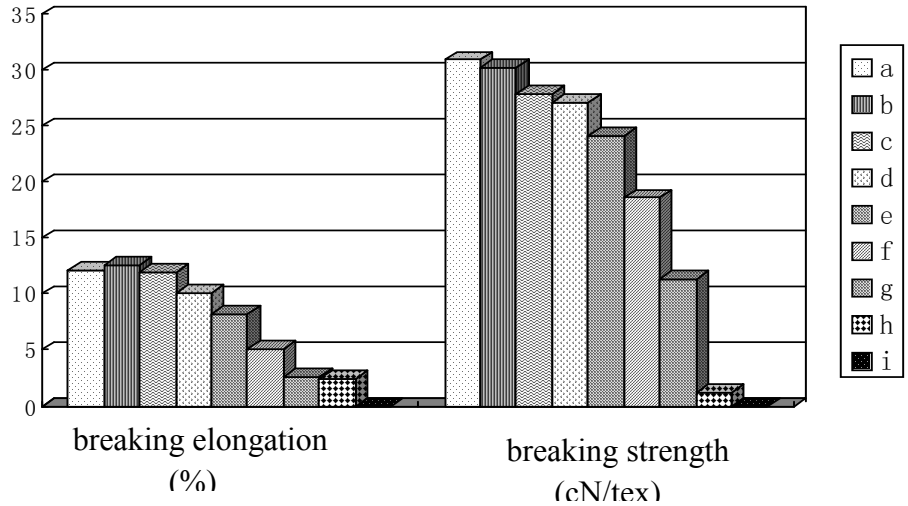


Fig. 4 Breaking strength and breaking elongation of irradiated silk fibers
Each data point was averaged from ten samples
(a)0 kGy, (b)30 kGy, (c)50 kGy, (d)100 kGy, (e)200 kGy,
(f)500 kGy, (g)1000 kGy, (h)2000 kGy, (i)3000 kGy

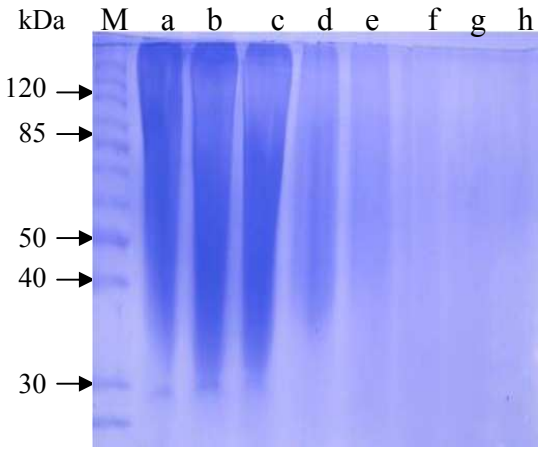


Fig. 5 Gel electrophoresis analysis of irradiated silk fibroin in deionized water
(a)0 kGy, (b)30 kGy, (c)50 kGy, (d)100 kGy, (e)200 kGy,
(f)500 kGy, (g)1000 kGy, (h)2000 kGy

Table 1 shows the yields of silk fibroins that were dissolved and dialyzed by the membrane with a molecular weight cutoff of 12-14 kDa. The concentration of silk fibroin after dialysis decreased remarkably with the increasing radiation intensity. The results from fig. 5 and Table 1 indicated that gamma radiation weakened bonding strength in fibroin's molecule, such as peptide bonding, hydrogen bond and intermolecular bonding.

Table 1 Concentration of silk fibroin after dialyzing against deionized water
with a molecular weight cutoff of 12-14 kDa

| Sample | Intensity of $Co^{60}$-γ radiation (kGy) | | | | | | | | |
|---|---|---|---|---|---|---|---|---|---|
| | 0 | 30 | 50 | 100 | 200 | 500 | 1000 | 2000 | 3000 |
| Concentration (g/ml)×100% | 2.67 | 2.18 | 2.16 | 2.06 | 1.99 | 1.95 | 1.49 | 1.22 | 1.03 |

**Summary**

From the FTIR and XRD curves, crystalline structure and peaks of β-sheet in the irradiated silk fibers were observed, which has no significant change compared to the untreated fibers. However, the evidence demonstrates that the clefts between microfiber lacertus and fragments formed. The breaking strength and breaking elongation decreased gradually, and when the radiation intensity was up to 1000 kGy, both of them almost vanished. The solubility of the silk fibers after treatment with the $Co^{60}$-γ radiation could be improved, and the molecular weight of dissolved and dialyzed silk fibroin from the irradiated silk fibers became lower. When the gamma radiation intensity was less than 100 kGy, the molecular weight of silk fibroin mainly was distributed within the range of 30~85 kDa. Our study indicated that the effects of $Co^{60}$-γ radiation on molecular structure of the silk fibroin were the clear weakening of the bonding strength among the fibroin molecules, such as peptide bonding, hydrogen bond and intermolecular bonding force, and the effects were enhanced gradually with the increase of gamma radiation intensity.

**Acknowledgements**

This work was supported by the National Basic Research Program of China (No. 2005CB623902), the Natural Science Foundation of Jiangsu Province of China (No. BK2009147 and BK2010253) and the Development Foundation of Suzhou City of China (No. SS0829 and SYG201001).

## References

[1] X.H. Zhang, C.B. Baughman and D.L. Kaplan: Biomaterials, Vol.29(2008), p. 2217

[2] H.F. Liu, H.B. Fan, S.L. Toh, et al: Biomaterials, Vol.29(2008), p. 1443

[3] B.B. Mandal and S.C. Kundu: Biomaterials, Vol.30(2009), p. 2956

[4] B.D. Lawrence, J.K. Marchant, M.A. Pindrus, et al: Biomaterials, Vol.30(2009), p. 1299

[5] H.B. Fan, H.F. Liu, E.J.W. Wong, et al: Biomaterials, Vol.29(2008), p. 3324

[6] C. Huang, H. Wang, Y.H. Xu, et al: Journal of textile research, Vol.29(2008), p. 59

[7] X.W. Ge and J.G.Chu: Acta Polymerica Sinica, Vol.2(2000), p. 205

[8] M. Tsukada, G. Freddi and N. Minoura: Journal of Applied Polymer Science, Vol.51(1994), p. 823

[9] A. Kojthung, P. Meesilpa, B. Sudatis, et al: International Biodeterioration & Biodegradation, Vol.62(2008), p. 487

*Advanced Materials Research Vols. 175-176 (2011) pp 90-94*

*doi:10.4028/www.scientific.net/AMR.175-176.90*

# Effect of Wet Post-Drawn on Structures and Properties of PA6/MWNTs Nanofiber Filaments

Yang Liu[1, a], Jie Li[1, b], Zhi-juan Pan[1, 2, c]

[1]College of Textile and Clothing Engineering, Soochow University, Suzhou,215021, China

[2]National Engineering Laboratory for Modern Silk,Soochow University, Suzhou, 215123, China

[a]Liuy@suda.edu.cn, [b]lijie_050901@126.com, [c]Corresponding author, zhjpan@suda.edu.cn

**Key words:** electrospinning; PA6; MWNTs; wet-draw; mechanical properties.

**Abstract.** Electrospining technique is one of the hotest topics all over the world. The main form of the electrospun products is generally nonwoven fiber web with the poor mechanical properties. Consecutive PA6/MWNTs nanofiber filaments were successfully fabricated by an improved electrospining method. Peregal O was used as the bath to post-draw the as-spun filaments and the effects of draw ratio on their structures and properties were studied. The results show that with the increase of the draw ratio, the diameters of filament and fiber decrease; while the degree of orientation arrangement and crystallinity of the fibers is obviously improved and the breaking strength and initial modulus of the filaments increase. As the maximum draw ratio reaches 1.7, the breaking strength and initial modulus of the filament are 2.64 times and 4.2 times as compared to those of the control sample respectively.

## Introduction

Carbon nanotube (CNT), which possesses excellent mechanical properties, favourable chemical and thermal stability, good conductivity and outstanding optical properties as well as the unique one-dimensional nanostructures, has attracted tremendious attention from its discovery in 1991[1]. Moreover, it has been widely used as high-performance structural material, multifunctional material, information material, biomedical material, catalyst, and so on [2-7].

For CNTs/polymer composite fibers, although some researchers had successfully obtained PA6/CNTs, PANI/CNTs, etc. by melt spinning , gel spinning and dry-wet spinning, its poor dispersion in organic polymer matrix remains unsolved. Recently, the development of electrostatic spinning technology has provided an effective way to prepare the CNTs/polymer composite fibers. Electrospinning can be conducted under the room temperature, the diameter and surface structure of the electrospun fiber can be easily controlled. With these advantages, electrospinning has recently became one of the most attractive manufacturing technologies in making nanofibers. But most of the products by electrospinning are porous nonwovens with randomly oriented nanofiber, which usually has poor mechanical properties. Since it is hard to control the structure of the assembled mats and its secondary process is limited, the electrospun nonwovens could only be used in a single form. In this paper, the continuous electrospun PA6/MWNTs nanofiber filaments were successfully obtained by our self-made electrospinning device.

In the processes of chemical fiber spinning, some researchers had studied the effect of post-drawn on the structures and properties of the as-spun yarns. The result reveals that, post-drawn

is helpful to enhance the strength and the modulus of the as-spun yarns, and results in the improvement of the mechanical properties [8-10]. Chen Fangquan etc[8]. have studied the effects of hot-drawn and vapor-drawn on the structures and properties of PAN fiber. He found that the strength of fiber stretched by vapor-drawn was higher than that by hot-drawn, and thought that the presence of water molecules increased the distance between PAN molecules and decreased the interactions between macromolecules, which not only reduced the relaxation activation energy and facilitated the movement of the segment and macromolecular chain, but also improved the crystallinity of PAN macromolecules. There are still few report on the wet post-drawn of the parallel-arranged electrospun nanofibers. In this article, on the basis of successful spinning of the continuous electrospun nanofiber filaments, the as-spun yarns were stretched with different draw ratios in reactive bath, and the effects of wet-drawing on the structures, thermal stability and mechanical properties of the fibers were studied.

## Experimental

**Materials.** Pure polyamide 6 copolymer pellets (Sigma Aldrich Inc.), 88% formic acid(W/W), MWNTs（Nano Ltd., Shenzhen）.

**Sample preparation**

***Acidification of MWNTs.*** MWNTs were added into the mixture solvents of 65% $HNO_3$ and 95% $H_2SO_4$ (v/v=1:3). The solution was centrifugated after the sonication for 4 hours at room temperature. Then MWNTs were separated from the mixture solvents and purificated with deionized water until the PH value reached 7. Finally MWNTs were dried in oven at 90℃ for the further use .

***Preparation of electrospinning solution.*** The pure polyamide 6 copolymer pellets were dissolved in 88% formic acid at the room temperature. After that, acided MWNTs were added into the solution, followed by sonication treatment for 1h. Then the PA6/fomic acid spinning solution was obtained after well mixing by magnetic stirrer. The concentration of PA6 in the PA6/fomic acid solution is 25wt%, and the content of MWNTs in the spinning solution are 1wt%, 2 wt%, 3 wt%, 4 wt%, and 5 wt% respectively.

***Electrospinning.*** As shown in Fig. 1, the continuous PA6/MWNTs nanofiber filaments were electrospun by our home-made electrospinning device. A circular reservoir was full of 0.5wt% peregal O aqueous solution. The horizontal distance from the tip of a spinneret to the left-wall of the reservoir was 2.5cm. The spinning solution was drawn from a syringe with a stainless spinneret (ID 0.85mm). The spinneret was connected with the positive pole of high power supply (HV) by a wire. A mandrel with diameter 11.4mm rotated at 150 rpm, and the corresponding linear speed was 5.4m/min. The temperature and length in the heater region were 100℃ and 10cm respectively.

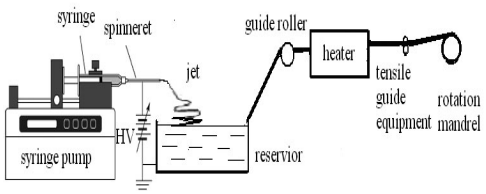


Fig. 1 Schematic diagram of electrospinning device

***Wet post-drawn.*** Unwinded the as-spun filaments from the mandrel to the 0.5%wt peregal O aqueous solution, and then the filaments were rolled after drying at 100℃. Draw ratios were

controlled by the ratio of unwinding speed to rolling speed. After the wet post-drawing, the filaments was naturally stored at room temperature.

**Measurements of structures and properties**

***Measurement of filament morphology and diameter.*** SEM (HITACH S-4700) was employed to characterize the morphology of the longitudinal surface of the filaments. The diameter of the yarn were measured by CU-2 fiber fineness tester. Each sample was measured 50 times and then calculate the average value.

***Measurement of thermal stability.*** Thermal stability was measured by Diamond 5700 of USA PE company. The temperature was increased from 25℃ to 300℃ at a rate of 10℃/min under nitrogen atmosphere (20ml/min).

***Mechanical property of filament.*** The mechanical property of PA6/MWNTs wet post-drawn filaments was tested by an Instron 3365 mechanical testing machine with a gauge length of 10mm, crosshead speed 10mm/min, temperature 20±2℃ and relative humidity 65±5%. Each sample was measured 10 times.

## Results and discussion

**Effect of wet post-drawn on structures and properties of PA6/MWNT nanofibers.** Fig. 2 shows SEM images of PA6/MWNTs filaments with different wet post-drawn ratios. The spinning voltage was 18KV and the spinning distance was 6cm. The changes of the fiber diameter and filament diameter were listed in Table 1. From Fig.2 and Table1, we can find that, with the increase of the wet post-drawn ratio, both the filament diameter and fiber diameter decreased, while the degree of fiber orientation arrangement obviously improved, which is induced by the straightening of the curved fibers under the external force during the drawing. The larger post-drawn ratio, the higher straight degree of the fiber. With the further drawing, the molecular chains begin to move, resulting in the decrease of the fiber diameter. As the draw ratio exceeded 1.7, both fibers and filaments began to fracture.

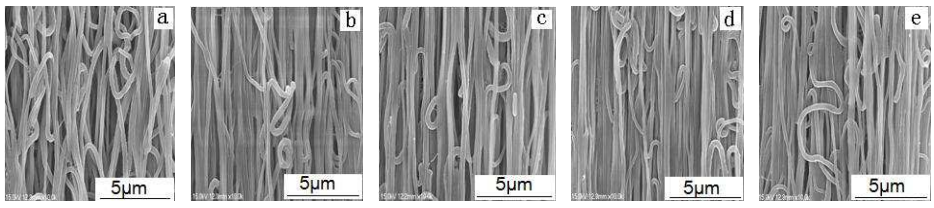


Fig.2 SEM images of PA6/MWNTs nano filaments(a~e : 1, 1.4 1.5, 1.6 ,1.7 time, 10 KX)

Table1 Average diameters of PA6/MWNTs nano-fiber

| Wet post-drawn ratio | Diameter of nano-filament /μm | coefficient of variation / % | Diameter of nano-fiber/nm | coefficient of variation / % |
|---|---|---|---|---|
| As-spun | 42.85 | 15.98 | 268.25 | 17.38 |
| 1.4 | 35.50 | 10.67 | 223.38 | 21.29 |
| 1.5 | 27.57 | 11.38 | 204.85 | 14.62 |
| 1.6 | 29.40 | 9.38 | 186.10 | 19.54 |
| 1.7 | 27.20 | 11.12 | 190.54 | 16.67 |

**Effects of wet post-drawn on thermal stability.** Fig. 3 is the DSC curves of the control and treated samples. The melting point, melting heat and melting enthalpy is listed in Table 2. With the increase of wet post-drawn ratio, the melting enthalpy increased, but the melting point changed slightly. It means wet post-drawn promotes the thermal stability of the nano-filament. Because of the recombinationaction of the surfactant and water during the drawing, the movement of the segment and macromolecular chain become easier. Also the external force facilitate the relative movement between fibers and molecular chains, thus promote the crystallization of the fiber in the wet post-drawn process.

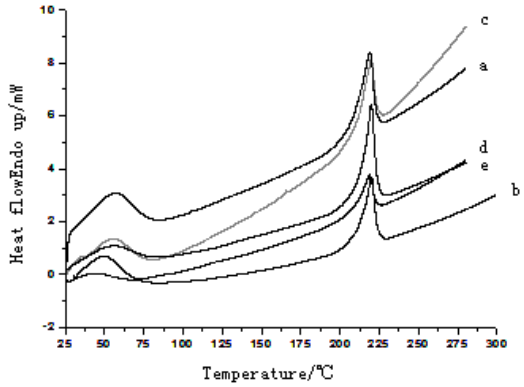


Fig. 3 DSC curves of PA6/MWNTs nano filaments
(the post-drawn ratios of a~e is 1, 1.4 1.5, 1.6 ,1.7 time respectively)

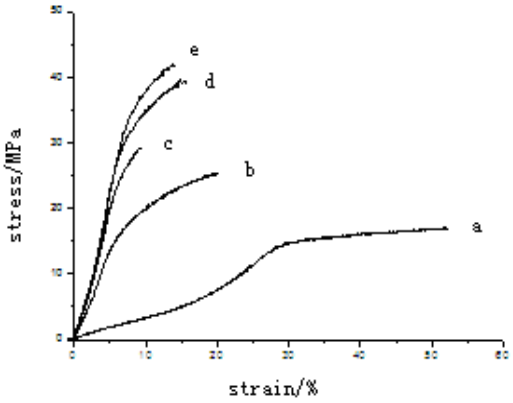


Fig. 4 Stress-strain curves of PA6/MWNTs filaments
(the post-drawn ratios of a~e is 1, 1.4 1.5, 1.6 ,1.7 time respectively)

Table 2 Melting point and mechanical properties of PA6/MWNTs nano-filaments

| Wet post-drawn ratio | $T_m$/℃ | Melting heat/mJ | Melting enthalpy/J·g$^{-1}$ | Strain at break/% | Initial modules/Mpa | Stress at break/Mpa |
|---|---|---|---|---|---|---|
| As-spun | 219.47 | 149.792 | 59.9168 | 50.3 | 88.9 | 14.2 |
| 1.4 | 219.83 | 143.728 | 51.3315 | 23.0 | 256.5 | 25.7 |
| 1.5 | 218.87 | 195.580 | 65.1935 | 8.0 | 249.7 | 25.1 |
| 1.6 | 219.79 | 200.015 | 71.4338 | 13.0 | 355.7 | 35.6 |
| 1.7 | 219.79 | 200.015 | 71.4338 | 11.1 | 373.3 | 37.5 |

**Effect of wet post-drawn on mechanical properties of PA6/MWNTs filament.** (Table 2) showed the mechanical properties of PA6/MWNTs filaments with different wet post-drawn ratios,

including the breaking strength, breaking elongation, and initial modules. Each data in Table 2 is the average value of 10 samples. Fig.4 is the typical stress-strain curve. The results show that with the increase of the draw ratio, the breaking strength and initial modulus of the filaments increase while the elongation at break decrease. This is because that the surfactant in the bath makes the fiber surface smoother, and further promotes the relative movement between fibers, resulting in the straightness of the curved fibers. Meanwhile the penetration of the surfactant molecular into the fibers makes it easier for the molecular chains and MWNTs to arrange along the axis of the fibers under rolling tension, therefore the mechanical properties of the PA6/MWNTs nanofiber filaments are improved.

## Summary

The modified method of wet post-drawn for PA6/MWNTs nanofiber filament can improve the fiber alignment along the axis of electrospinning. With the increase of the draw ratio, both the filament diameter and fiber diameter decrease. With the increase of the wet post-drawn ratio , the thermal stability of PA6/MWNTs filament is improved. The breaking strength and initial modulus follow the same trends. As the draw ratio reaches 1.7, the breaking strength and initial modulus of the filament are 2.6 times and 4.2 times larger than those of the control samples respectively.

## Acknowledgements

Financial support for this work was provided by the Science and Technology Project of Jiangsu Province (BK2008151) and Creative Research Project for Graduate Students of Jiangsu Province （CX09B_026Z）

## References

[1] H.W. Zhu, D.H.Wu, C.L. Xu: Carbon nanotube, (China Machine Press, Beijing2003).

[2] H.W. Li, X.S. Gao, Y. Tong: Chinese Journal of Materials Research, Vol.17(2003), p. 444

[3] X.Y. Gong, J. Liu, S. Baskaran, et al: Chem Mater, Vol.12(2000), p. 1049

[4] J. Sandler, M. P. Shaffer: Polymer, Vol.40(1999), p. 5967

[5] Z. H.Yang, X. H. Li, Z. G.Chen,et al: New chemical materials,Vol.27(1999), p. 22

[6] Y.Yu, Y. Zeng, W. J. Wang, et al: Journal of Central China Normal University (Natural Sciences), Vol.36(2002), p. 319

[7] K.A. Watson, J. R. Smith, G. Joseph, et al: Inter SAMOE Tech conference, Vol.33(2001), p. 1551

[8] F.Q. Chen，J. Gao，H. F. Chen et al: China Synthetic Fiber Industry, Vol.31(2003), p. 4

[9] X.Y. Lu, T.B.Zhao, Y.Y. Xu,et al: Guangzhou Chemical Industry,Vol.37(2009), p. 140

[10] M.Y. Li，T.J. Zhang: China Synthetic Fiber Industry, Vol.32(2009), p. 21

*Advanced Materials Research Vols. 175-176 (2011) pp 95-99*

*doi:10.4028/www.scientific.net/AMR.175-176.95*

# Preparation of braided silk as a tubular tissue engineering scaffold

Huijing ZHAO[1, a], Mingzhong LI[1, b]

1.National Engineering Laboratory for Modern Silk, College of Textile and Clothing Engineering,

Soochow University, No. 199 Ren'ai Road, Industrial Park, Suzhou 215123, China

[a]zhhj@suda.edu.cn, [b]Corresponding author, mzli@suda.edu.cn

**Keywords:** silk; braiding; small diameter; tissue engineering scaffold; tube.

**Abstract.** Silkworm silk has been recognized as a satisfactory biomaterial for long time due to its exceptional biocompatibility, biodegradability, mechanical properties etc. For example, silk fibers in the form of sutures have been used for centuries. The aim of this study is to discuss the potential usage of silk as the novel biomedical devices, such as blood vessels. In this study, cuit silks prepared from degummed raw silks were twisted as threads with four different yarn linear densities. A specific braiding machine was used to weave those threads into a tube. Subsequently two different groups of silk tubes were prepared. One was treated by ethanol and the other without. Thickness, porosity, mass per unit area of two groups of braided tubes were measured. Its mechanical properties were also studied. The influence of ethanol treatment and various yarn linear densities on its structural and mechanical properties was also studied. Results indicated that structural and mechanical properties of the tubes were significatly changed by the yarn linear densities and ethanol treatment. Conclusively, braided silk tube could be a potential blood vessel tissue engineering scaffold.

## Introduction

Blood vessels are important components of human's life. They function to carry blood from and to the heart, as well as to and from the tissues and organs. They form a branched system of arteries and veins that vary in size, mechanical properties, biochemical and cellular content, depending on their location and specific function. However, because of diseases and damages, the pathology of blood vessels is one of the major causes of death all over the world. Although synthetic vascular grafts such as ePTFE and PET have been used successfully in treating the pathology of large arteries (> 6mm internal diameter), these have generally not proved successful in replacing the smaller diameter (6 mm internal diameter and below) vessels [1-3]. An alternative supply of small diameter blood vessels become a massive clinical need. However, in spite of many years of research using a wide variety of biomaterials, clinical success for small diameter (< 6 mm) vessels has not yet to be demonstrated due to disappointing structural and mechanical properties and complications such as occlusion, thrombosis, intimal hyperplasia, and compliance mismatch. References have told us that the mechanical properties are critical to blood vessel function. How to prepare a small diameter graft with good biocompatibility and mechanical properties has been a challenge for a long time. Silkworm silk has been agreed as a satisfying biomaterial for a long time because of its good biocompatibility, biodegradability, mechanical properties etc. Being used in the form of sutures for centuries could prove its satisfying biocompatibility and mechanical properties [4]. Braiding silk fibroin fibers as tubes offers the potential of replacing diseased and damaged native small diameter blood vessels. Recently, researchers from Japan studied silk fibroin fibers being woven as small

diameter tubular grafts. They studied the biological properties of the grafts and reported that they had good long-term patency [5]. However, the morphological and mechanical properties of the grafts have not been studied systematically. In this paper, the preparation of small diameter tubes braided by silk fibroin threads with different yarn linear densities and some of their basic properties will be studied, which will provide the foundation of further study on the small diameter tubular grafts that can be used clinically.

## Materials and Methods

**Materials.** Cuit silks prepared by degummed raw domestic silkworm silks were twisted as threads with four different yarn linear densities (44, 88, 176, 352 denier). A special braiding machine was used to weave those threads into tubes with different internal diameters (3, 4, 5, and 6 mm). In order to keep a stable shape and reduce its porosity, the tubes were then treated with 4% (w/w) silk fibroin aqueous solution for 4 hours and dried in oven with 60℃ for 4 hours. Those oven-dried tubes were divided into two groups. One group of tubes was treated by 75% (v/v) ethanol for 2 hours, to make silk fibroin water-insoluble.

**Scanning electron microscopy (SEM).** In order to determine the morphology of the samples, they were viewed under a scanning electron microscope. The accelerating voltage was 15 kV. Specimens were mounted on aluminum stubs using conductive carbon tape. They were then coated with gold/palladium to obtain a conductive coating.

**Porosity.** Since the overall porosity of the tube could not be measured directly, it was calculated by an indirect approach using the mass per unit area, thickness, and silk density of the tubes. Porosity was calculated by Equation (1) [6].

$$P = 100 \times \left( 1 - \frac{M}{t \times \rho \times 1000} \right)\% \tag{1}$$

Where P is porosity (%), M is mass per unit area (g/m2), t is thickness (mm), $\rho$ is density of the silk (1.38 g/cm3). The thickness of the specimen was measured by a thickness gauge YG(B)141D. The mass of the specimen was measured after they had been cut into 3 cm lengths.

**Mechanical testing.** The specimen were cut into 6 cm lengths and then tested in INSTRON 3365 which was made in USA. A 0.5 N load cell was used with a crosshead speed of 50 mm/min. The length between the two clamps was 4 cm. The values of peak load (N) and peak strain (%) are reported in the next Section.

## Results and Discussion

**Surface morphology.** The braided tubes were treated with silk fibroin aqueous solution and dried in oven. Some of the oven-dried tubes were treated by ethanol, to make silk fibroin water-insoluble. After those treatment, the specimens could keep a stable tubular shape and not be dissolved in water. The other important reason for the tubes being treated by silk fibroin aqueous solution was that the solution could form silk fibroin films after being dried in oven, and it could form a cover on the surface of the tubes and prevent leakage of the blood when the tubes were implanted into human's body. With the increase of the time in human's body, the silk fibroin film would be degraded faster than the braided tubes, therefore, the pore sizes of the tubes become bigger, which is good for the cells ingrowth.

As can be seen in Fig.1, the silk fibroin went in between the filaments of silk threads, as well as made a cover-like layer on the internal and external surfaces of the threads. It was also observed that the surface morphology of specimens treated with and without ethanol has no significant differences. The general view of the samples was showed in Fig. 2.

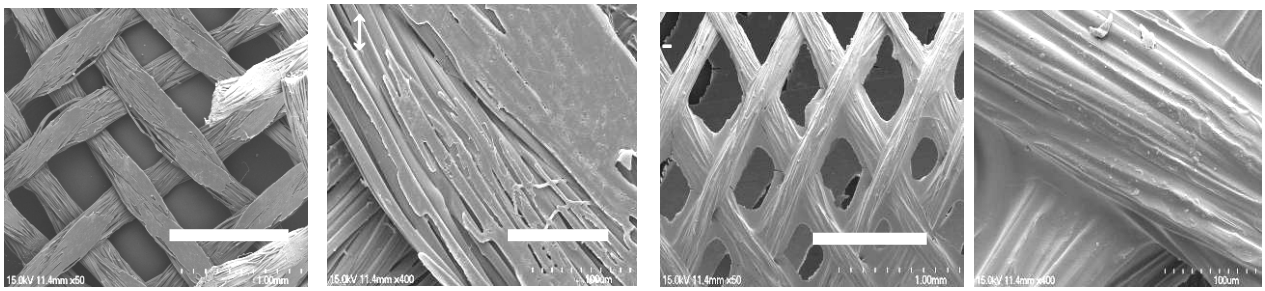

Fig. 1 The internal surface (A: 50×, B: 400×) and the external surface (C: 50×, D: 400×) of the braided silk tubes

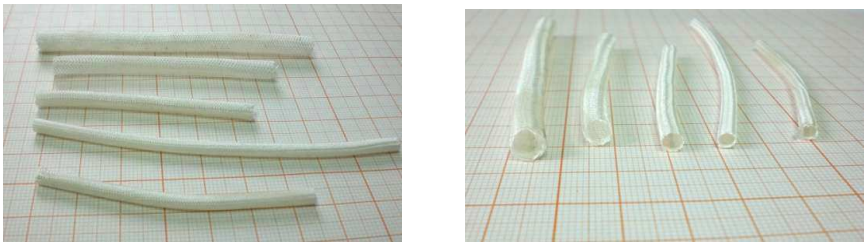

Fig. 2 The photos of the samples with different internal diameters

**Influence of ethanol treatment.** Ethanol treatment could make the specimens water-insoluble. However, it also had some other influences on the morphological and mechanical properties. As can be seen in Table 1, no matter what the internal diameter and the yarn linear density were, the thickness of most ethanol treated specimens had significant increase. The yarn linear density of specimens in Fig. 3 and 4 was 352 denier. There is no significant change of the peak load after ethanol treating, as can be seen in Fig. 3. However, the peak strain of the majority ethanol treated specimens decreased significantly, which was showed in Fig. 4. Before ethanol treating, the silk fibroin mainly contains random coil structure, and the molecular chain can be stretched relatively easily. Ethanol treatment induced the transformation from random coil structure to β-sheet crystalline structure, and the molecular chain was relatively difficult to be stretched. Therefore, the peak strain of the samples decreased after ethanol treatment [7].

Table 1 Thickness of braided silk tubes with and without ethanol treatment

| Yarn linear density | 352 denier | | | 176 denier | | |
|---|---|---|---|---|---|---|
| Internal diameter (mm) | No ethanol | Ethanol treated | p value | No ethanol | Ethanol treated | p value |
| 3 | 0.38+0.04 | 0.47+0.07 | 0.02 * | 0.20+0.01 | 0.20+0.04 | 0.41 |
| 4 | 0.37+0.04 | 0.41+0.03 | 0.06 | 0.19+0.02 | 0.21+0.01 | 0.03 * |
| 5 | 0.31+0.02 | 0.39+0.07 | 0.02 * | 0.18+0.02 | 0.22+0.03 | 0.03 * |
| 6 | 0.34+0.03 | 0.32+0.03 | 0.26 | 0.18+0.02 | 0.23+0.02 | 0.01 * |

**Influence of yarn linear density.** Yarn linear density had obvious influence on the morphological and mechanical properties of the samples. It was showed in Table 2 that with the decrease of yarn

linear density, thickness and mass per unit area diminished no matter what internal diameter was. Apparently, yarn linear density determined the thickness and mass per unit area of the samples directly. For the porosity of specimens with the internal diameter of 3 millimeters, they increased with the decrease of yarn linear density. The reason of that was also obvious. With the same internal diameter, the thinner the silk thread was, the bigger pores the tubes had. However, it seemed that there was no certain relationship between yarn linear density and porosity of the specimens with the internal diameters of 3 and 4 millimeters. It was probably because the samples were soaked in silk fibroin aqueous solution and dried in oven after they were braided, silk fibroin film filled in some of the voidage of the samples. Fig. 1 could also explain this phenomenon.

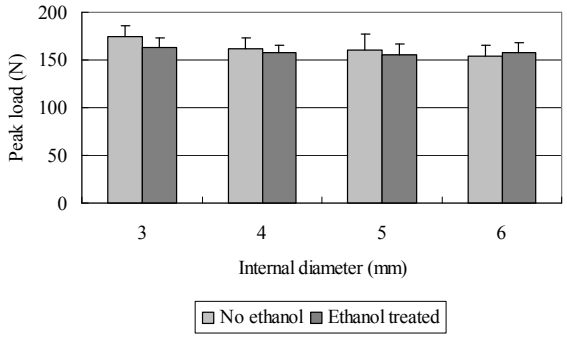


Fig. 3 Peak load of braided silk tubes with and tubes with and without ethanol treatment

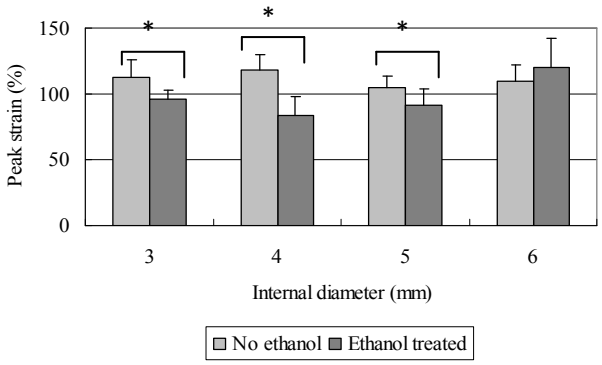


Fig. 4 Peak strain of braided silk without ethanol treatment

Table 2 Average Performance Properties of Samples

| Silk linear density (denier) | Internal diameter 3 mm Thickness (mm) | Mass (g/m2) | Porosity (%) | Internal diameter 4 mm Thickness (mm) | Mass (g/m2) | Porosity (%) | Internal diameter 5 mm Thickness (mm) | Mass (g/m2) | Porosity (%) |
|---|---|---|---|---|---|---|---|---|---|
| 352 | 0.38+0.04 | 75.30 | 85.75 | 0.37+0.04 | 58.47 | 88.42 | 0.31+0.02 | 46.07 | 89.37 |
| 176 | 0.20+0.01 | 38.46 | 86.20 | 0.19+0.02 | 31.61 | 87.62 | 0.18+0.02 | 28.00 | 88.97 |
| 88 | 0.11+0.01 | 18.37 | 87.45 | 0.12+0.03 | 17.73 | 89.11 | 0.10+0.01 | 13.14 | 89.87 |
| 44 | 0.05+0.01 | 8.35 | 88.36 | 0.04+0.01 | 6.16 | 88.85 | 0.06+0.01 | 9.26 | 88.02 |

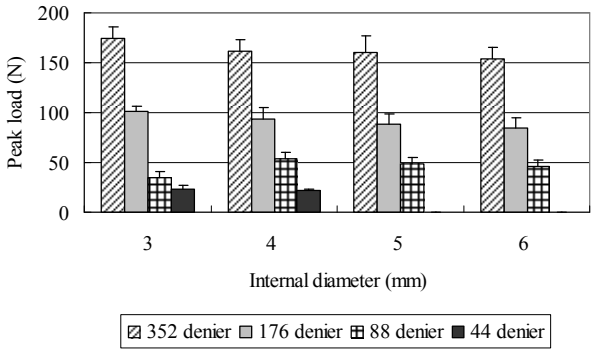


Fig. 5 Peak load of the silk tubes with different different silk linear density

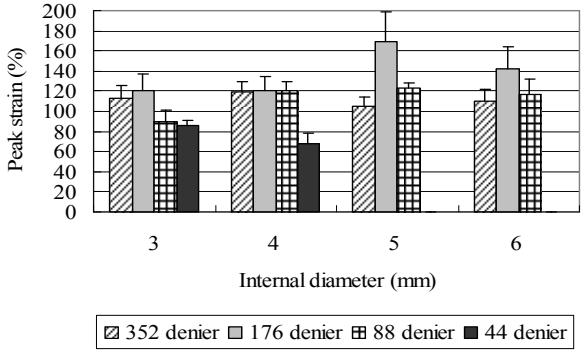


Fig. 6 Peak strain of silk tubes with silk linear density

With the decrease of yarn linear density, the peak load decreased remarkably no matter what internal diameter was, as can be seen in Fig. 5. It indicates that the strength of braided tubes depended on the strength of silk threads significantly. Normally, the coarser the silk threads, the stronger they are. Fig. 6 showed that it has no certain trend of peak strain with the decrease of yarn